

STERNOCLEIDOMASTOID FUNCTION

LEMIEUX

DETERMINATION OF THE STERNOCLEIDOMASTOID  
MUSCLE FUNCTION USING HEAD LIFT

By

D. RENALD LEMIEUX, B.Sc.

A Thesis

Submitted to the School of Graduate Studies  
in Partial Fulfilment of the Requirements

for the Degree

Master of Engineering

McMaster University

April 1984

Master of Engineering (1984)  
(Engineering Physics)

McMASTER UNIVERSITY  
Hamilton, Ontario, Canada

TITLE : Determination of the Sternocleidomastoid  
Muscle Function Using Head Lift

AUTHOR : Daniel Renald Lemieux, B.Sc.  
Bishop's University, Lennoxville,  
Quebec, Canada (1982)

SUPERVISOR : Dr. L. David Pengelly

NUMBER OF PAGES : X; 190

## ACKNOWLEDGEMENTS

I would like to gratefully acknowledge the generous support of my advisor, Dr. L.D. Pengelly of the Department of Engineering Physics and Medicine who provided me with guidance and expertise in the undertaking of this research project. My thanks are also directed to Dr. H. de Bruin who provided interesting discussions about EMG modelling and instrumentation. Furthermore, I would like to thank Dr. L.D. Pengelly for his useful advice and for the provision of facilities necessary to this study.

I wish to especially thank the following persons who submitted themselves to being subjects for this study:

Lawrence Torsher

Paul J. Moroz

Atheling Seunarine

Colin Wu

Special thanks are extended to Donald B. MacHattie for his assistance in preparing and testing the instrumentation used during this study.



## ABSTRACT

Forces associated with head lifting efforts as well as mouth pressure were measured on four supine normal men, at five different lung volumes from FRC to TLC, and with the head positioned at two different heights above the bed. Positioning the head at one of the two heights ( 3cm and 10cm ) provided for a change in length of the sternocleidomastoid (SCM) muscle.

Graded efforts of head lift, and graded inspiratory pressure manoeuvres were executed and corresponding electromyograms of the SCM were measured.

The mass lifted during efforts of head lift under static conditions (HSL) was measured with a self-contained transducer system located under the head of the subject. The muscle pressures at different lung volumes were obtained from pressure transducer records by adding the pressure-volume relaxation curve to the inspiratory mouth pressure-volume curve. The electromyogram of the SCM was obtained from surface electrodes, amplified and processed with a smoothing integrator to obtain the mean rectified electromyogram (MRE).

For every subject, the relationships between MRE and MASS LIFTED, and between MRE and MUSCLE PRESSURE were linear for every lung volume at every head height above the bed (  $r^2 >$

0.95 ). Data from all subjects were put together to form a single linear relationship ( MRE vs MASS LIFTED and MRE vs MUSCLE PRESSURE ) for every head height above the bed. The variability was greater at 3cm than at 10cm of head height. For both the head lift manoeuvre and the respiratory manoeuvre, there was a greater variability due to lung volume, on the slope and intercept of the curves at 3cm, than at 10cm of head height. Furthermore, more EMG was generated at 10 cm than at 3cm for a constant mechanical output, i.e., head lift or muscle pressure.

Statistical tests were performed on the curves. Slope and intercept of the curves at different lung volumes, for a specific manoeuvre and head height above the bed were not significantly different (  $p < 0.05$  ). The curves at different lung volumes were then put together to form a single linear relationship for both manoeuvres at both heights. Slope and intercept of the "pooled" curves, at both 3cm and at 10cm, were tested for both head lift and respiratory manoeuvres. It was found that the slopes were significantly different (  $p < 0.05$  ) while the intercepts were not. Using the input variable, MRE, as the common factor, a linear relationship between the two output variables, MASS LIFTED and MUSCLE PRESSURE, was determined at each head height. Interpretation of the resulting relationships shows that:

(a) About 50% of the maximum inspiratory muscle pressure can be generated without using the SCM muscle.

(b) For the head located at 3cm above the bed, the production of muscle pressure from 50% to 100%  $P_{muscle}$

max) corresponds to lifting, with the head, a mass equivalent to 4.5 times the head mass, while at 10cm above the bed, the same respiratory manoeuvre corresponds to lifting a mass equal to 1.3 times the head mass.

(c) Changes in lung volume do not bring about as great changes in length of the SCM muscle as do changes in head height.

## TABLE OF CONTENTS

	page
CHAPTER I - INTRODUCTION	1
CHAPTER II - RESPIRATORY FUNCTION ASSESSMENT STUDY AND ITS IMPORTANCE	4
2.1 Respiratory function assessment	4
2.2 Importance of the proposed study	5
CHAPTER III - THE STERNOCLEIDOMASTOID MUSCLE	8
3.1 Anatomy	8
3.2 Physiology	9
3.2.1 Functions of the SCM muscle	9
3.2.2 Importance of the other muscle involved	10
CHAPTER IV - THE EMC SIGNAL	15
4.1 Introduction	15
4.2 Physiology of the nerve and the muscle	16
4.2.1 The nerve cell and its action potential	16
4.2.2 The motor unit	19
4.2.3 The neuromuscular junction	19
4.2.4 The muscle fibre	21
4.3 Model for the myoelectric signal	22
4.3.1 Introduction	22
4.3.2 The MUAP	23
4.3.3 The MUAPT	24
4.3.4 The ME signal	29

	4.4 The Force-EMG relationship	34
CHAPTER V	- MATERIAL AND PROTOCOL	39
	5.1 Introduction	39
	5.2 Subjects	39
	5.3 Instrumentation	39
	5.4 Protocol	53
	5.5 Data manipulation	56
	5.5.1 Mean values	56
	5.5.2 Normalization	56
	5.5.3 Modelling	58
CHAPTER VI	- RESULTS	61
	6.1 Force levels	61
	6.2 Force-EMG relationship	64
	6.3 Reorganization of the data	71
CHAPTER VII	- DISCUSSION	83
	7.1 Introduction	83
	7.2 Summary of the results	83
	7.3 Sources of variability	85
	7.4 Discussion of the results	90
	7.4.1 The Sternocleidomastoid dual function	90
	7.4.2 Force-EMG relationship	91
	7.4.3 Importance of the Force-Length curve	97
	7.5 The SCM muscle function	103
	7.6 Future steps of this study	105
CHAPTER VIII	- CONCLUSIONS	107
APPENDIX A	- THE MYOELECTRIC SIGNAL	110
APPENDIX B	- BASIC LISTINGS	118

B-1	Principle of Least Squares	119
B-2	Statistical analysis	125
APPENDIX C	- TABULATED DATA	132
C-1	Raw data	134
C-2	Normalized data	147
C-3	Regression lines from normalized data	160
C-4	Pooled data	165
C-5	Final relationships	168
C-6	Relaxation manoeuvre	170
C-7	Reproduction	173
APPENDIX D	- A MODEL OF THE NECK	183
REFERENCES		186

## LIST OF ILLUSTRATIONS

Figure	page
3.1 Musculature of the neck	12
4.1 Scheme of a motor unit	20
4.1 Schematic representation of the generation of the motor unit action potential	25
4.3 Schematic model for MUAPT	30
4.4 Explanation of some of the terms of the myoelectric signal	30
4.5 Schematic representation of the model for the generation of the ME signal	31
4.6 Theoretical expressions for parameters of the ME signal and their relation to physiological correlates of a contracting muscle	33
5.1 Instrumentation used to record EMG	42
5.2 Instrumentation used to record respiratory function	46
5.3 Instrumentation used to record head lift	48
5.4 Instrument's general requirements	48
5.5 Construction of mechanical system of prototype	50
5.6 The mechanical system	50
5.7 Block diagram of the electrical system	51
5.8 Circuit design	52
5.9 Output of the chart recorder	57
6.1 Reproduction of the data for the Head Lift manoeuvre	63
6.2 Data for subject PM, and for HL manoeuvre	68
6.3 Data for pooled subjects	77
6.4 Data for pooled subjects and lung volumes	78

6.5	Relationship between the two mechanical outputs	82
7.1	Respiratory Manceuvre	95



## LIST OF TABLES

Table	page
3.1 Main muscles involved in forward bending of the neck and in forced inspiration	13
5.1 Subject description	40
5.2 Instruments description	47
5.3 Values used to normalize the subject's data	59
6.1 F-Values due to lung volume (FRC+2L) affecting the reproducibility of the linear Force-MRE relationship of a manoeuvre	62
6.2 HL(max) and P <sub>muscle</sub> (max) for the maximum voluntary contractions	65
6.3 MRE generated by a maximum voluntary contraction	66
6.4 Linear Force-MRE relationship: HL manoeuvre	69
6.5 Linear Force-MRE relationship: Respiratory Function manoeuvre	70
6.6 t-Values due to variation in lung volume from FRC to FRC+0.5L	72
6.7 F-Values due to lung volumes affecting the linear Force-MRE relationship	72
6.8 F-Values due to the subject's variation affecting the linear Force-MRE relationship	74
6.9 Linear Force-MRE relationship: pooled subjects	76
6.10 Linear Force-MRE relationship: pooled subjects and lung volumes	76
6.11 F-Values due to lung volumes affecting the linear Force-MRE relationship: pooled subjects	80
6.12 MRE ratios between 10cm and 3cm of Head Height	80
6.13 Linear Force-Force relationship	80
7.1 Slope ratio for a change in lung volume from FRC to FRC+0.5L	99

## CHAPTER I

### INTRODUCTION

It has been known for many years that the contraction of a muscle is accompanied by a substantial electrical activity. This electrical activity can be considered as an information source of the muscle activity. By the use of suitable electrodes and amplification, the electrical activity of muscles can be measured. This measured activity is called an electromyographic (EMG) signal.

It has also been known for many years that the EMG signal changes with the length of the studied muscle for a constant level of contraction, and with the contraction level for a constant muscle length.

The work presented in this thesis was initiated in an effort to determine an easy method of measuring the respiratory status of weak patients in an ICU unit by studying the neck muscle called " Sternocleidomastoid ".

To clearly understand the importance of this study, the main reasons why this study will help ICU patients and physicians

are discussed in Chapter II. This chapter mentions the actual method used by physicians to determine the respiratory status of their ICU patients. It concludes with a discussion of the benefits a simple method of determining the respiratory status of ICU patients can provide to them.

The muscle studied was the sternocleidomastoid (SCM) muscle. For this reason, Chapter III details the anatomy and physiology of this muscle. It also explains its dual function and its relation to the other neck and respiratory muscles.

The most important instrument of work used in this study is the EMG source signal. The physiology and physical parameters which are the basis of recorded EMG signals are investigated. These parameters belong to the most recent existing model developed by Carlo de Luca. This model is presented in Chapter IV. It helps to understand how the recorded EMG is related to the muscle physiology.

Chapter V details the material used during the experiment. This aspect is important because it has been reported in the literature that different recording devices have different output signals for the same input signal because their electrical properties are different. The choice of recording electrodes, their characteristics and their geometrical arrangement relative to the muscle fibres are very important features and are discussed in this chapter. Finally, the chapter outlines the protocol used during the experiment and details the methods used to analyze the results.

The results are presented in Chapter VI. In Chapter VII, an interesting discussion of the results is presented. It

outlines the meaningful results, it discusses the weaknesses of the experiment; it argues the results presented in chapter VI, it explains the SCM dual function from the obtained results, and it describes the future steps one should follow to continue the study of the SCM muscle.

The thesis ends with a concluding chapter, Chapter VIII, outlining the meaningful conclusions that help to understand the SCM dual function. It also explains from the final results, how the method used to do the experiment can become a simple method to determine the main respiratory function parameter of weak subjects, i.e., muscle pressure.

## CHAPTER II

### RESPIRATORY FUNCTION ASSESSMENT

#### STUDY AND ITS IMPORTANCE

##### 2.1 Respiratory function assessment.

It has been noted by the clinicians of the Intensive Care Unit of the Hamilton General Hospital that a simple method of assessing respiratory function of critically ill patients does not exist. There are two reasons for this:

- 1) these patients require a mechanical ventilatory support system, and respiratory function assessment is difficult because the respirator must be removed from the patient, which in certain cases may jeopardise the patient's life.
- 2) These critically ill patients may be fatigued or sleep deprived, and are not equipped to cooperate in respiratory function assessment.

One way to assess respiratory function is to ask the patient to deliver a vital capacity (VC) manoeuvre, i.e., the patient is asked to exhale as much as possible after making a maximum inhalation, or to deliver a maximum inspi-

ratory pressure manoeuvre under static conditions (MIPS), i.e., the patient is asked to inspire as hard as he/she can while the airways are blocked. These two manoeuvres activate the SCM muscles which are also used for performing forward flexion of the neck. For an ICU patient, forward bending of the neck is equivalent to lifting the head off the pillow. This requires less coordination and cerebral involvement than doing a VC or a MIPS manoeuvre.

The proposed study consists of assessing the SCM muscle which acts like a skeletal muscle for performing forward flexion of the neck, and as a respiratory muscle for performing forced inspirations. The ultimate objective of this study is to define a correlation between head lift and respiratory function. From this correlation, an easy method of determining the respiratory status of these patients can be defined.

## 2.2 Importance of the proposed study.

The respiratory assessment done by the clinicians on ICU patients is of primary importance in weaning the patients from mechanical respiratory support. A review of nine month's caseload through the 15-bed ICU of the Hamilton General Hospital, done by J.R. Hewson, MD, revealed that 599 patients had required mechanical respiratory support during their stay in the ICU. Of this total, 361 patients had respiratory support for less than 24 hours, 137 pa-

tients for a duration of 1 to 3 days, 52 for 4 to 7 days, 21 for 8 to 14 days, and 19 for greater than 14 days duration.

An extrapolation revealed that a total of 800 patients would require ventilatory support in the course of a year in this ICU. The nine month sample of patients, projected to twelve months, indicates that in the ICU almost 1000 ventilatory days of mechanical ventilatory support are given to the small group of patients who have not been weaned from mechanical respiratory support by day 14 of their respiratory support regimen.

In this same review of cases, it appeared that the average occupancy rate of the ICU is greater than 95%, which is well above the national standards advised by the Ministry of Health and Welfare in Ottawa. This clearly indicates an overutilization of the ICU resources. Besides, 17.5% of the total available ICU resources have to be utilized for the mechanical respiratory support of patients after they have already received 14 days of mechanical ventilatory support. It is clear then that prolonged ventilatory support is a major problem from a resource utilization point of view.

Prolonged mechanical ventilatory support also creates ventilatory dependence. That is, the patient loses his ability to breathe because of a lack of utilization. The respirator pushes the air inside the lungs and the patient makes no effort. The result of this is that the weaning becomes much more difficult to perform and demands much

more energy from both patient and clinician.

The weaning consists of reeducating these ventilatory dependent patients how to breathe because the breathing mechanism is lost. The respiratory muscles have become atrophic and have lost their coordination.

By defining a simple way of assessing respiratory status of critically ill patients, weaning can be performed sooner. This will reduce mechanical ventilatory dependence of the patients, and will improve resource utilization of the ICU.



## CHAPTER III

### THE STERNOCLEIDOMASTOID MUSCLE

#### 3.1 Anatomy

The sternocleidomastoid (SCM) muscle is located very superficially in the neck. It can be seen and palpated easily. The muscle passes obliquely down across the side of the neck and forms a prominent landmark, especially when contracted.

The SCM muscle has the shape of the eleventh letter of the Greek alphabet, lambda. It has three attachment points. Its lower attachment points are the upper part of the anterior surface of the manubrium sterni and the upper surface of the medial third of the clavicle. These two heads are separated at their attachments by a triangular interval; but as they ascend, the clavicular head passes behind the sternal head and blends with its deep surface below the middle of the neck forming a thick, rounded belly. Above, the muscle is inserted by a strong tendon into the lateral surface of the mastoid process of the skull, from its apex to its superior border, and by a thin aponeurosis into the lateral half of the superior nuchal line, i.e., a slight

curved ridge, which runs laterally from the external occipital protuberance to the mastoid process of the temporal bone.

The SCM muscle is innervated by two sets of motor nerves: the eleventh cranial nerve called "The Accessory Nerve", and the cervical spinal nerves C2 and C3. The Accessory Nerve has two portions: a cranial portion and a spinal portion. The cranial portion derives from four to five rootlets at the side of the medulla, runs laterally below the vagus nerve (or cranial nerve X) at the jugular foramen where it is joined by the spinal portion which arises from the motor cells in the anterior gray column as low as the fifth cervical segment. In order to join the cranial portion inside the skull, the spinal portion enters the skull through the foramen magnum. Both portions leave the skull through the jugular foramen. The cranial portion innervates the pharynx, the upper larynx, the uvula, and the palate. The spinal portion innervates the sternocleidomastoid and the trapezius muscles.

### 3.2 Physiology.

#### 3.2.1 Functions of the SCM muscle

One action of the SCM muscle is to tilt the head towards the shoulder of the same side; it also rotates the head so as to carry the face towards the opposite side. When both SCM muscles act, the rotation of the head is prevented by the cancellation of the lateral forces, and the final ac-

tion is the forward bending of the neck such that the chin touches the upper sternum.

The other action of this muscle is to help to perform an inspiration. The SCM muscle is considered to be an accessory inspiratory muscle. This function does not occur in normal breathing ( Mountcastle 1980 ), but it becomes of major importance during forced inspiration and during exercise where hyperventilation occurs. In a normal situation both functions are present, but one can voluntarily stabilize the head to perform a forced inspiration as well as one can voluntarily stabilize the chest to perform a forward flexion of the neck.

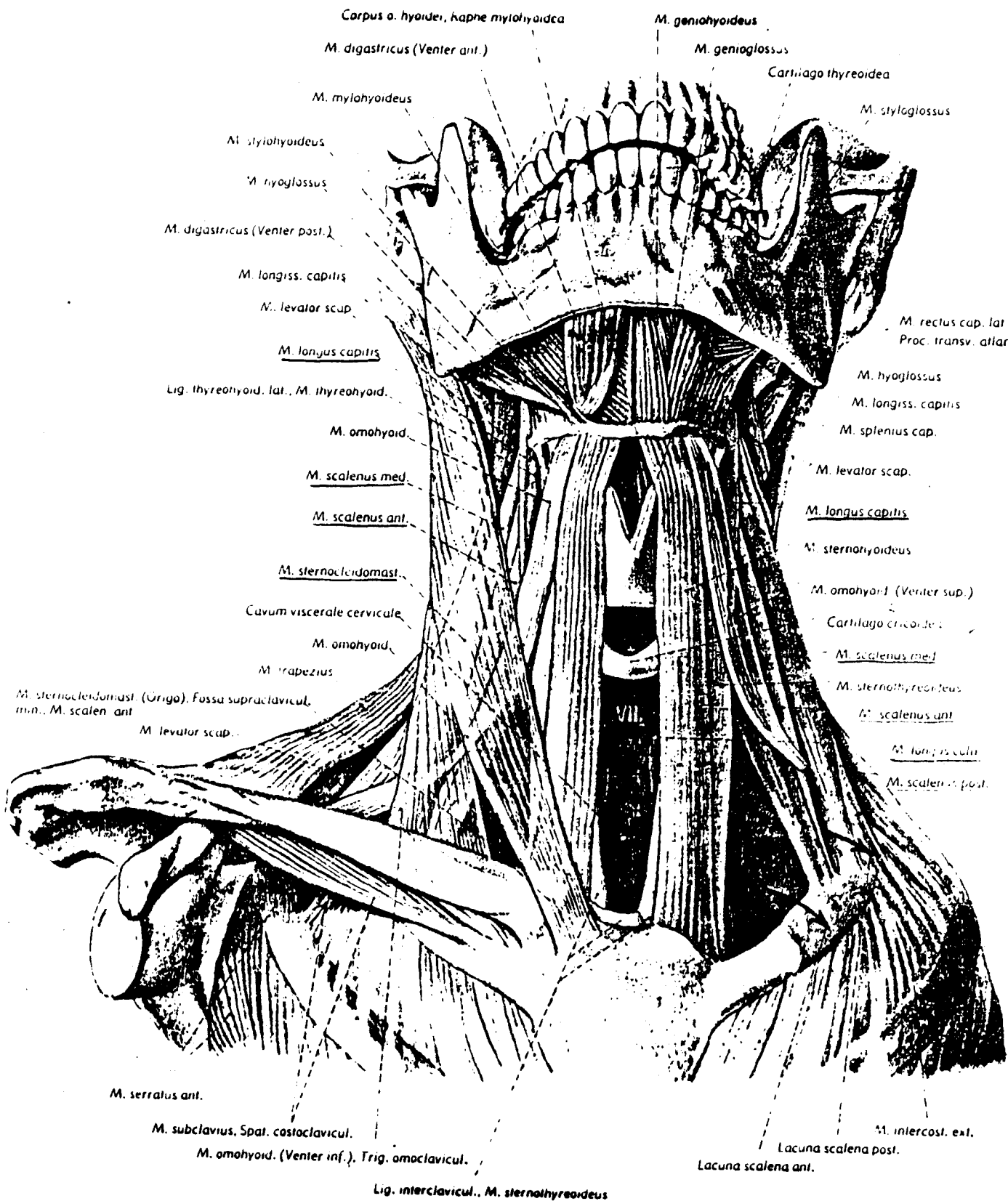
### 3.2.2 Importance of the other muscles involved.

As mentioned in the previous section, the SCM muscle has a dual function; it bends the neck forward, and it is used as an accessory inspiratory muscle. Other muscles are also involved in these functions.

In forward bending of the neck, three other muscles in addition to the SCM muscle are involved: the Longus Colli (Sup. Oblique, vertical) muscles, the Longus Capitis muscle, and the Scalenes (Anterior, Middle, Posterior) muscles. The SCM muscle is the prime muscle of the action (Warwick 1973). These muscles, except for the anterior and middle scalene muscles, do not touch the SCM muscle. They are located deeper in the neck (Fig. 3.1).

The same phenomenon occurs during hyperventilation. The SCM muscle as well as the scalene muscle are acces-

sory inspiratory muscles while the diaphragm muscle and the external intercostal muscles are the main inspiratory muscles (Tokizane 1952). During normal breathing the SCM muscle is not activated while the three others are (Raper 1966); the scalene is less activated than the external intercostal muscles which are less activated than the diaphragm muscle (Campbell 1955a, Murphy 1958). The order of activation of the intercostal muscles is from the first to the eleventh intercostal muscle (Murphy 1958). The SCM muscle is activated during hyperventilation to help the other inspiratory muscles to perform an adequate inspiration to obtain an appropriate gas exchange in the lungs (Campbell 1955b). Table 3.1 lists the main muscles involved in both manœuvres, i. e., inspiration and forward bending of the neck.



(Pernkopf 1963)

FIGURE 3.1: Musculature of the neck

(The underlined muscles are the ones used in both manoeuvres, Head Lift and Respiratory Manoeuvre.)

Name	Origin	Insertion	Action	Nerve
Longus Capitis	Ant. tubercle, Trans. process vertebrae C3-6	Basilar part of occipital bone	Flexes head	C1,2,3
Longus Colli Sup. Oblique	Ant. tubercle, Trans. process vertebrae C3-5	Tubercle on ant. arch of Atlas	Flexes neck, slight rota- tion of cer- vical part.	C2-7
Vertical	Bodies of ver- tebrae C5-7, T1-3	Bodies of C2-4	Flexes neck	C2-7
Ant. Scalene	Ant. tubercle, Trans. process vertebrae C3-6	Scalene tu- bercle, rid- ge on upper first rib	Bends neck, Raises 1 <sup>st</sup> rib	C5-8
Mid. Scalene	Post. tubercle Trans. process vertebrae C2-7	Upper 1 <sup>st</sup> rib, behind subclav. groove	Bends neck Raise first rib	C5-8
Post. Scalene	Post. tubercle, Trans. process vertebrae C5-7	Outer 2 <sup>nd</sup> rib	Bends neck, Raises 2 <sup>nd</sup> rib	C6-8
Sternocleido- mastoid	Sternum, Clavicle	Mastoid pro- cess of the skull	Bends head to same side Rotates head Raises chin to opposite side, toge- ther bend head forward + elevate chin. When head stabili- ze, it eleva- tes sternum + clavicle.	Accesso- ry (XI) spinal part, i.e. C2-4, C2 and C3

TABLE 3.1: Main muscles involved in forward bending of the neck and in forced inspiration

TABLE 3.1: (continuing)

Name	Origin	Insertion	Action	Nerve
External intercostal (11 pairs)	Lower border of rib	In upper border of rib below	Elevates rib below	Intercostal nerves T1-T12
Diaphragm	Xiphoid process of the sternum, Ribs 7-12, Lumbo-costal arches and crura	Central tendon	Descent of the central tendon	C4, (also C3 and C5)

## CHAPTER IV

### THE EMG SIGNAL

#### 4.1 Introduction

The electromyographic signal obtained from an active muscle is essentially the summation of the activities of a large number of physiological units. To effectively use this signal as an information source, a knowledge of the basic structural and functional units in striated muscle is required.

This chapter briefly reviews the characteristics of each physiological unit. In addition to giving a brief description of the electrical events, a model of the myoelectric signal will be presented in order to define the mathematical expressions of the most used parameters of the myoelectric signal, i.e.: (a) the mean rectified value, (b) the mean integrated rectified value, and (c) the root-mean-squared value. Finally, a brief discussion of the models of the Force-EMG relationship will be given.



## 4.2 Physiology of the nerve and the muscle.

### 4.2.1 The nerve cell and its action potential.

The nervous system is composed of two different parts: (a) the central nervous system which controls the voluntary actions, and (b) the peripheral nervous system which controls the reflex actions and controls certain functions (Somatic and Autonomic nervous system). The nerve cell is the basic element of any nervous system. It is composed of three parts: (a) the dendrites, (b) the body, and c) the axon. The dendrites are small, less than 10um diameter, and numerous. They transmit the information they receive to the cell body which is the living part of the nerve cell. It contains the nucleus and when it dies, the whole cell dies with it. The axon is unique in the nerve cell. It transmits the information it receives from the cell body to the dendrites of the following nerve cell, or to the muscle fibres of a muscle. Since our main interest is in the EMG signal, total attention will be directed to the nerve-muscle transmission of the action potential (AP). At its end point, the axon is divided into 3 to 150 terminal branches. The diameter of the axon varies between 1 and 20um, and its length can reach one meter. The nerve fibres whose axonal diameters are more than 2um are called myelinated fibers because their axon is covered with myelin. This myelin is positioned at interval of 1 to 2mm along the length of the axon. The uncovered parts are called nodes, and the covered parts are called internodes. The other nerve fibers (less than 2um diameter) are called non-myelinated fibers. The action of the myelin will be discussed later.

The information transmitted through a nerve cell is simply a depolarization process which is transmitted along the nerve cell. This depolarization process allows the propagation of a current along the cell. The skin of the nerve cell is a bilipid layer membrane. This membrane offers a very high resistance to the passage of electrical current, and has a biological capacitance of about  $1\mu\text{F}/\text{cm}^2$ . At rest, the nerve cell is in a state of active equilibrium. With the help of a sodium ( $\text{Na}^+$ )-potassium ( $\text{K}^+$ ) active pump which keeps the  $\text{K}^+$  ions inside the cell and the  $\text{Na}^+$  outside the cell, the nerve cell sustains a resting membrane potential ( $V_m$ ) of about  $-90\text{ mV}$  (inside relative to outside). The transmembrane potential ( $V_m$ ) can be expressed as:

$$V_m = \frac{-RT}{F} \ln \left[ \frac{P_{\text{Na}}[\text{Na}^+]_i + P_{\text{K}}[\text{K}^+]_i + P_{\text{Cl}}[\text{Cl}^-]_o}{P_{\text{Na}}[\text{Na}^+]_o + P_{\text{K}}[\text{K}^+]_o + P_{\text{Cl}}[\text{Cl}^-]_i} \right] \quad (4.1)$$

where  $P$  = permeability of the ion,  $F$  = Faraday's constant,  $T$  = absolute temperature, and  $R$  = gas constant.

The expression " $RT/F \ln$ " can be replaced by " $60 \log$ ". The above equation is called the "Goldman-Hodgkin-Katz" equation or the "GHK" equation.

When the nerve cell is excited, biochemical phenomena, still unknown, increase the membrane permeability to these ions by opening different channels and by letting the ions flow through them. Investigators believe that there are specific channels for specific ions (Selkurt 1976). The driving force existing, when the nerve cell is at rest, attracts the  $\text{Na}^+$  inside the cell and pushes the  $\text{K}^+$  outside the cell. This phenomenon first induces an increase of the sodium conductance ( $G_{\text{Na}}$ )

which depolarizes the nerve membrane towards zero millivolt to reach an overshoot of +30mV. During that time, a slow increase in the potassium conductance ( $G_K$ ) starts to repolarize the cell. The peak of  $G_K$  is reached after the  $G_{Na}$  peak so that an overshoot of +30mV could be reached. After a few milliseconds, the  $Na^+-K^+$  pump is activated to continue the repolarization of the nerve membrane to its resting value of -90mV after a period of hyperpolarization due to the potassium flow. The phenomenon just described is called an Action Potential (AP). This AP is generated at every axon-dendrite synapse and propagates along the nerve cell. The propagation along the axon can be continuous or saltatory. The continuous conduction is a slow conduction ( 1-5m/s ) found in the non-myelinated fibres. The saltatory conduction ( 50m/s ) is a characteristic of the myelinated fibres.

The action potential (AP) is an all or none phenomenon. When the depolarization of the nerve membrane reaches a threshold potential, the depolarization is automatic and instantaneous. This characteristic is useful for the propagation of the AP. Each point of the nerve membrane which is in contact with the extracellular medium becomes depolarized if the threshold is overcome. Because of this, the local depolarization, with local currents, is propagated along the non-myelinated fibres while it is from node to node in the myelinated fibres. The myelin provides a very good electrical insulation. Depolarization cannot occur in the internode space. When an AP train reaches a muscle, it depolarizes many muscle fibres synchronously. These muscle fibres belong to a motor unit.

#### 4.2.2 The motor unit.

The motor unit (Fig. 4.1) is the functional unit of the motor system. It is composed of one motoneuron and many muscle fibres (3-150). The number of muscle fibres in one motor unit is determined by the function of the whole muscle. Muscles controlling fine movements and adjustments have the smallest number of muscle fibres per motor unit (eg. eye ball muscles), while larger muscles producing gross movements have a larger number of muscle fibres per motor unit (eg. limb muscles).

The same muscle contains motor units of different size. Larger motor units may consist of a larger number of muscle fibres, or the muscle fibres themselves may be larger (de Bruin 1976). When a muscle contracts, it does so smoothly. The muscle fibres of the same motor unit contract synchronously while the muscle fibres of different motor units contract asynchronously.

#### 4.2.3 The neuromuscular junction.

The muscle fibre contraction is the mechanical result of the muscle fibre membrane depolarization. In order to reach the muscle fibre and cause a muscle fibre action potential, the nerve action potential (AP) has to pass through the neuromuscular junction (NMJ) or End Plate. The NMJ is the interface between the motor nerve ending and the muscle fibre. It serves as an impedance matching device to provide sufficient current to drive the muscle fibre membrane beyond threshold.

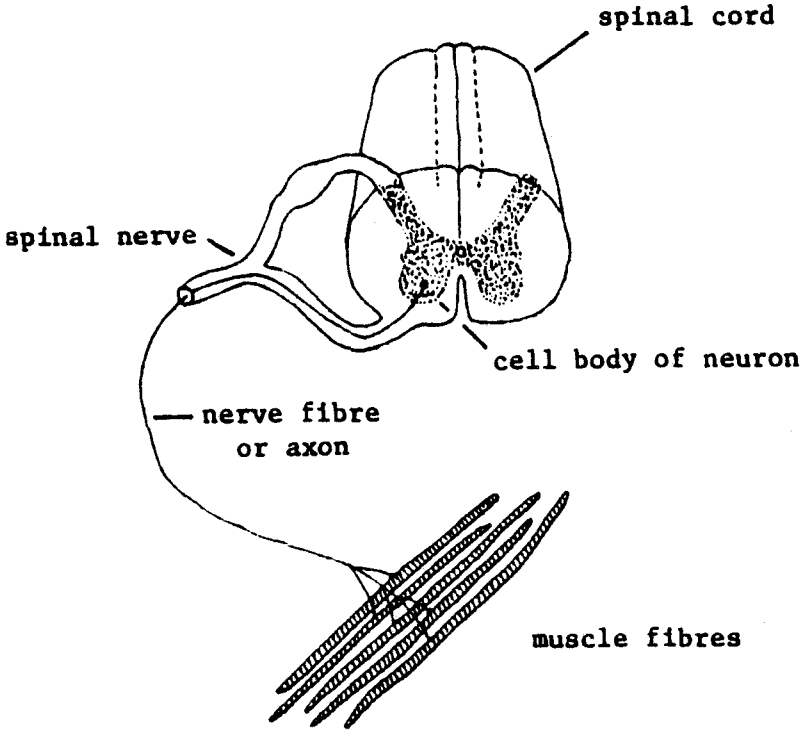


Figure 4.1 Scheme of a motor unit.

(Basmajian, 1974)

The transmission of the nerve AP from the presynaptic membrane to the postsynaptic membrane is essentially chemical. The nerve AP makes the presynaptic vesicles, with the help of the calcium ion, liberate acetylcholine (ACh) which makes the transition across the synapse gap, separating the nerve and the muscle fibre membranes. After ACh binds to the postsynaptic receptors, located on the muscle fibre membrane, the permeability suddenly increases to  $\text{Na}^+$  and  $\text{K}^+$ . These cations move according to their concentration and electrical gradient causing a depolarization of the membrane beyond threshold, which induces a self-propagating impulse called the End Plate Potential (EPP). The delay for producing a EPP is around 1.2msec. of which 0.7msec. is required for the synaptic transmission.

#### 4.2.4 The muscle fibre.

The muscle fibre is the basic component of a motor unit, and is also the basic structural unit of contraction. Under a microscope, the muscle fibre is a fine thread with a diameter varying from 10 to 100 $\mu\text{m}$ , and a length that can reach 30cm.

Once the EPP is generated, the depolarization propagates in both directions from the end plate, located in the middle of the muscle fibre, at a speed of 5m/s. The delay from the NMJ to both ends is around 5msec..

The depolarization of the muscle fibre membrane by the conducted impulse is followed by a brief phasic contraction of the muscle fibre, a twitch, followed by a rapid and complete relaxation. The duration of the twitch and of the relaxation,

from a few msec. to 0.2 sec., depends on the type of fibres involved. There are two types of muscle fibres: (a) the fast twitch fibres, and (b) the slow twitch fibres. A muscle contains both types of fibre, while a motor unit contains only one type of muscle fibre. Consequently, there exists: (a) fast twitch motor units, and (b) slow twitch motor units (Basmajian 1974).

### 4.3 Model for the myoelectric signal

#### 4.3.1 Introduction

A muscle can contract in three different ways. It can perform: (a) an isometric contraction, i.e., the muscle generates a tension while its length is fixed, (b) a concentric contraction, i.e., the muscle generates a tension while its length is shortening, and (c) an eccentric contraction, i.e., it generates a tension while its length is lengthening (Knuttgen 1982).

Many investigators have studied muscle function using a technique called "Electromyography" which records, with the use of various type of electrodes, the electrical event which induces a known mechanical event, i.e., a contraction.

The model presented in this section summarizes the work done by Carlo de Luca whose contributions (1968-1979) were very important in modelling the myoelectric (ME) signal. The derived expressions are only applicable to the ME signal as it exists on the surface of the active muscle fibres. The conductive medium between the motor unit fibres and the recording site

is considered to be purely resistive. The expressions do not take into account the filtering effect of the ME signal caused by the muscle tissue, fascia, fat, skin, and recording electrodes. This allows simple addition of the motor unit potentials. The model presented in this section will also give mathematical expressions for three out of four parameters used by investigators to describe the ME signal during a constant force isometric contraction: (a) the mean rectified value, (b) the mean integrated rectified value, and (c) the root-mean-squared value. The fourth parameter, the power density spectrum, describes an entirely new method of analysing the ME signal. This method has not been used to study the SCM muscle and will not be described.

The description of the model will be divided into three parts. The first part will describe the formation of the motor unit action potential (MUAP). The second part will discuss the motor unit action potential train (MUAPT) and its main parameters. The third part will explain how the MUAPT's are added together to form the ME signal.

#### 4.3.2 The MUAP

The depolarization of the muscle fibre membrane, from its resting potential of about  $-85\text{mV}$ , results in a brief monophasic wave of 2 to 4 msec. duration. The propagation of the muscle fibre action potential, at a speed of about  $5\text{m/s}$ , is seen by bipolar recording electrodes, located in the vicinity of the muscle fibre and arranged in a parallel alignment relative to the fibre, as a biphasic action potential. The



time duration of this action potential depends on the distance between the two electrodes. Its amplitude depends on the radius [a] of the muscle fibre, [  $V = ka^{1.7}$  where k is a constant (de Luca 1979)], the distance [D] between the muscle fibre and the recording site, [  $V = k/D$  where k is a constant (de Luca 1979)], and the filtering properties of the electrodes.

Since the nerve action potential depolarizes quasi-synchronously all the muscle fibres of a motor unit, the resultant signal seen at the recording site, the MUAP symbolized by  $h(t)$  (Fig. 4.2), will constitute a spatial-temporal superposition of the contributions of the individual muscle fibre action potentials.

The shape of the MUAP will generally vary due to the unique geometric arrangement of the motor unit fibres with respect to the recording site. The amplitude varies from a few  $\mu V$  to 10mV peak to peak with a typical value of 300 $\mu V$ . The number of phases may vary from one to four: 3% monophasic, 49% biphasic, 37% triphasic, and 11% quadriphasic (reported by de Luca 1979).

#### 4.3.3 The MUAPT

The MUAPT represents a sequence of MUAP's produced by the same motor unit during a sustained muscle contraction. It can be described by its inter-pulse intervals (IPI's) and the shape of the MUAP.

The assumptions made to create the MUAPT model are:

- 1) the IPI between every MUAP of one MUAPT remains cons-

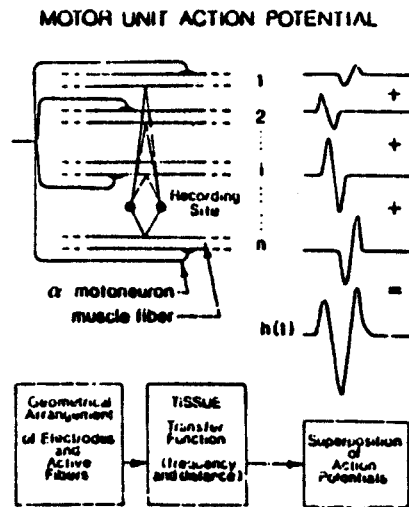


FIGURE 4.2: Schematic representation of the generation of the motor unit action potential

(de Luca 1979)

tant

2) the shape of the MUAP's remains constant

Manns et al (1977) reported a change in the firing frequency (the reciprocal of IPI) toward low frequencies, as a function of the contracting time, during a constant-force isometric contraction. Many other investigators reported a change in firing rate during an isometric contraction. This goes against the first assumption. However, it is very difficult to record only one MUAPT such that it is distinguishable. The myoelectric signal recorded using electrodes is mostly composed of several MUAPT's. Consequently, the individual firing rates  $\lambda_i(t)$  cannot be measured. To overcome this barrier, de Luca (1968) (reported by de Luca 1975) introduced the concept of the generalized firing rate  $\lambda(t)$ . It is defined as the mean value of the firing rates of the MUAPT's detected during a contraction. This value represents the constant firing rate of one MUAPT. The IPI's between two adjacent MUAP's in the same MUAPT have a tendency to be statistically independent (de Luca 1975), but this independence of adjacent pulses is not as strong as that between every other pulse in the same train.

$$\lambda(t) = \left[ \int_{-\infty}^{\infty} p_x(x,t) dx \right]^{-1} \quad (4.2)$$

where  $x$  represents the inter-pulse interval, and  $p_x(x,t)$ , the probability distribution function fitted from a IPI histogram (de Luca 1979).

The second assumption can be fulfilled if the following

conditions are respected:

- 1) the geometric relationship between the electrodes and the active muscle fibres remains constant
- 2) the properties of the recording electrodes do not change
- 3) there are no significant biochemical changes in the muscle tissue because that could affect the muscle fibre conduction velocity and the muscle tissue filtering properties.

The first two conditions can be verified for short recording time. The third condition cannot be verified but one can suppose that such biochemical changes occur in muscle and neuromuscular junction diseases.

It would be extremely difficult to give a unique mathematical description of the MUAP because there are many possible shapes. Thus, to uniform the shape, it is convenient, from a mathematical point of view, to decompose the MUAPT into a sequence of Dirac delta impulses  $\delta(t-t_{ik})$  (Fig. 4.3) which pass through a linear system whose impulse response is  $h_1(t)$ . The expression  $t_{ik}$  represents the time location of the impulse and the subscript  $i$  represents the  $i^{\text{th}}$  MUAPT. The resultant MUAP can be expressed as:

$$h_1(t-t_k) = \int_0^{\infty} h_1(t-u) \delta(u-t_{ik}) du \quad (4.3)$$

The motor unit is a physical system  $h(t-u) = 0, t < u$  (i.e. it does not respond before an input pulse is applied at the NMJ). The variable  $t_k$  can be expressed as:  $t_k = \sum_{l=1}^k x_l$  for  $k, l = 1,$

2, ..., n where x expresses the IPI. Finally the MUAPT, represented by the summation of the MUAP's, can be expressed as:

$$u_i(t) = \sum_{k=1}^n h_i(t-t_k) \quad (4.4)$$

where n represents the total amount of IPI's in the MUAPT. The description of the distribution of x is far beyond the purpose of this chapter. A more complete treatment is given by de Luca (1975).

Now that the two time dependent elements characterizing the MUAPT are known: (a)  $\lambda(t)$  and (b)  $h(t)$ , the expressions for the two most commonly used parameters of the ME signal (at the MUAPT level), i.e., the mean rectified value and the root-mean-squared value can be given.

Mean rectified value:

$$E[|u_i(t)|] = \int_0^{\infty} \lambda_i(\hat{t}) |h_i(t-\hat{t})| d\hat{t} \quad (4.5)$$

Root-mean-squared value:

$$(MS[u_i(t)])^{\frac{1}{2}} = \left( \int_0^{\infty} \lambda_i(\hat{t}) h_i^2(t-\hat{t}) d\hat{t} \right)^{\frac{1}{2}} \quad (4.6)$$

For the convolution expressions such as those in the above equations, the MUAP,  $h_i(t)$ , can be conveniently represented by a Dirac delta impulse,  $\delta_i(t)$ , multiplied by a constant that is equal to the area of the MUAP. From this approximation, the above expressions are greatly simplified to:

$$E[ |u_i(t)| ] \cong \lambda_i(t) \underline{|h_i(t)|} \quad (4.7)$$

$$MS[ u_i(t) ] \cong \lambda_i(t) \underline{h_i^2(t)} \quad (4.8)$$

where  $\underline{|h_i(t)|} = \int_0^{\infty} |h_i(t)| dt$  and  $\underline{h_i^2(t)} = \int_0^{\infty} h_i^2(t) dt$ .

This approximation introduces an error less than 0.001% (de Luca 1975) (Fig. 4.4).

#### 4.3.4 The ME signal

The ME signal  $m(t, F)$  (Fig. 4.5), for a constant force isometric contraction  $F$ , is modelled as a linear, spatial and temporal summation of all the MUAPT's detected by the electrode. The signal  $m_p(t, F)$  is not observable. When the signal is detected, an electrical noise  $n(t)$  is introduced, and the filtering properties of the recording electrode  $r(t)$  and possibly other instrumentation affecting  $m_p(t, F)$  are also introduced. The resulting signal,  $m(t, F)$ , is the observable ME signal. The derivation of the following expressions assumes that: (a) the noise,  $n(t)$ , is negligible, and (b) the effect of the recording electrodes and instrumentation remain constant with time ( $m(t, F) = m_p(t, F)$ ) (Stulen 1978). These considerations can be realized with proper experimental procedures.

The ME signal can be expressed as:

$$m(t) = \sum_{i=1}^S u_i(t) \quad (4.9)$$

The subscript  $F$  was removed because it only indicates the for-

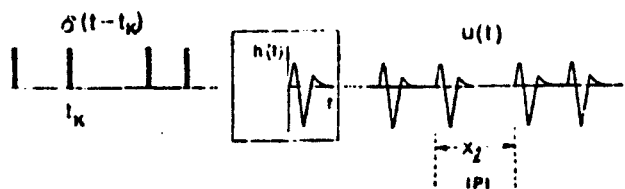


FIGURE 4.3: Schematic model for the MUAPT

(de Luca 1979)

TERM	DIAGRAM	EXPRESSION
a) GENERALIZED FIRING RATE OF A TYPICAL MOTOR UNIT		$(f(t)) = \frac{1}{\tau} \text{rect}(t)$
b) MOTOR UNIT ACTION POTENTIAL		$h(t)$
c) AREA UNDER THE RECTIFIED MOTOR UNIT ACTION POTENTIAL		$m_1(t) = \int_0^t h_1(\tau) d\tau$
d) AREA UNDER THE SQUARE OF A MOTOR UNIT ACTION POTENTIAL		$m_2(t) = \int_0^t h_1^2(\tau) d\tau$

FIGURE 4.4: Explanation of some of the terms in the expressions in the text.

(de Luca 1979)

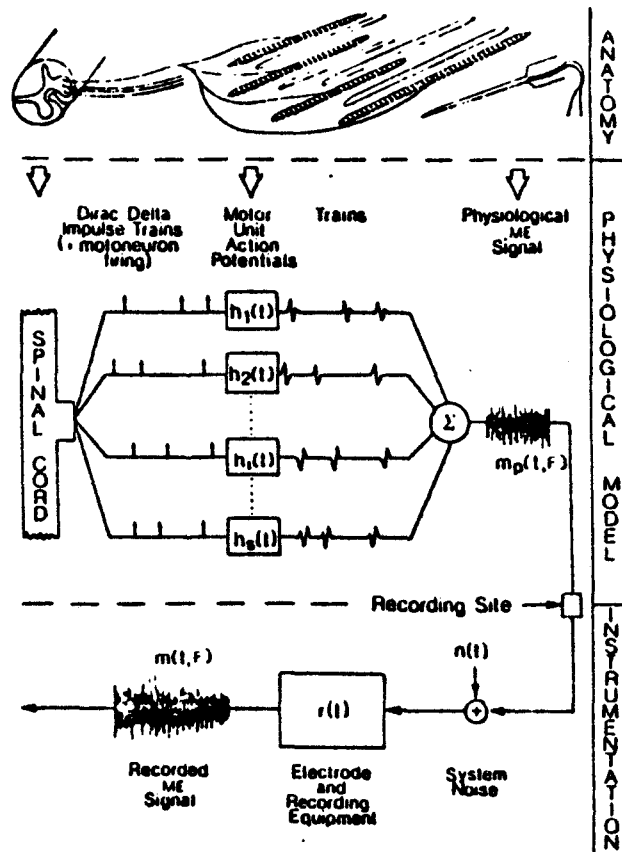


FIGURE 4.5: Schematic representation of the model for the generation of the ME signal.



ce at which the isometric contraction was performed and therefore, adds nothing to the analysis.

As demonstrated in Appendix A, the correlation function is used to defined the main parameters of the ME signal ( Fig. 4.6).

Mean rectified value:

$$E[|m(t)|] = \lambda(t) \sum_{i=1}^s \underline{|h_i(t)|} + J(t) \quad (4.10)$$

where  $\underline{|h_i(t)|} = \int_0^{\infty} |h_i(t)| dt$ , and where  $J(t)$  is a non positive term which represents the cancellation of MUAP's superimposed with a  $180^\circ$  phase shift.

Mean integrated rectified value:

$$E\left[\int_0^T |m(t)| dt\right] = \int_0^T E[|m(t)|] dt \quad (4.11)$$

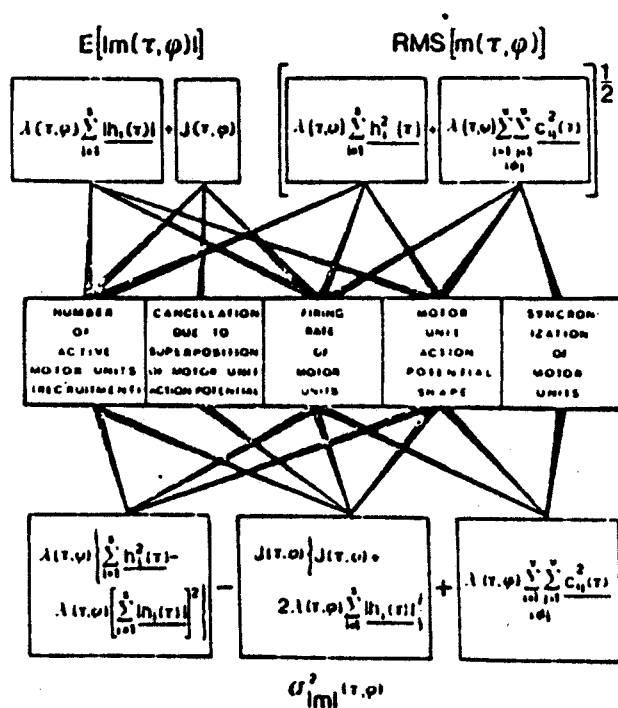
Root-mean-squared value:

$$\text{rms}[m(t)] = \lambda(t)^{\frac{1}{2}} \left( \sum_{i=1}^s \underline{h_i^2(t)} + \sum_{i=1}^v \sum_{j=1}^v \underline{c_{ij}^2(t)} \right)^{\frac{1}{2}} \quad (4.12)$$

where  $\underline{h_i^2(t)} = \int_0^{\infty} h_i^2(t) dt$ , and where the second term within the parenthesis represents the synchronization of the MUAP's,  $v < s$ . Furthermore,  $\underline{c_{ij}^2(t)} = \int_0^{\infty} h_i(t+T_{ij}) h_j(t) dt$ . The details of these expressions are presented in Appendix A.

This general model, including the mathematical expressions of its main parameters, defines the ME signal during a constant-force isometric contraction. The basic function is the autocorrelation function of the ME signal (Appendix A). Many as-

## MEAN RECTIFIED AND RMS VALUES



## VARIANCE OF THE RECTIFIED SIGNAL

FIGURE 4.6: Theoretical expressions for parameters of the ME signal and their relation to physiological correlates of a contracting muscle.

assumptions have been used to define this model. Meanwhile, the parameters, presented in this model, are dependent on: (a) the firing rate,  $\lambda(t)$ , of the motor units, (b) the number of motor unit action potential trains (MUAPT's) comprising the ME signal, (c) the shape of the MUAP, and (d) the number of synchronized MUAPT's.

The approach used thus far has been directed at relating the measurable parameters of the ME signal to the behavior of the individual MUAPT's. However, when the recording electrodes detect a large number of MUAPT's (greater than 15 (de Luca 1979)), such as would typically be the case for surface electrodes, the law of large numbers can be involved to consider a simpler, more limited approach. In such cases, the ME signal can be effectively represented as a signal with a Gaussian distributed amplitude. By using this approach, it has been demonstrated that the mean rectified value of the ME signal can be expressed as:

$$E[|m(t)|] = \sqrt{2/\pi} \sigma(t) \quad (\text{de Luca 1979}) \quad (4.13)$$

where  $\sigma(t)$  is the standard deviation of the amplitude distribution.

#### 4.4 The Force-EMG relationship

Considerable confusion seems to exist regarding the mathematical relationship between the IEMG and the force produced

in human muscle contraction. Theoretical considerations suggest that the EMG recordings from surface electrodes represent a very complex summation of varying numbers of motor unit action potentials which vary both in size and in wave form. Using certain simplifying assumptions such as: (a) the adoption of an arbitrary biphasic, symmetrical impulse to represent the muscle fibre action potential, (b) no cancellation, and (c) no synchronization, it has been suggested that the most likely relationship would be one in which the IEMG (either rms or average values) would vary as the square root of the force (Moore 1967). Actual observations of the relationships have most often led to report a linear relationship (Hudgins 1979, Hof 1977) but some investigators have reported curvilinear relationships with IEMG varying in positively accelerated fashion as force of contraction increases (Komi 1975, Zuniga 1969). Furthermore, among the curvilinear relationships, a few have been decomposed into two parts: (a) a linear relationship in the submaximal force range, and (b) a non-linear relationship in the force range closer to the maximal voluntary contraction (Kuroda 1970, Zuniga 1969).

The Force-EMG relationship is not unique and varies from muscle to muscle. Workers who studied the Force-EMG relationship in situations in which only one muscle could be involved, as Lawrence (1983), found a linear relationship. When, on the other hand, the muscle under study is one of a group of synergists, often a considerable controversy about this linearity exists in literature (Kuroda 1970, Komi 1976, Lawrence 1983). Even the biceps brachii, a muscle that is very often used in

this kind of study and for which rather different Force-EMG relationships are reported, clearly falls in this category as it is a synergist of the brachialis and the brachioradialis muscles for elbow flexion (Zuniga 1969).

All this controversy leads one to believe that the Force-EMG relationship is determined by the muscle under investigation. A variety of phenomena that may contribute to the muscle-dependent difference in the Force-EMG relationship can be identified. Some of them are:

- 1) motor unit recruitment and firing rate properties
- 2) relative amounts and location of slow-twitch and fast-twitch muscle fibres within the muscle
- 3) cross talk from ME signals of adjacent muscles
- 4) agonist-antagonist muscle interaction
- 5) viscoelastic properties of the muscles.

The viscoelastic properties of the muscles, although they may be an influential factor, remain difficult to verify. The agonist-antagonist muscle interaction is important during isometric contractions where the joints have to be stabilized. The net force produced is usually assumed to be linear with respect to the agonist muscle of interest. However, this relationship may be modified by numerous factors such as joint angle, limb position, and pain sensation. The electrical cross talk from adjacent muscles is unquestionably a possible factor and cannot be eliminated. This factor is of prime importance when one uses bipolar surface electrodes because they detect MUAPT fields from a large volume.

The relative amounts and location of slow-twitch and fast-

twitch muscle fibres within a muscle is very important. The fast-twitch fibres have a larger diameter than the slow-twitch fibres (Lawrence 1983). Since the amplitude of the ME signal is dependent on the diameter of the muscle fibre (de Luca 1979), a different ME signal amplitude will be recorded whether slow-twitch or fast-twitch fibres are used during the contractions. The larger motor units (containing the larger diameter fast-twitch fibres) are preferentially recruited at high force levels according to the "size principle" (Milner-Brown 1973b). Therefore, the relative location of the fast-twitch fibres within the muscle and with respect to the recording electrodes determines how the electrical signal from these motor units affects the surface ME signal.

The motor unit recruitment and firing rate properties must not be neglected. Larger muscle fibres have higher thresholds of excitation (Milner-Brown 1973b). They are recruited at higher force levels. Moreover, recruitment has much less effect at high force levels than the firing rate (Kurcda 1970). It has been suggested that the recruitment of more motor units should cause a linear increase of force, since the number of the activated fibers is directly related to the force (Moore 1967). This suggests that each muscle fibre in a muscle exerts nearly the same amount of force at any given frequency of stimulation. Consequently this suggests that the non-linearity in the Force-EMG relationship is due to the firing frequency alone since it gives a saturation of the output force with increasing frequency. The controversy in the literature shows clearly that each study is unique and cannot be reproduced. The electrode arrange-

ment is a crucial factor which affects the Force-EMG relationship tremendously. Once the electrodes are removed, it is quasi-impossible to put them back exactly the way they were. The Force-EMG relationship can vary from linear to highly non-linear with different slopes, and no evidence has been presented that any one relationship is most correct.

## CHAPTER V

### MATERIAL AND PROTOCOL

#### 5.1 Introduction

Surface electromyographic (EMG) signals, mass lifted with the head, and total inspiratory pressure generated by the SCM muscle were recorded at various levels of voluntary isometric contraction and at different lung volumes.

This chapter serves as a description of the experimental procedure including the experimental instrumentation, protocol, data collection and data management.

#### 5.2 Subjects

Four normal male volunteers (ages 24 to 25 years) were studied. See Table 5.1 for a full description of the subjects. All volunteers were aware that the experimental procedure was not invasive, and only surface electrodes were to be in contact with the skin.

#### 5.3 Instrumentation



SUBJECT	SEX	AGE	HEIGHT cm	BODY MASS Kg	HEAD MASS Kg	MAX. MASS LIFETD(Kg)	IC Liters	VC Liters
LT	M	24	185.0	74.8	4.6	12.6	4.13	5.28
PM	M	24	174.0	77.0	5.3	17.1	3.53	4.03
AS	M	24	170.0	73.0	4.6	23.6	3.25	3.75
CW	M	25	166.5	54.2	4.6	9.6	2.55	3.25

TABLE 5.1: SUBJECT DESCRIPTION

The instrumentation used during the experiment can be divided into three main sections: (a) the instrumentation used to record the EMG signals, (b) the instrumentation used to record head lift, and (c) the instrumentation used to record mouth pressure and lung volume.

The block diagram of Figure 5.1 shows the total instrumentation used to record EMG. The input transducer was two Beckman Ag-AgCl bipolar surface electrodes. They were located on the belly of the SCM muscle right in the middle of the neck. They were arranged in a parallel alignment with respect to the fibres. The diameter of the electrodes was 4mm, and the distance from center to center was 14mm. The skin was rubbed with alcohol and a chloride paste was used in order to reduce the total electrode impedance. The wires of the pair of electrodes were twisted with each other to reduce the 60Hz magnetic coupling.

Ag-AgCl electrodes have interesting characteristics: (a) low impedance, (b) low noise, and (c) non-polarizable, i.e., reversible. However, they have two main drawbacks: (a) they are current limited (1nA), and (b) they produce a steady potential resulting in a dc offset that must be removed during calibration, or through AC coupling.

The choice of an electrode is very important. There are five main types of electrodes used by investigators:

- 1) Monopolar needle
- 2) Coaxial needle
- 3) Bipolar needle
- 4) Bipolar fine wire

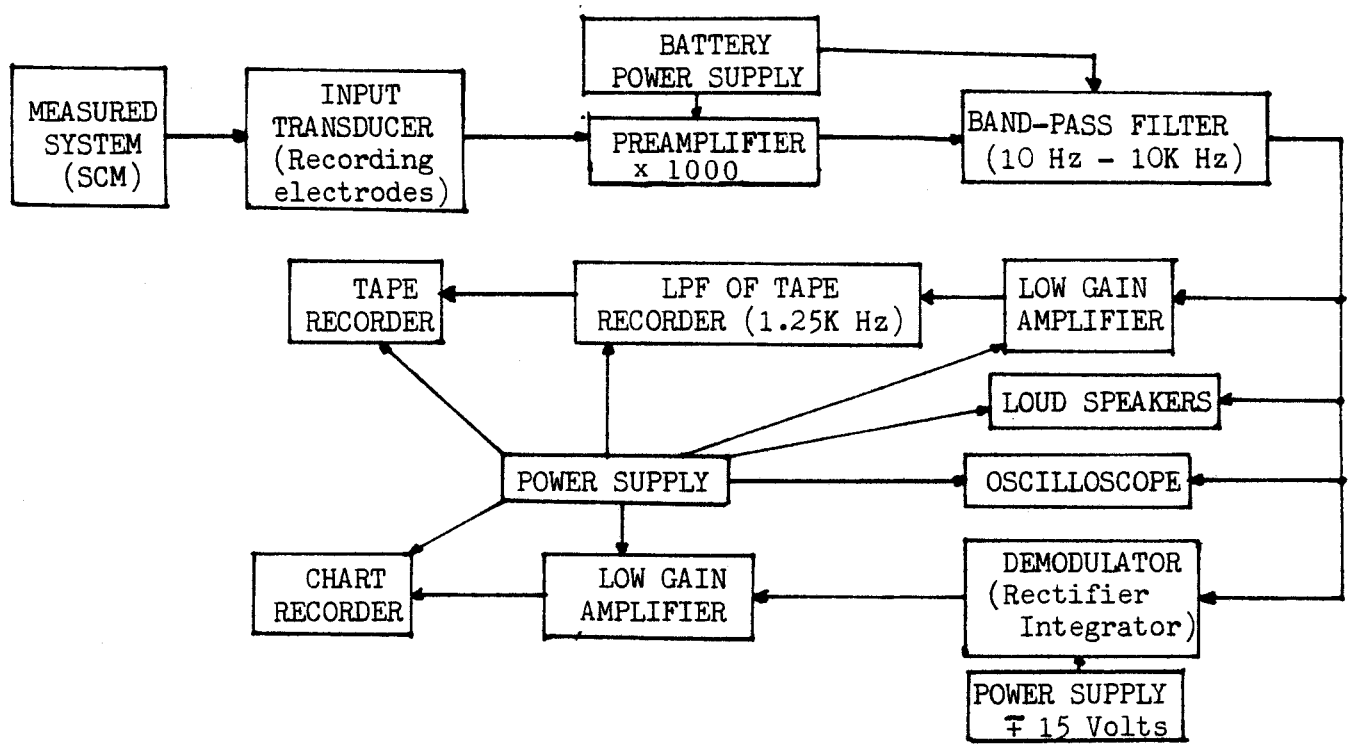


FIGURE 5.1 : INSTRUMENTATION USED TO RECORD EMG

### 5) Bipolar surface

A detailed discussion of these electrodes is beyond the objectives of this chapter. Since bipolar electrodes were used during the present experiment, it is necessary to mention a few characteristics defining their behavior.

There are many factors affecting the characteristics of the recorded signals. Some of them are:

- a) the distance from the muscle fibres to the recording site
- b) the size of the electrodes used
- c) the spacing between the electrodes
- d) the geometrical arrangement of the muscle fibres with respect to the recording orientation.
- e) the electrode-external medium interface transfer function or filtering effects.

When the distance between the muscle fibres and the recording site increases, the amplitude of the recorded signals decreases. This phenomenon is due to the reduction of the electrical field strengths at the recording site. A second effect of the distance between fibres and electrodes is that of low pass filtering. The impedance of the external medium is such that high frequency signals are more severely attenuated than low frequency signals. As the distance increases, the bandwidth of the low pass filter decreases.

The size of the electrodes will determine the electrode impedance and its effective field pick up area. Larger electrodes have smaller impedance. The net field the electrode detects is then the spatial integration of the fields adjacent to it, over its whole area. Furthermore, spatial inte-

gration reduces the high frequency components of travelling field waves.

The effect of the spacing between the electrodes is that of differentiating. As the spacing decreases, the recorded signal becomes closer and closer to being the derivative of the travelling wave. Reducing spacing increases recorded signal bandwidth. Generally, reduced spacing causes reduced signal amplitude. This effect is due to the potential difference between the electrodes. It is that potential difference that is amplified, and as the electrodes are moved closer together, the potential difference between electrodes generally decreases.

The geometrical arrangement of the muscle fibres with respect to the recording site determines, partially, the shape of the recorded signals. As soon as any change occurs, the recorded signals look totally different: (a) the spatial integration is different, (b) the distance between the fibres and the recording site is changed, a different bandwidth and a different signal amplitude are induced, (c) the direction of the field relative to the electrode orientation, etc.

The electrode-external interface is very important in determining the electrodes impedance per unit area and subsequently its filtering effects on the recorded signal. The type of materials used for the electrode and the electrolyte interfacing the tissue with the electrode determines the impedance per unit area of the electrode-external medium interface.

In order to summarize, the size of the surface electrodes determines the amount of spatial averaging done and thus

affects the bandwidth of the recorded signals. Spacing of the electrodes determines the amount of differentiating of the detected fields, the volume of muscle mass recorded from, and the bandwidth of the recorded signal. Since distances between the surface electrodes and the muscle generator are relatively large, tissue filtering effects are significant and affect the bandwidth of the signals recorded.

The other instruments also have their own characteristics. It would be superfluous to describe them in detail but it is essential to mention them. Table 5.2 summarizes some of their important characteristics.

The instrumentation used to record respiratory function, i.e., mouth pressure and lung volume is summarized in Figure 5.2. The pneumotach is connected to the flow transducer. Their main characteristics are summarized in Table 5.2.

Figure 5.3 shows the block diagram of the instrumentation used to study the head lifting manoeuvre. The most important device, the head lift meter, has not been presented yet. The purpose of the head lift meter was to provide a convenient method of measuring the SCM function through the amount of head lift in subjects in the supine position. As indicated in the block diagram of Figure 5.4, the input to such an instrument was the mass lifted by the head and the output was a reading on the calibrated scale of a simple meter. To be useful, the instrument had to be simple, easy to use, and had to require a minimum of patient movement. For ease of transportation and use, the instrument had to be hand held and battery powered.

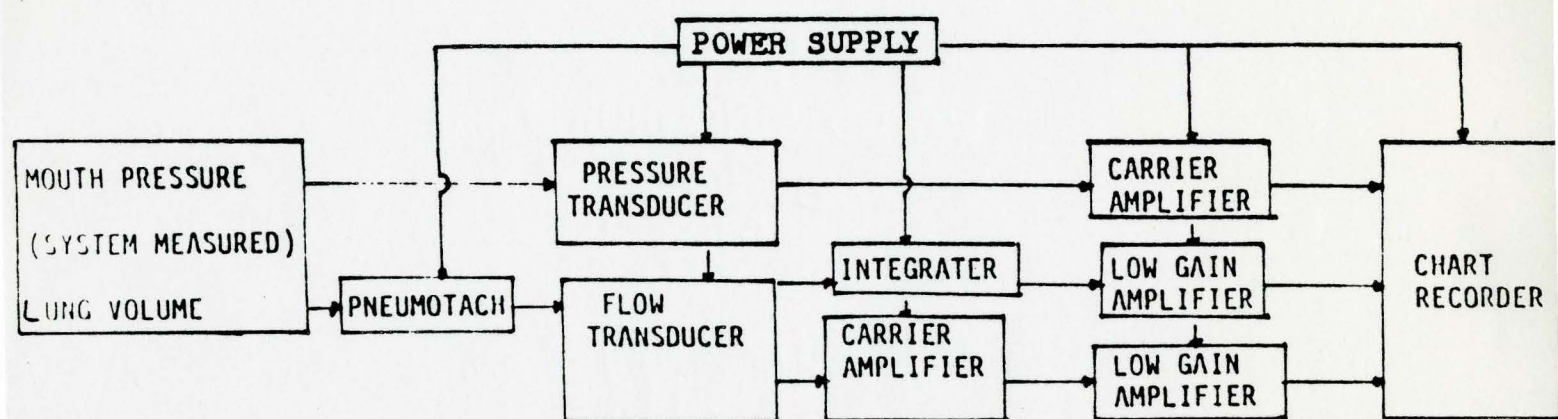


FIGURE 5.2 : INSTRUMENTATION USED TO RECORD RESPIRATORY FUNCTION

TABLE 5.2

	8-Channel chart recorder	Low gain amplifier	Carrier amplifier	Pressure transducer	Flow transducer
Model	HP 7758 A	SANBORN 8081A	SANBORN 8085A	HP 267 B	HP 47304 A
$R_{input}$	50 K ohms	500 K ohms	10 K ohms		
$R_{output}$		50 ohms	10 ohms		
CMRR		>48 dB			
Linearity range				-100 mmHg to +400 mmHg	$\pm 2.25\%$ of reading
Hysteresis				<1.5% Full Scale	
Output voltage				40 $\mu$ V/Volt excitation/mmHg	
Excitation freq. range			440Hz to 4800Hz (stan- dard value 2400Hz)		
Excitation voltage			4.5V to 5V r.m.s. when driven with 10V r.m.s.		
3dB point			200Hz		
gain stability					$\pm 0.05\%$ of rea- ding per $^{\circ}$ C
Output noise					5mV r.m.s. Max. at $\pm 4.0$ V output level



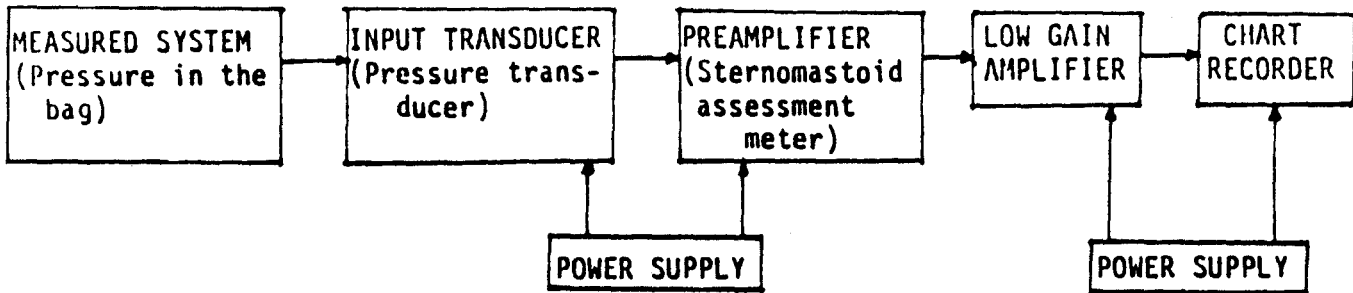


FIGURE 5.3 : INSTRUMENTATION USED TO RECORD HEAD LIFT

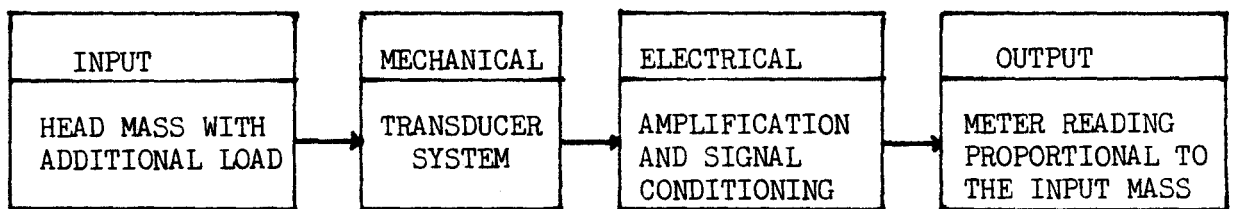


FIGURE 5.4: INSTRUMENT'S GENERAL REQUIREMENTS

The function of the mechanical system was to couple the subject's head mass to a force transducer. To minimize disturbance of the subject, a design consisting of a fluid-filled bag and a pressure transducer was developed (Figure 5.5). As shown in Figure 5.6, the fluid-filled bag can be slipped under the head with minimal effort required from the subject and from the investigator. The weight of the head and additional load causes an increase in fluid pressure which changes the state of the pressure transducer. The resulting electrical signal was used as the input for the electronic circuitry.

A Bell and Howell resistive bridge pressure transducer (type 4-327-0109, No. 3263) was used in the construction of the prototype. From tests done on the pressure transducer, it was found that with 6 volts dc excitation of the bridge, the output voltage (mV) was linear with respect to the transducer pressure in the expected range of operation;  $Y \text{ (mV)} = 1.200 + 0.038 P \text{ (mm. Hg)}$ .

The circuit developed for processing the transducer bridge voltage is very simple. The essential components of the circuit are shown in the block diagram of Figure 5.7. The "full scale" output voltage was chosen to be 5 volts. This consequently required a total amplification of about 60 dB. The design of the circuit is shown in Figure 5.8.

The head lift meter was found to perform well. Good results were obtained when it was tested. The meter was consequently used on a regular basis, during the whole experiment.

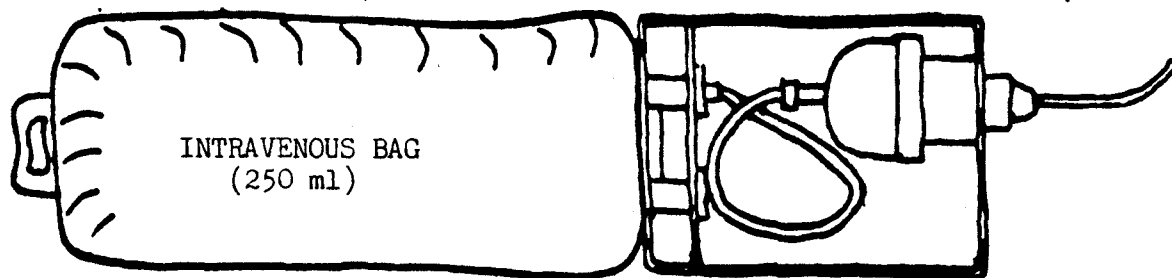


FIGURE 5.5: CONSTRUCTION OF MECHANICAL SYSTEM OF PROTOTYPE

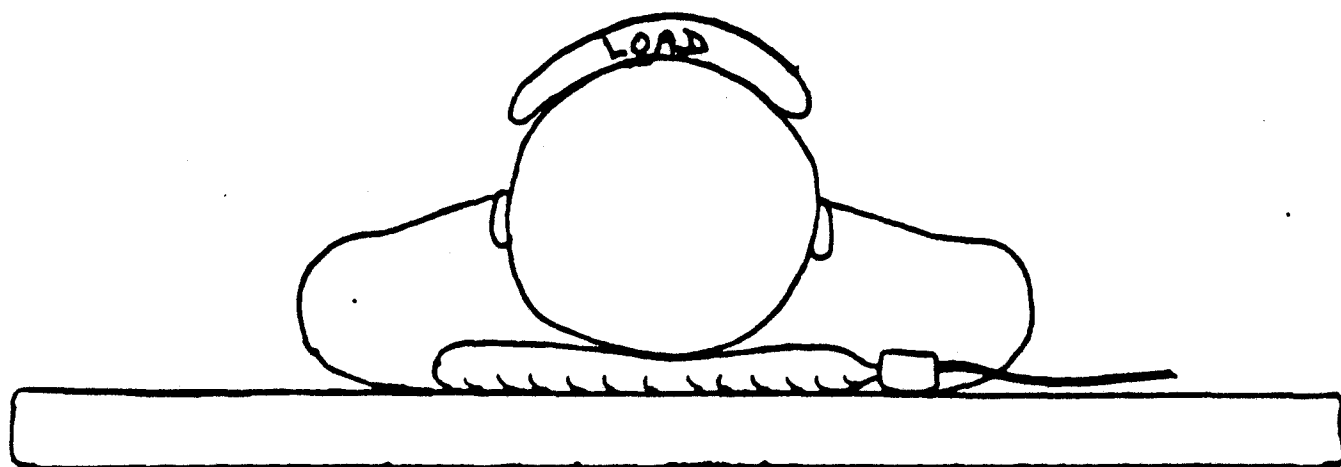


FIGURE 5.6: THE MECHANICAL SYSTEM

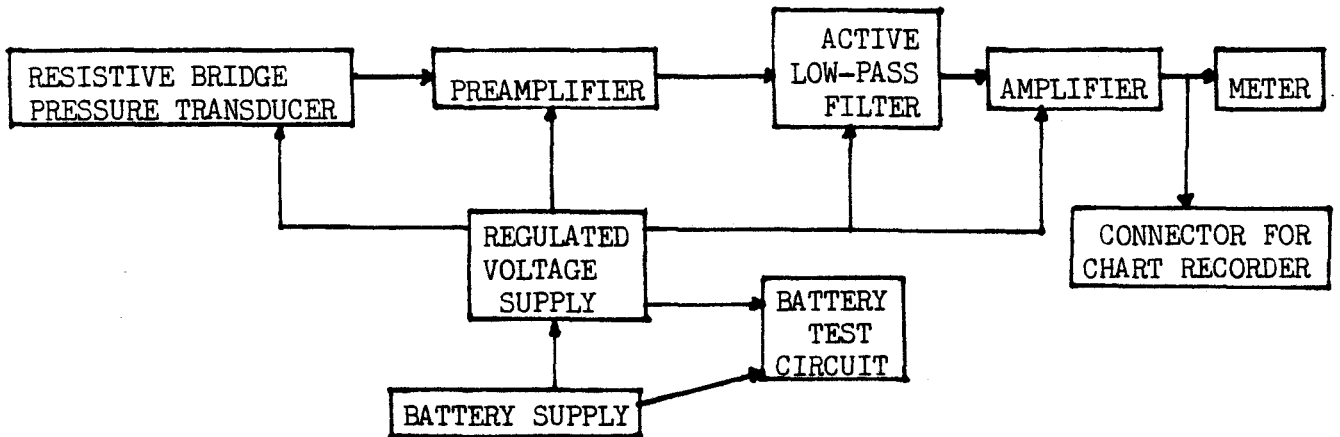


FIGURE 5.7: BLOCK DIAGRAM OF THE ELECTRICAL SYSTEM

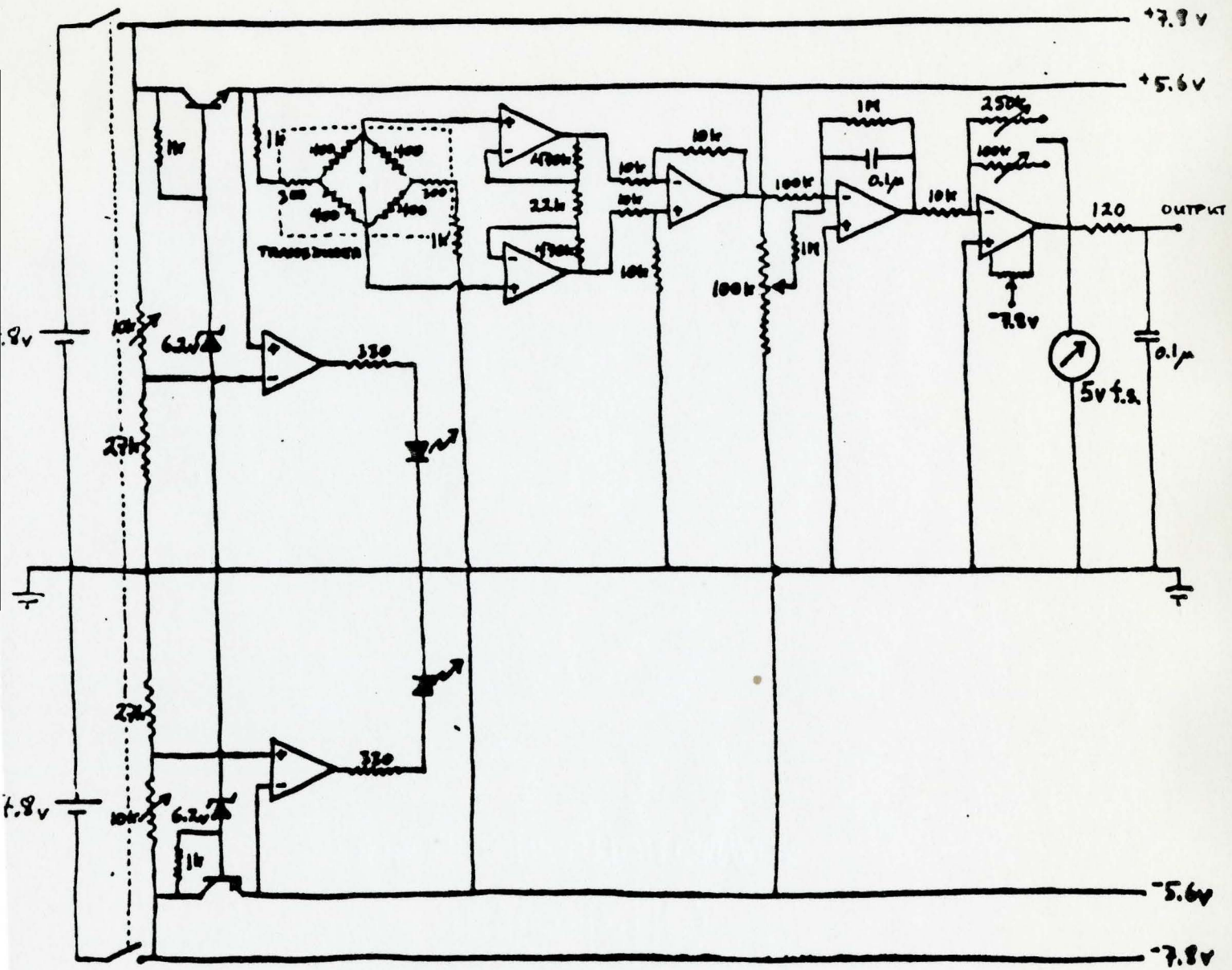


FIGURE 5.8: CIRCUIT DESIGN

5.4

PROTOCOL

## A) PREPARATION

- 1) Arrival of the subject
- 2) Signing of the consent form
- 3) Personal data ( age, sex, height, weight, etc. )
- 4) Measurement of the head weight
- 5) Measurement of the maximum weight lifted by the neck muscles
- 6) Five minutes rest
- 7) Placement of the electrodes

- B) VC (x2) (VC = Vital Capacity)  
 IC (x2) (IC = Inspiratory Capacity)

## C) LIFTING OF THE HEAD

Every manoeuvre will be maintained 5 seconds .

- |                  |   |                     |             |
|------------------|---|---------------------|-------------|
| 1) Wmax (x2)     |   |                     | FRC         |
| 2) 85% Wmax (x2) |   | 3cm of head height  | FRC + 0.5 L |
| 3) 75% Wmax (x2) | X | 10cm of head height | X FRC + 1 L |
| 4) 65% Wmax (x2) |   |                     | FRC + 2 L   |
| 5) 50% Wmax (x2) |   |                     | TLC         |

## D) RESPIRATORY FUNCTION

I Relaxation manoeuvre (x2)

II Every manoeuvre will be maintained 5 seconds

- |                  |   |                     |             |
|------------------|---|---------------------|-------------|
| 1) MIPS (x2)     |   |                     | FRC         |
| 2) 85% MIPS (x2) |   | 3cm of head height  | FRC + 0.5L  |
| 3) 75% MIPS (x2) | X | 10cm of head height | X FRC + 1 L |
| 4) 65% MIPS (x2) |   |                     | FRC + 2 L   |
| 5) 50% MIPS (x2) |   |                     | TLC         |

The expression FRC stands for Functional Residual Capacity and is defined as the volume of air remaining in the lungs after a passive expiration. When the subject performs a maximum inspiration, i.e., until no more air is able to enter in the lungs, then the volume of air in the lungs is called Total Lung Capacity or TLC. When the subject performs a forced, active expiration until he is not able to push any more air out of the lungs, the remaining lung volume is called the Residual Volume or RV. The difference between TLC and FRC, i.e.,  $TLC - FRC$ , is called Inspiratory Capacity or IC. The difference between TLC and RV is called Vital Capacity or VC,  $TLC - RV = VC$ . The expression  $w_{max}$  indicates the maximum weight lifted, and the expression MIPS indicates Maximum Inspiratory Pressure performed under Static conditions, i.e., with blocked airways.

The protocol was followed exactly as listed. The positions of the head were 3cm and 10cm above the bed. The 3cm is the thickness of the fluid-filled bag on which the subject's head was resting during the experiment. The 10cm was arbitrarily chosen to reduce the length of the SCM muscle. This position was obtained by adding many boards under the bag. During the experiment, the subject was lying down on a hard surface in order to provide stability of the body, especially during the head lift manoeuvre.

In order to avoid muscle fatigue, a resting period of twenty minutes was given to the subject between the 3cm and the 10cm manoeuvres, for both head lift manoeuvres, section C, and respiratory manoeuvres (RM), section D. During that period of time, the subjects were allowed either to sit or get up and walk.

Furthermore, a resting period, varying between 1.5 and 2 minutes was given between each and every manoeuvre.

Every manoeuvre was performed twice and was performed the following way. The subjects took two or three big breaths, went to FRC during 1 sec., took a slow inspiration up to the desired lung volume, and then performed the HL manoeuvre with their glottis closed, or the RM manoeuvre with the glottis open. After the manoeuvre was performed, a resting period of 1.5 to 2min. was allowed and the subjects were breathing freely. After the rest, the same manoeuvre was performed a second time, using the same method. Between each set of HL manoeuvre (eg.  $w_{max}$  (x2) at 3cm above the bed and at FRC, for head lift (part C.1 in the protocol)), all subjects asked, and were allowed to move their head and rub their neck to remove the pain and the discomfort caused by the manoeuvre. Between each set of RM manoeuvres (eg. part D.1 in the protocol), the subjects were allowed to remove the mouth piece from their mouth and move their head. During those short resting periods, the subjects were not allowed to sit or get up.

Because the experiment was long and demanding for the subjects, it had to be done in two sessions. The first session contained parts A, B, and C, while the second session contained the remaining. The whole experiment lasted six hours; the first session lasted four hours and the second, two hours.

During the experiment, there was no visual feedback to the subject because of the type of experiment. Meanwhile, the investigator took a careful and particular attention in guiding the subjects for performing the submaximal manoeuvres. This



way, variability was reduced to the least that could possibly be obtained. One example of the output obtained on the chart recorder, for both HL and RM manoeuvres, at FRC, is shown in Figure 5.9.

## 5.5 Data manipulation

### 5.5.1 Mean values

As mentioned before, every manoeuvre was performed twice. The mean and the standard deviation of the mean were found from the two recorded values for the same manoeuvre. The mean and the standard deviation of the mean of each manoeuvre are listed in Appendix C as VALUE and SD. These tabulated values represent the mean values of Head Lift, Head Lift EMG, Pmusc, and Pmusc EMG.

The normalized values, listed in Appendix C, were calculated from these mean values. Furthermore, the modelling, using the Least Squares method, was done on the normalized mean values.

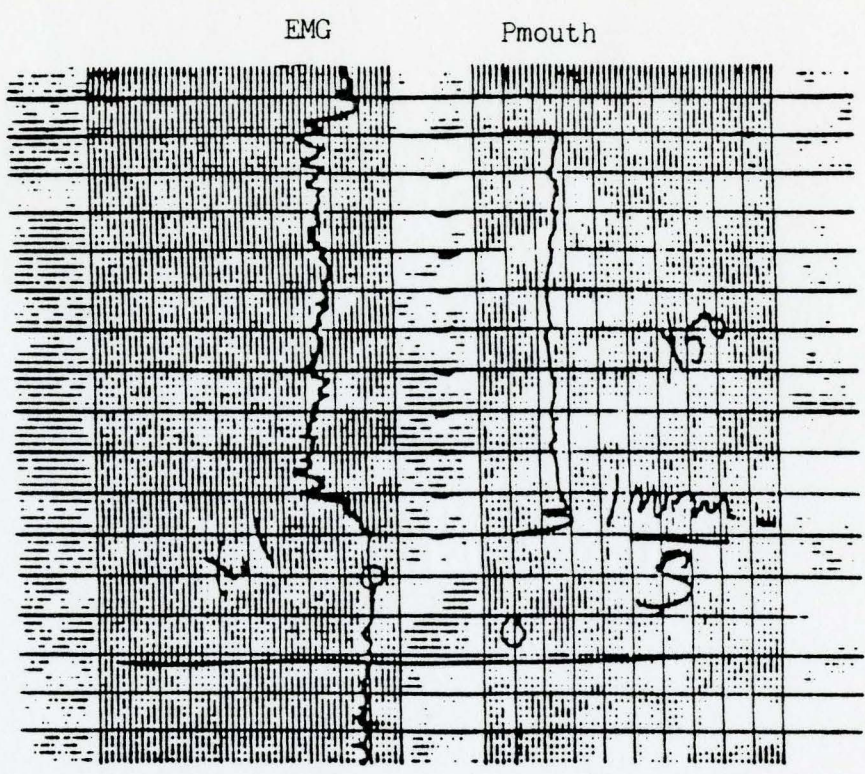
### 5.5.2 Normalization

The analysis of the results of this experiment required modelling and simplifying such that simple relationships could be found to be representative of the four normal subjects studied. Since the purpose of the study was to find a relationship between head lift and respiratory function, the SCM EMG was used as the common factor in the analysis.

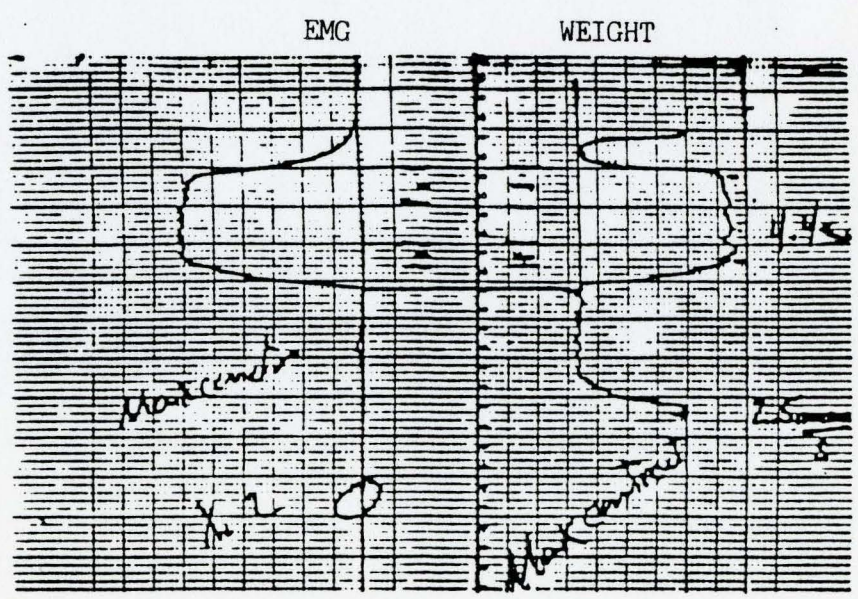
The first step was to normalize the data. Table 5.3 summarizes the normalization process. Mass lifted was normalized with the head mass value of every subject. The corresponding EMG

FIGURE 5.9: OUTPUT OF THE CHART RECORDER

MOUTH PRESSURE VS STERNOCLEIDOMASTOID EMG



WEIGHT LIFTED VS STERNOCLEIDOMASTOID EMG



of the mass lifted was normalized with the corresponding EMG of the head mass. Consequently, the scaling of the y axis was in multiples of the head mass and the scaling of the x axis was in multiples of the head mass EMG.

For respiratory manoeuvres, muscle pressure had to be found. It is defined as:

$$P_{\text{musc}} = P_{\text{mouth}} + P \text{ (at a specific lung volume)} \quad (5.1)$$

The second term,  $P$ , was found by asking the subject to execute a relaxation manoeuvre. The subject took a big inspiration up to TLC and when the airways were blocked, the subject relaxed completely. A positive pressure was noted in the airways. Step by step, the investigator unblocked the airways and positive pressure at different lung volumes were recorded. From these values, the pressure-volume curve was drawn. The normalization of  $P_{\text{musc}}$  was done by using the maximum value  $P_{\text{musc}}(\text{max})$  and the head mass EMG was again used to normalize the  $P_{\text{musc}}$  EMG values.

The above normalization process was performed separately at both head heights, 3cm and 10cm. As shown in Table 5.3, the data at a head height of 3cm were normalized with the values of Head Mass, Head Mass EMG, and  $P_{\text{musc}}(\text{max})$  at 3cm, and the data at 10cm were normalized with the values of Head Mass, Head Mass EMG, and  $P_{\text{musc}}(\text{max})$  at 10cm. The values in Table 5.3 represent the mean values calculated from the two values recorded for each of these manoeuvres.

### 5.5.3 Modelling

The second step of the analysis was to model the nor-

	3cm above the bed for head height				10cm above the bed for head height			
	LT	PM	AS	CW	LT	PM	AS	CW
Head Mass (Kg)	4.6	5.3	4.6	4.6	4.6	5.3	4.6	4.6
Head Mass EMG (uV)	600.0 (1L)	140.0 (FRC)	512.0 (FRC)	355.6 (FRC)	640.0 (FRC)	271.7 (FRC)	520.7 (FRC)	625.2 (FRC)
Max. P <sub>musc.</sub> (cm H <sub>2</sub> O)	88.025 (1L)	125.6 (1L)	108.2 (1L)	89.1 (1L)	79.7 (2L)	132.5 (FRC)	140.5 (2L)	90.8 (0.5L)

TABLE 5.3: VALUES USED TO NORMALIZE THE SUBJECT'S DATA

The subscripts indicate the lung volume where the value has been taken

malized relationships. After studying the curves, it was found that the linear relationship represented an appropriate approximation. Other relationships were tried: second order and third order curvilinear, and exponential relationships. The use of a more complex model did not result in a substantial increase in the coefficient of determination, and thus to simplify the interpretation, we stayed with the linear model. The modelling process was performed by using the "Least Squares Principle". Appendix B-1 details the method, and a listing of the program is provided.

Once the regression line equations were found, a statistical test was done on the slope and intercept of many lines to see whether they were really coincident or parallel or had a common intercept. The technique used is an ANOVA technique, and it has nothing to do with the one-way or two-way ANOVA techniques one already knows. It is a specific technique used only for straight line testing. It uses a F-test. The technique employs tests based on variance ratios to determine whether or not significant differences exist among the means of several groups of observations, where each group follows a normal distribution. This analysis of variance technique determines the effect of one independent variable (lung volume) on two dependent variables (slope and intercept). Appendix B-2 details the method used to allow the pooling of the data, and also a listing of the program is provided.

## CHAPTER VI

### RESULTS

#### 6.1 Force levels

The subjects performed two different types of manoeuvre: head lift manoeuvre (HL), and respiratory manoeuvre (RM) which consisted of doing inspiratory pressures. These manoeuvres were performed at different lung volumes and at two specific head positions. MRE, mass lifted with the head (HL), and muscle pressure (P<sub>musc</sub>) were tabulated. P<sub>musc</sub> was defined as being the transthoracic pressure difference when the subject performed a static inspiratory pressure manoeuvre at a given lung volume above FRC.

The first step of the analysis was to see whether the manoeuvres were reproducible. Table 6.1 reveals that the second measurement (EMG-WT or EMG-P<sub>musc</sub>) is not significantly different than the first one, for the same manoeuvre. One may say that the measurements are reproducible. It also reveals, because of the low F-values, that the mean of the two measurements can be taken to represent the manoeuvre. Figure 6.1 shows an example of the closeness of the curves for the

SUBJECT	LUNG VOLUME	HL MANOEUVRE		RM MANOEUVRE	
		SLOPE	INTERCEPT	SLOPE	INTERCEPT
LT	FRC	.757	.507	.321	.700
	FRC+2L	.213	.101	.326	.017
PM	FRC	.031	.012	1.284	1.833
	FRC+2L	1.692	.557	19.455 *	11.919 *
AS	FRC	.269	.274	.424	.699
	FRC+2L	.002	.016	.089	.177
CW	FRC	.155	.046	.075	.095
	FRC+2L	5.648	4.118	1.128	.148

\* significant for  $p < 0.05$

TABLE 6.1: r<sup>2</sup>-Values Due to Lung Volume (FRC+2L)  
Affecting the Reproducibility of the  
Linear Force-MRE Relationship of a  
Manoeuvre



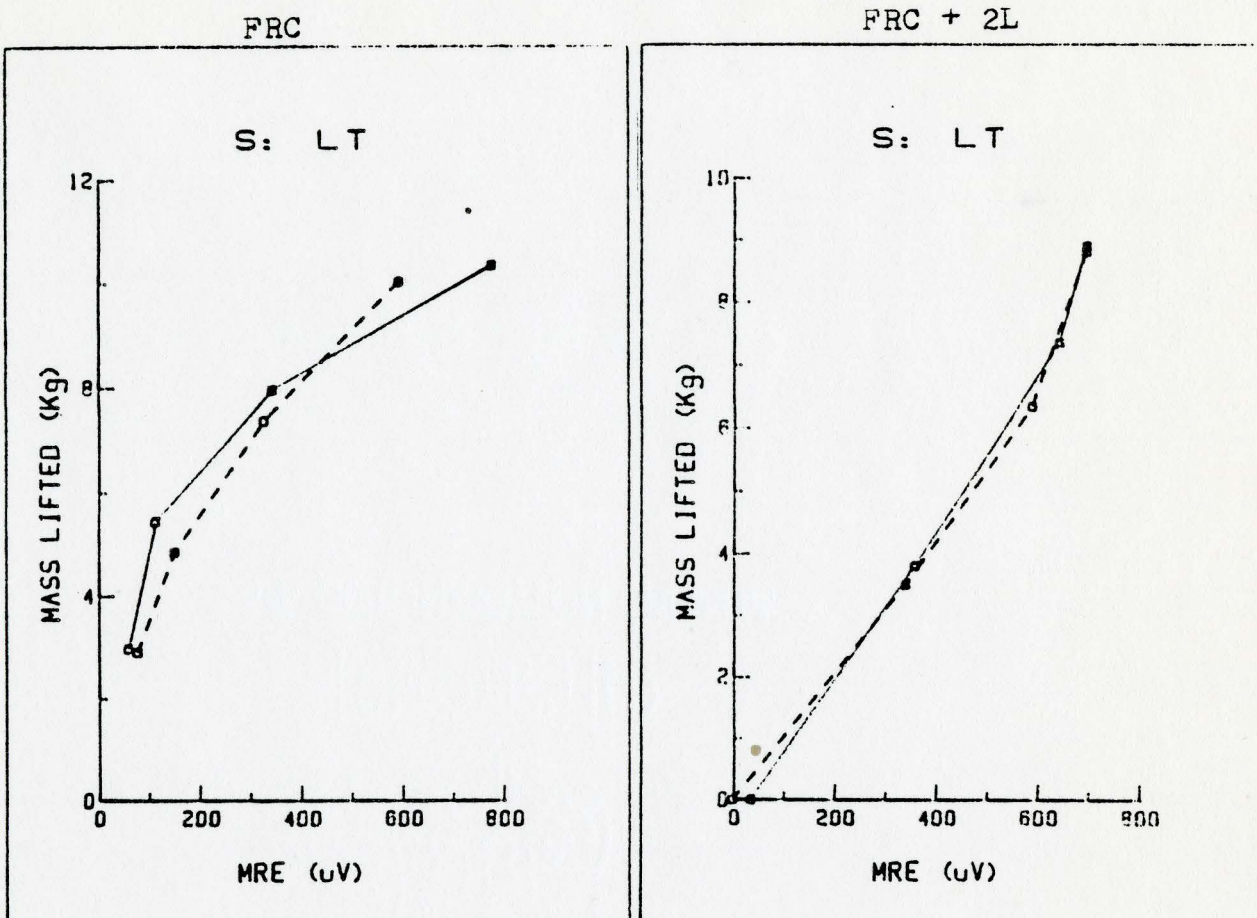


FIGURE 6.1 : Reproduction of the data for the Head Lift Manoeuvre



Head Lift manoeuvre. The data are presented in Appendix C (RE-PRODUCIBILITY). In addition, Table 6.1 reveals that breathing to a specific lung volume does not introduce more variability than the performance of the manoeuvre. The F-values are not significantly lower when the manoeuvres are performed at a lung volume of FRC + 2L than at FRC.

A careful examination of Tables 6.2 and 6.3 reveals:

- 1) no specific pattern in the variation of HL(max), Pmusc(max), and MRE(max) with increasing lung volume, from FRC to TLC, for every subject and head height
- 2) a decrease in HL(max), and an increase in Pmusc(max) with increasing lung volume over the range of tidal lung volume ( $V_t$ ) for both head heights. ( $V_t$  is defined as the amount of air inspired during normal breathing, at rest.)
- 3) no specific pattern in the variation of HL(max), Pmusc(max), and MRE(Pmusc(max)), but an increase in MRE(HL(max)) occurs with increasing head height for every subject and lung volume
- 4) for every subject, head height, and lung volume, MRE(HL(max)) is greater than MRE(Pmusc(max)).

## 6.2 Force-EMG relationship

After keeping the data that were believed to represent the action of only the Sternomastoid muscle, a linear relationship seems to exist between force (HL or Pmusc) and mean-rectified-

Subject	Lung Volume	3 cm above the bed		10 cm above the bed	
		HL Man. (kg)	Resp. Man. (cm H <sub>2</sub> O)	HL Man. (kg)	Resp. Man. (cm H <sub>2</sub> O)
LT	FRC	15.600	60.000	7.400	65.000
	FRC+0.5L	10.700	74.870	5.400	79.500
	FRC+1L	8.800	88.025	5.650	71.275
	FRC+2L	10.800	72.238	8.850	79.738
	TLC	10.700	31.750	10.900	31.750
PM	FRC	13.900	71.750	12.900	132.500
	FRC+0.5L	12.900	123.082	12.967	119.332
	FRC+1L	14.200	125.564	12.600	120.064
	FRC+2L	14.272	101.408	14.031	90.158
	TLC	13.287	33.500	13.968	33.500
AS	FRC	21.400	86.250	23.600	123.750
	FRC+0.5L	16.200	83.005	22.500	103.005
	FRC+1L	15.100	108.213	20.040	123.213
	FRC+2L	14.031	89.209	19.744	140.459
	TLC	13.500	32.000	17.238	32.000
CW	FRC	9.600	65.625	9.000	86.250
	FRC+0.5L	7.281	65.796	7.719	90.796
	FRC+1L	7.400	89.091	7.900	81.591
	FRC+2L	6.982	68.977	7.900	81.477
	TLC	7.100	31.500	7.600	31.500

TABLE 6.2: HL(max) and P<sub>musc</sub>(max) for the maximum voluntary contractions

Subject	Lung Volume	3 cm above the bed		10 cm above the bed	
		HL Man. ( $\mu$ V)	Resp. Man. ( $\mu$ V)	HL Man. ( $\mu$ V)	Resp. Man. ( $\mu$ V)
LT	FRC	865.454	462.220	782.220	586.670
	FRC+.5L	676.368	448.000	800.000	584.000
	FRC+1L	720.000	435.560	728.890	266.670
	FRC+2L	702.220	382.230	844.450	524.000
	TLC	728.890	148.890	862.220	144.450
PM	FRC	398.400	418.750	660.000	370.000
	FRC+.5L	400.000	660.000	694.000	375.000
	FRC+1L	440.000	510.000	675.000	240.000
	FRC+2L	390.000	250.000	595.000	235.000
	TLC	365.000	200.000	560.000	300.000
AS	FRC	880.000	592.000	1504.000	436.000
	FRC+.5L	992.000	296.000	1440.000	308.000
	FRC+1L	1344.000	428.000	1544.000	492.000
	FRC+2L	1184.000	528.000	1496.000	496.000
	TLC	1104.000	640.000	1616.000	440.000
CW	FRC	711.110	193.900	786.670	146.670
	FRC+.5L	680.000	200.000	791.110	137.780
	FRC+1L	751.110	244.440	960.000	150.330
	FRC+2L	773.330	137.780	1066.700	111.110
	TLC	791.110	37.778	1031.110	120.000

TABLE 6.3: MRE generated by a maximum voluntary contraction

ENG (MRE) for a single subject, lung volume, and head height (Fig. 6.2c). Linearity offered a satisfying model with a mean coefficient of determination  $r^2 > 0.95$  for both manoeuvres and both head heights. As mentioned previously, the Least squares method was used to find the regression lines. As there was no strong physiological basis for assuming otherwise, the regression was not designed to force the fitted line through zero. This implies that it is possible to get a mechanical output (HL or P<sub>musc</sub>) without any electrical input (MRE). This is true only if it is assumed that the output is due to the synergist muscles whose electrical input could not be recorded because they were too far away from the recording site. Secondly, this also implies that it is possible to record the electrical input signal without getting any mechanical output, assuming that the recorded signal comes from the muscles located in the vicinity of the recording site but whose action is secondary to the manoeuvre performed. More details will be given in the next chapter.

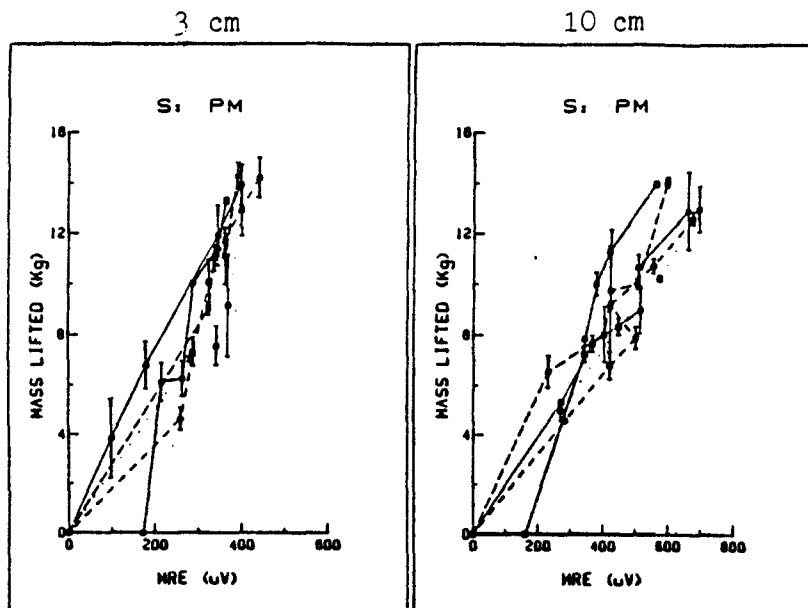
Tables 6.4 and 6.5 list the values of the regression line's coefficients A and B. The equation adopted was:

$$F = A + B \times \text{MRE} \quad (6.1)$$

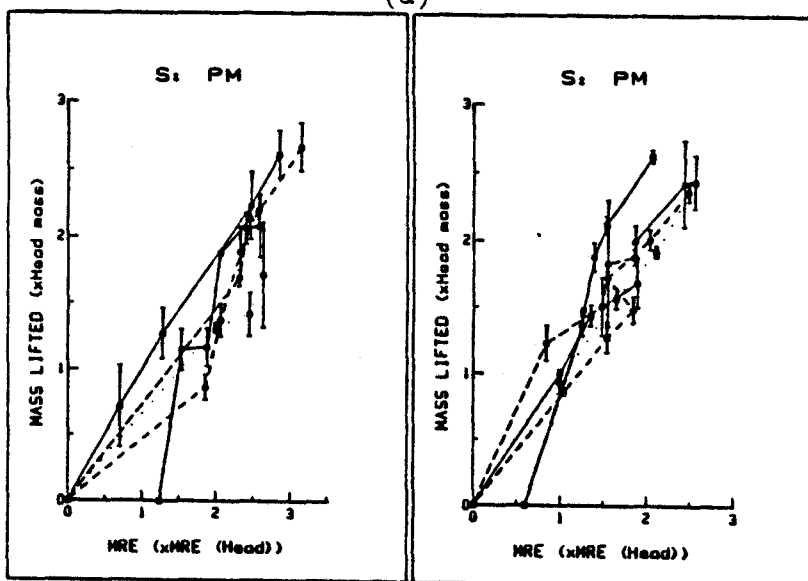
where F is the mechanical output, Force, i.e., HL or P<sub>musc</sub>. The equation is applicable to a single subject, head height, and lung volume. As well, coefficients of determination which describe the goodness of the fit of the relation to the data are listed.

Examination of these tables reveals:

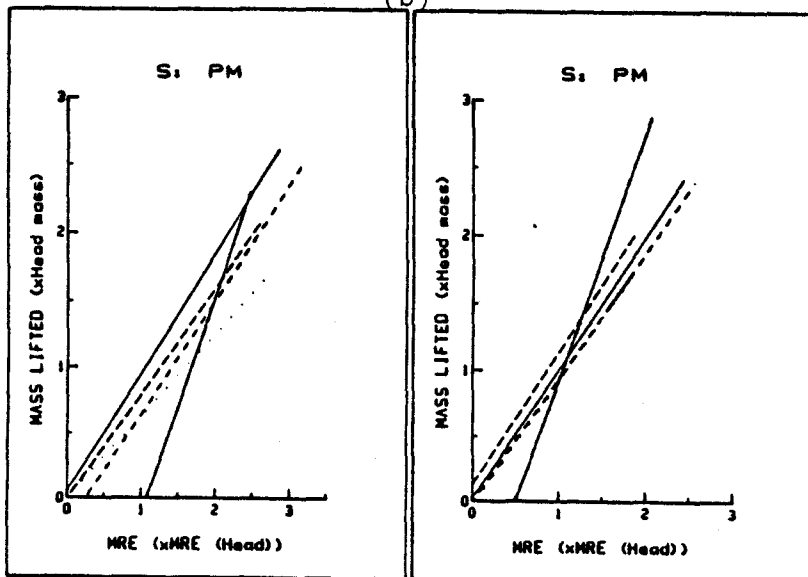
- 1) negative intercepts exist only for the head lift ma-



(a)



(b)



(c)

Figure 6.2: (a) raw data; (b) normalized data; (c) regression line; for subject PM, HL Manoeuvre.

Subject	Lung Volume	3 cm above the bed			10 cm above the bed		
		A	B	r <sup>2</sup>	A	B	r <sup>2</sup>
LT	FRC	.691	1.421	.927	.562	.503	.925
	FRC+.5L	1.144	1.051	.998	.092	.922	.973
	FRC+1L	-.091	1.453	.959	.097	1.107	.955
	FRC+2L	-.088	1.640	.986	.115	1.433	.983
	TLC	-.412	2.345	.949	-.034	1.584	.822
PM	FRC	.054	.899	.998	.020	.985	.981
	FRC+.5L	.006	.624	.988	-.032	.947	.996
	FRC+1L	-.210	.857	.907	-.009	.940	.948
	FRC+2L	-.007	.803	.984	.131	1.006	.947
	TLC	-1.765	1.654	.882	-.905	1.833	.954
AS	FRC	-.011	1.671	.990	-.038	1.139	.973
	FRC+.5L	.006	1.369	.999	.904	.901	.860
	FRC+1L	-.080	1.250	.993	.108	1.135	.972
	FRC+2L	-.048	1.078	.990	-.111	1.210	.927
	TLC	-.202	1.224	.972	-.259	1.191	.971
CW	FRC	.025	1.008	.993	.018	1.126	.977
	FRC+.5L	.326	.425	.990	.029	1.079	.985
	FRC+1L	.321	.410	.990	.096	1.041	.972
	FRC+2L	-.032	.708	.978	.039	.990	.994
	TLC	-.094	.703	.927	-.050	1.055	.990

Force = A + B x MRE

r<sup>2</sup> = coefficient of determination

TABLE 6.4: Linear Force-MRE Relationship: HL Manoeuvre

Subject	Lung Volume	3 cm above the bed			10 cm above the bed		
		A	B	r <sup>2</sup>	A	B	r <sup>2</sup>
LT	FRC	.293	.528	.985	.491	.360	.993
	FRC+.5L	.444	.549	.948	.576	.472	.952
	FRC+1L	.415	.783	.995	.511	.923	1.000
	FRC+2L	.448	.588	.974	.502	.618	.927
	TLC	-	-	-	-	-	-
PM	FRC	.403	.065	.782	.324	.499	.982
	FRC+.5L	.427	.119	.977	.367	.402	.967
	FRC+1L	.473	.136	.957	.343	.467	.862
	FRC+2L	.416	.150	.973	.381	.366	.945
	TLC	-	-	-	-	-	-
AS	FRC	.426	.326	.980	.507	.453	.949
	FRC+.5L	.474	.514	.978	.351	.663	.980
	FRC+1L	.511	.581	.999	.450	.458	.986
	FRC+2L	.595	.232	.952	.446	.583	.997
	TLC	-	-	-	-	-	-
CW	FRC	.442	.557	.926	.367	1.902	.957
	FRC+.5L	.452	.588	.654	.379	2.177	.994
	FRC+1L	.480	.764	.952	.379	1.623	.997
	FRC+2L	.435	.928	.927	.456	1.684	.844
	TLC	-	-	-	-	-	-

$$\text{Force} = A + B \times \text{MRE}$$

r<sup>2</sup> = coefficient of determination

TABLE 6.5: Linear Force-MRE Relationship: Resp. Funct. Manoeuvre

noeuvre

- 2) no specific pattern in the variation of slopes with increasing lung volume from FRC to TLC, for every subject, head height, and type of manoeuvre
- 3) a decrease in slope with increasing lung volume in the range of tidal volume, for the HL manoeuvre, for every subject, and for every head height (except for subject LT at a head height of 10cm)
- 4) an increase in slope with increasing lung volume in the range of tidal volume, for the respiratory manoeuvre, for every subject, and for every head height (except for subject PM at the head height of 10cm).

A one-tail paired t-test was performed to see whether the change in slope with increasing lung volume over  $V_t$ , i.e., from FRC to  $FRC + 0.5L$ , for a specific manoeuvre (HL or RM) and a specific head height was significant (Table 6.6). The change in slope was not significant at a head height of 10cm for every subject while it was for a few subjects at a head height of 3cm. Furthermore, the change in slope was observed in head lift manoeuvre (HL) at a head height of 3cm.

### 6.3 Reorganization of the data

Pooling the data helps to define a more general Force-MRE relationship. Table 6.7 shows the results of the F-test performed on slope and intercept of the regression line at different lung volumes. The results showed that the slope and



Manoeuvre	Head Height (cm)	Subject			
		LT	PM	AS	CW
HL	3	1.311	5.044*	2.444	9.601*
	10	2.581	.511	.749	.343
RM	3	.154	2.070	3.110*	.091
	10	1.381	1.667	2.109	.890

\* significant for  $p < 0.05$

TABLE 6.6: t-Values Due to Variation in Lung  
Volume from FRC to FRC + 0.5 L

Manoeuvre	Head Height		Subject			
			LT	PM	AS	CW
HL	3cm	Slope	.822	.810	1.253	1.274
		Interc.	2.433	.761	.121	.396
	10cm	Slope	.604	1.309	.062	.070
		Interc.	.292	.754	.285	.091
RM	3cm	Slope	.578	.657	5.602*	.114
		Interc.	.858	.230	5.979*	.019
	10cm	Slope	.633	.311	.675	.187
		Interc.	.202	.126	1.790	.099

\* significant for  $p < 0.05$

TABLE 6.7: F-Values Due to Lung Volumes Affecting  
the Linear Force-MRE Relationship

and intercept of these lines were not significantly different than the slope and the intercept of the regression line calculated from the pooled data. Meanwhile, the subject AS showed significant variations of both slope and intercept at 3cm of head height for the respiratory manoeuvre. A more intensive study showed that the significance was due to the regression line at a lung volume of FRC +2L. Thus, the first source of variation that could affect the Force-MRE relationship, the change in lung volume, did not affect much the Force-MRE relationship. The data from the different lung volumes could be pooled and could be represented by a single Force-MRE relationship. This relationship was applicable to a single subject, head height, and type of manoeuvre (HL or RM).

The second source of variation that could affect the Force-MRE relationship, the variation between subjects, was tested. Table 6.8 summarizes the results of the F-test performed on slope and intercept of the regression line of each subject compared to the one from the pooled subjects, for each lung volume. By examining the Table, one notices in the respiratory manoeuvre more variation between subjects than in the head lift manoeuvre. Furthermore, the slopes showed a significant difference between them while intercepts did not (except for HL at 3cm and at a lung vol. of FRC + 0.5L). Finally, the variation between subjects had a greater effect on the Force-MRE relationship than the variation between lung volumes.

To get a more general Force-MRE relationship for normals, the data from all the subjects were pooled. A new Force-MRE relationship was defined for a specific lung volume, head

Manoeuvre	Head Height		Lung Volume				
			FRC	FRC+.5L	FRC+1L	FRC+2L	TLC
HL	3cm	Slope	3.515	22.195*	1.619	3.757*	1.844
		Interc.	2.021	21.698*	.169	.023	.775
	10cm	Slope	.497	.033	.201	.243	.586
		Interc.	.741	1.078	.029	.058	.371
RM	3cm	Slope	5.766*	1.626	9.499*	4.583*	-
		Interc.	.918	.021	.262	2.526	-
	10cm	Slope	4.509*	7.218*	7.492*	.598	-
		Interc.	1.601	3.854	1.347	.155	-

\* significant for  $p < 0.05$

TABLE 6.8: F-Values Due to the Subject's Variation

Affecting the Linear Force-MRE Relationship

height, and type of manoeuvre (Table 6.9). By pooling the subjects, more variability was introduced in the data; the values of the coefficient of determination were smaller than the ones listed in Tables 6.4 and 6.5. Furthermore, the regression line fitted better the data at a head height of 10cm than at 3cm. In addition, the slope showed a constant increase with increasing lung volume for RM, while no specific pattern occurred for HL.

The underlined values in table 6.9 indicate the variability between the subjects for the IC manoeuvre. These values indicate the amount of MRE taken to perform a maximum inspiration. The mechanical output of this manoeuvre was the transthoracic pressure generated by the inspiration. The variability increases with increasing head height. Figure 6.3a and b show the variability of the data with respect to the regression line at every lung volume.

An even more generalized Force-MRE relationship can be found by pooling the lung volumes in order to get a unique relationship for a single head height and type of manoeuvre. Figure 6.4a and b show the resultant lines. As seen in Figure 6.4, the scattering between the data points is now very large. It is larger for the respiratory function manoeuvre than for the head lift manoeuvre, and it is larger at a head height of 3cm than at 10cm. This scattering is also seen in Table 6.10 by paying attention to the low values of the coefficient of determination.

The additional variability introduced by the resultant line from the pooled subjects' data reduced the effect due to

Manoeuvre	Lung Volume	3 cm above the bed			10 cm above the bed		
		A	B	r <sup>2</sup>	A	B	r <sup>2</sup>
HL	FRC	.420	.920	.704	.142	.967	.944
	FRC+.5L	.853	.490	.276	.082	1.066	.861
	FRC+1L	.101	.868	.761	.110	1.003	.229
	FRC+2L	.137	.813	.814	.115	1.084	.910
	TLC	.178	.792	.471	-.017	1.173	.872
RM	FRC	.511	.047	.099	.500	.362	.600
	FRC+.5L	.553	.091	.459	.494	.394	.466
	FRC+1L	.631	.108	.291	.482	.513	.455
	FRC+2L	.568	.110	.137	.495	.453	.542
	<u>TLC</u>	<u>.369</u>	<u>-.066</u>	<u>.954</u>	<u>.407</u>	<u>-.165</u>	<u>.817</u>

$$\text{Force} = A + B \times \text{MRE}$$

r<sup>2</sup> = coefficient of determination

TABLE 6.9: Linear Force-MRE Relationship: Pooled Subjects

Manoeuvre	3cm above the bed			10 cm above the bed		
	A	B	r <sup>2</sup>	A	B	r <sup>2</sup>
HL	.352	.789	.503	.089	1.058	.818
RM	.567	.088	.230	.493	.408	.504

$$\text{Force} = A + B \times \text{MRE}$$

r<sup>2</sup> = coefficient of determination

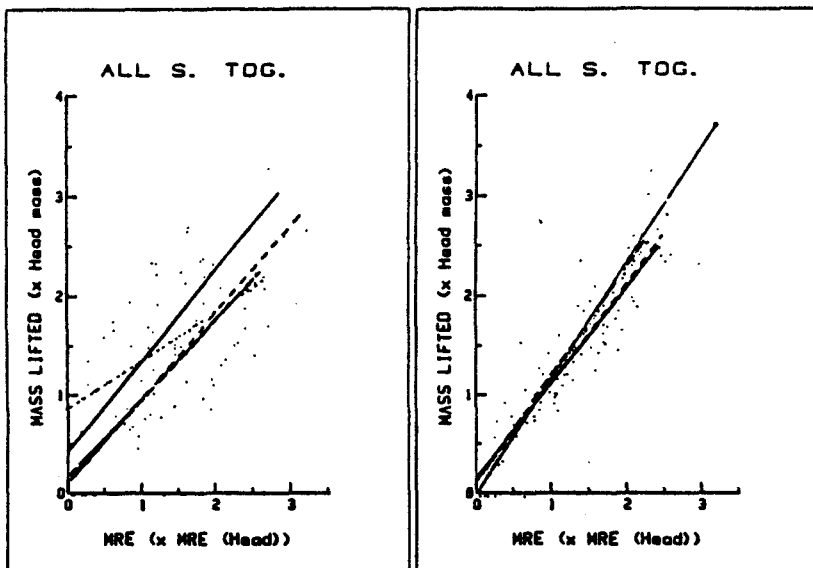
TABLE 6.10: Linear Force-MRE Relationship:

Pooled Subjects & Pooled Lung

Volumes

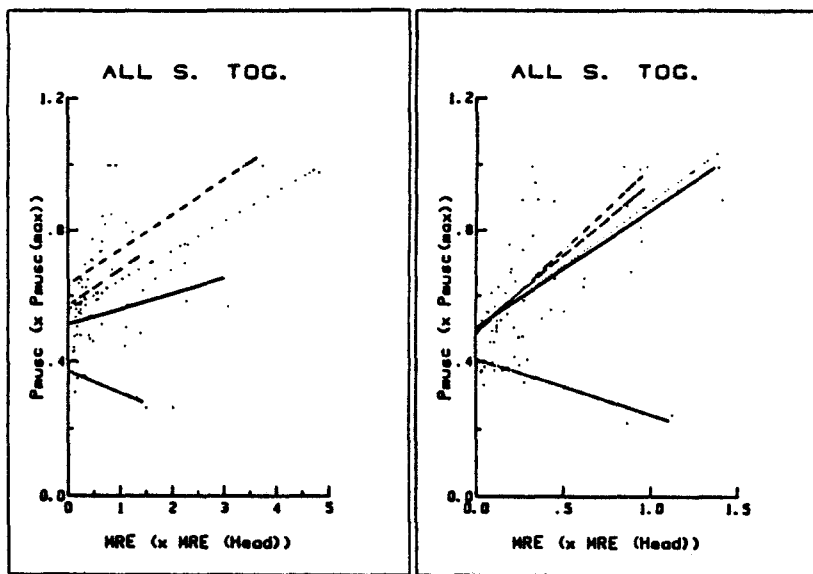
3 cm

10 cm



(a)

Lung Volume	Symbol
FRC	—————
FRC+.5L	.....
FRC+1L	- - - - -
FRC+2L	- . - . - .
TLC	.....

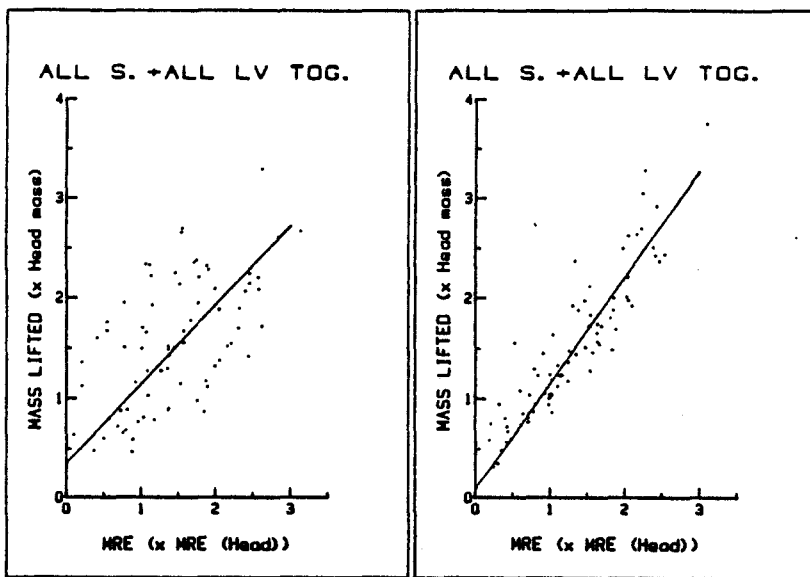


(b)

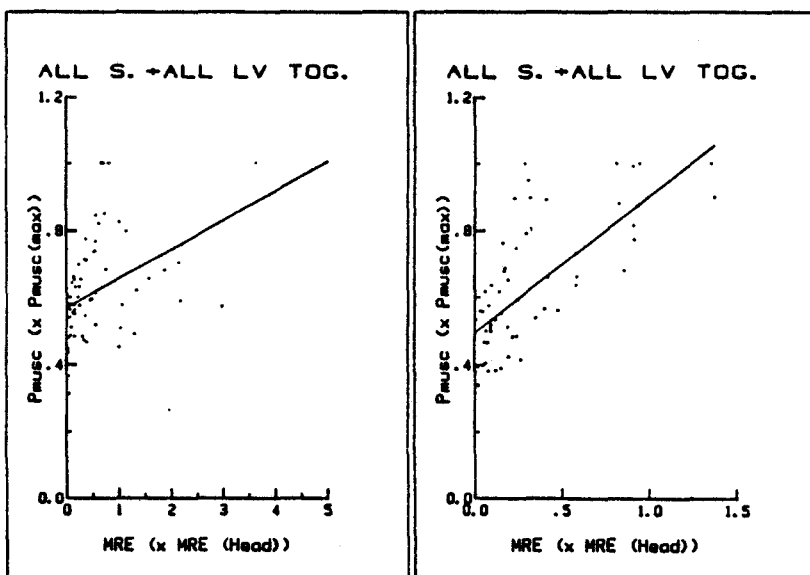
Figure 6.3: (a) HL Manoeuvre; (b) Resp. Manoeuvre; for all the Subjects pooled together at different Lung Volume.

3 cm

10 cm



(a)



(b)

Figure 6.4: (a) HL Manoeuvre; (b) Resp. Manoeuvre; for the Pooled Subjects and the Pooled Lung Volumes.

the change in lung volume. As seen in Table 6.11, this change is not statistically significant any more. This implies that the lung volume lines can be represented by a resultant line whose coefficients are calculated from the pooled subjects' and pooled lung volumes' data (Figure 6.4).

Because of the normalization, the lines at 3cm cannot be compared to the lines at 10cm of head height. Meanwhile, from the raw data, the amount of MRE taken to lift one head mass at a head height of 3cm can be compared to the amount of MRE taken to lift the same mass at a head height of 10cm. Similarly, the amount of MRE taken to perform an inspiratory capacity (IC) at 3cm can be compared to the amount of MRE taken to perform an IC at 10cm. Table 6.12 shows the ratio of MRE at 10cm over the MRE at 3cm. For the HL manoeuvre the ratio is greater than one for every subject, while for the RM manoeuvre, only one subject (AS) has a ratio much lower than one. Since the subjects were pooled, the mean ratio was found to be higher than one for both manoeuvres (around 1.5). One concludes that more electrical input is needed to drive the SCM muscle to perform a specific mechanical task at a head height of 10cm than at 3cm.

Using the electrical input (MRE) as the common factor, a linear relationship can be defined between the two mechanical outputs, head mass lifted (HL) and muscle pressure ( $P_{\text{musc}}$ ), for every head height. The results are shown in Figure 6.5a and the equations are presented in Table 6.13. Since the intercepts are close to each other, the mean value is used as the final intercept (Figure 6.5b). The final equations are:



Manoeuvre		Head Height above the bed ( cm)	
		3	10
HL	Slope	.222	.177
	Interc.	.375	.053
RM	Slope	.113	.065
	Interc.	.313	.004

TABLE 6.11: F-Values Due to Lung Volumes Affecting the Linear Force-MRE Relationship: Pooled Subjects

Manoeuvre	Subject				Mean Value
	LT	PM	AS	CW	
HL	1.067	1.941	1.016	1.758	1.446
RM	.970	1.500	.689	3.166	1.584

TABLE 6.12: MRE Ratios Between 10 cm and 3 cm Head Height

Head Height	A	B
	3 cm	.528
10 cm	.459	.386

$$P_{\text{muscle}} = A + B \times HL$$

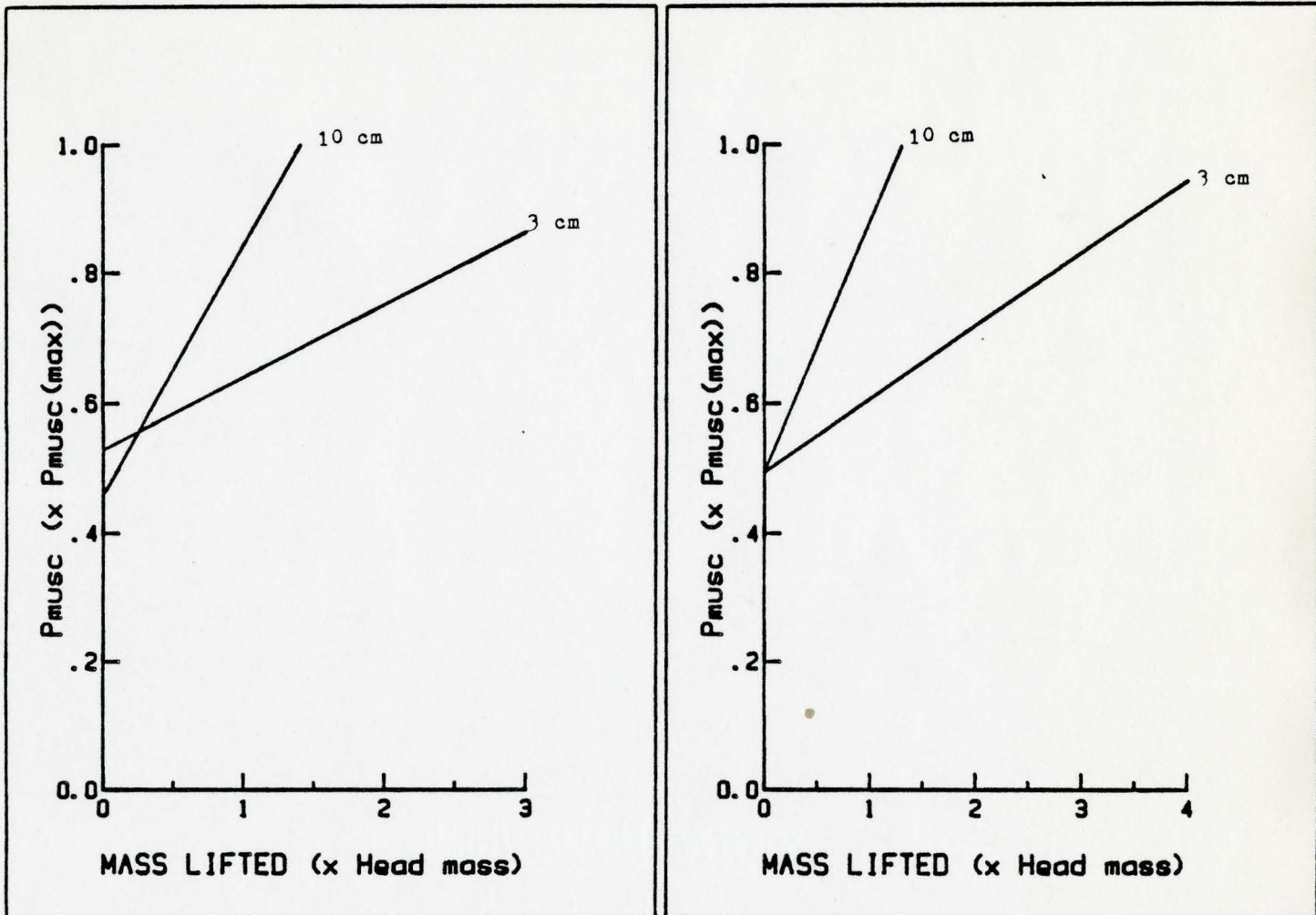
TABLE 6.13: Linear Force-Force Relationship

$$F_{cr\ 3cm} P_{musc} = 0.494 + 0.112 \times HL \quad (6.2)$$

$$F_{cr\ 10cm} F_{musc} = 0.494 + 0.386 \times HL \quad (6.3)$$

From the final graph (Fig. 6.5b), one can conclude that:

- 1) about 50% of the maximum inspiratory muscle pressure, performed under static conditions, (MIMPS), can be generated by a normal subject without using the SCM muscle
- 2) at a head height of 3cm above the bed, the amount of recruitment of the SCM muscle used to perform a MIMPS manoeuvre is the same as the amount used to lift a mass of 4.5 x Head Mass, while at 10cm, the SCM recruitment to do a MIMPS manoeuvre is the same as lifting a mass of 1.3 x Head Mass.



(a)

(b)

Figure 6.5: Relationship between the two mechanical output, i.e.,  $P_{musc}$  and Mass Lifted. (a) resultant lines; (b) resultant lines with a common intercept.

## CHAPTER VII

### DISCUSSION

#### 7.1 Introduction

The preceding chapter showed how the analysis was done to identify the main results. These results express the dual function of the SCM muscle. Finally, a relationship between the two mechanical outputs was determined for every head height.

In this chapter one will briefly summarize the meaningful results obtained from the experiment, one will comment on the experiment itself in order to know its weaknesses, one will discuss and argue the results, summarize the dual function of the SCM muscle from the discussion, and finally, one will introduce the future actions to take to continue the study of the SCM muscle.

#### 7.2 Summary of the results

The purpose of this section is to make sure that the results described in Chapter VI are clear to the reader. For

this reason, a point form summary will be used.

The meaningful results derived from the experiment are:

- 1) The MRE recorded from a maximum HL manoeuvre is greater than the MRE recorded from a maximum P<sub>musc</sub> manoeuvre for every subject, every lung volume, and every head height above the bed (except for subject PM at 3cm and lung vol. FRC, FRC+0.5L, and FRC+1L).
- 2) The linear Force-MRE relationship represents a satisfactory model for a single subject, head height, lung volume, and type of manoeuvre. The averaged coefficient of determination is 0.956 for HL, and 0.963 for RM.
  - 3a) The slope of every regression line is positive
  - b) For the HL manoeuvre, 50% of the intercepts are negative, while for the RM manoeuvre, all the intercepts are positive.
- 4) For the HL manoeuvre, a decrease in slope with increasing lung volume over the range of tidal volume was noticed, while the reverse occurred for the RM manoeuvre.
- 5a) Once the subjects are pooled, the variation in lung volume has no significant effect on the Force-MRE relationship, while the head position seems to have a larger one although it could not be formally tested because of the normalization process used.
  - b) For the RM manoeuvre, the slope increases with increasing lung volume, while for the HL manoeuvre, no specific pattern occurs.
- 6a) 50% of the maximum inspiratory muscle pressure (MIMPS) can be generated without using the SCM muscle.

- b) At a head height of 3cm above the bed, the amount of EMG recorded when a MIMPS manoeuvre is performed is the same as the amount of EMG recorded when a mass of 4.5 x Head Mass is lifted with the head, while at 10cm, the amount of EMG recorded when a MIMPS manoeuvre is performed is the same as the amount of EMG recorded when a mass of 1.3 x Head Mass is lifted with the head.'

### 7.3 Sources of variability

The striking point about the results of the preceding chapter is the great variability in the data. This variability is seen by the very low F-values in every test performed and also by the large standard deviation of EMG recorded. The causes of this variability can be divided into two sections: (a) during the manoeuvres, and (b) between the manoeuvres.

During the isometric manoeuvres, a possible cause of variability is the change of the contraction velocity of the internal structures of the muscle. Especially during strong contractions, the stretching of the series elastic components (tendons and their retinacula) allows substantial internal shortening of the contractile elements (Bigland 1954). This phenomenon may apply for both manoeuvres.' In the present experiment, the contraction period was 5 sec.. It is believed that the stretching of these elements occurs at the very beginning of the contraction such that no more stretching occurs during that contraction.' Furthermore, since fatigue was thought to be avoided,

it is possible that the muscle might not work much harder at the end of the contraction than at the beginning such that no significant stretching occurs. The contraction velocity, as a possible source of variability, may not be very important during a short isometric contraction, but deserves to be mentioned. In addition to this phenomenon, the inspiratory pressures performed under static conditions may not be isometric manoeuvres. The respiratory muscles changed their length because of the deformation of the chest wall during these breathing efforts (Agostoni 1966). This implies that the change in the contraction velocity may be a much more important cause of variability during the respiratory manoeuvres (RM) than during the head lift manoeuvres (HL). In the following section one will see why the respiratory manoeuvres may give rise to eccentric contractions of the SCM muscles.

A second important cause of variability is the use of the abdominal muscles during HL manoeuvres. The SCM EMG production changes with the degree of utilization of the abdominal muscles. The use of the abdominal muscles, especially the rectus abdominis muscles, changes the SCM muscle length. During the head lift manoeuvre, the contraction of the SCM muscle has the tendency to deform the chest wall by moving the sternum toward the chin although the lung volume is maintained constant during the manoeuvre. This results in a shortening of the muscle. By contracting the rectus abdominis muscles, an opposite force is created on the sternum. This new force has the tendency to move the sternum toward the umbilicus causing a lengthening of the SCM muscle. The resultant force

applied on the sternum, during the HL manoeuvre, is the sum of the two above opposite forces. This resultant force determines the sternum position and consequently, the length of the SCM muscle. The degree of utilization of the abdominal muscles, especially the rectus abdominis, changes the position of the SCM muscle on its force-length curve and consequently, changes the EMG production. Although careful attention was taken to avoid the use of these extra muscles, the natural tendency of the subject was to use them, especially for manoeuvres close to maximum. Although the effect of the abdominal muscles on HL manoeuvre was not systematically measured in this pilot study, it cannot be neglected. One way of studying the contribution of the abdominal muscles during the HL manoeuvre would be to record their EMG production and relate it to the mass lifted with the head to see whether the change in EMG is proportional to the change in mass lifted with the head.

Another cause of variability is the way people breathe, i.e., the use of their rib cage vs the use of their abdomen. Every subject had his own way of breathing. A few used more their rib cage, and the others used more their abdomen. Chest breathers use more their SCM muscles than abdomen-diaphragm breathers (Danon 1971). This aspect was important to consider during the respiratory manoeuvres performed during the experiment. This phenomenon increases the variability between the subjects. Furthermore, it is likely that this source of variability (use of rib cage and/or abdomen) was greater in a given subject during submaximal manoeuvres than during maximal manoeuvre. We made no effort to remove this variable. The



subjects were not asked to breathe with any specific pattern. One approach to this problem might have been to define a specific chest breathing pattern and to teach it to every one of our subjects. In addition, a specific way of approaching the defined lung volumes might have been taught to the subjects. One of the objectives of this experiment was to compare normals with weak ICU patients, and for that reason subjects were allowed to breathe with their normal pattern. It is clear that it is very difficult for a weak ICU patient to perform respiratory manoeuvres using an imposed pattern. Figure 6.3 shows clearly that the scattering of the points is larger for the respiratory manoeuvre than for the head lift manoeuvre. It seems that the way of breathing was a more important variable for RM than the use of the abdominal muscles for HL, for both head heights.

Table 6.1 showed that breathing up to a specific lung volume, during a manoeuvre, does not introduce more variability than doing the manoeuvre. Because the F-values are very small at FRC (Table 6.1), the amount of variability introduced by the way the manoeuvre is performed, is probably large. The comparable F-values at FRC + 2L (Table 6.1) indicate that the variability introduced by breathing to a specific lung volume, before performing a manoeuvre, is not larger than the one introduced by the manoeuvre itself, but may still be large. Consequently, Table 6.3 reveals that the increase in scattering of the points for the RM manoeuvres might probably be due to the way the subjects were performing the inspiratory pressures. Since the inspiratory pressures were done by breathing with

closed airways, the teaching of a breathing pattern is valid to approach a defined lung volume, and to perform an inspiratory pressure during RM manoeuvres.

Between the manoeuvres the main cause of variability was the change in the geometry of the muscle fibres relative to the recording site due to the movements of the subject's head. As described in Chapter V, the subjects expressed the strong wish to move their head between the manoeuvres for both RM and HL manoeuvres. This change of head position changed the orientation of the muscle fibres relative to the recording electrodes. As explained in Chapter V, the recorded EMG changes with the geometrical arrangement of the muscle fibres relative to the recording electrodes. Although care was taken to put the subject's head back in the same position, after the resting periods, it was impossible to get back the same electrode-muscle fibres orientation. Furthermore, because the experiment was lengthy, it had to be done in two sessions. The electrodes were not at the same place on the neck during the second session relative to the first session. Once the electrodes were removed, it was very difficult to put them back where they were before even if tremendous care was taken.

Another important source of variability is the action of the agonist and the antagonist muscles during the manoeuvre. The variability introduced by their action, introduced a variability in the action of the SCM muscle. The contribution of these muscles during the manoeuvres was not studied. It is difficult to determine their effects on the SCM muscle func-

tion. One way to approach this problem is to record the EMG of the main agonist and antagonist muscles activated during a specific manoeuvre. Statistical analyses might tell us whether their action is significant. For the moment, one knows that these muscles play an important role in the performance of a manoeuvre and that the variability they introduce might possibly be important.

Finally, the last but much less important variable to consider was "Fatigue". It was reported in the literature that to avoid fatigue, the contraction period should be less than ten seconds and the rest period between every contraction, at least two minutes (Cnockaert 1975, Kcni 1976). The contraction period and the rest period used in the experiment were 5 sec. and 1.5 to 2 min.. It was thought that fatigue was avoided, but still it remains a possible variable. The effect of fatigue on EMG is to increase the EMG production for a constant force, mainly due to an increase in synchronization (Missiuro 1962, Bigland-Ritchie 1979, Ralston 1961).

## 7.4 Discussion of the results

### 7.4.1 The sternocleidomastoid dual function

As explained in Chapter III, the SCM muscle has a dual function. It is used as a skeletal muscle to lift the head in subjects in the supine position, and it is used as an accessory respiratory muscle. The first finding of the experiment was that the EMG recorded during the maximum HL manoeuvre

vre was greater than the EMG recorded during the maximum RM manoeuvre. It indicates that during the maximum HL manoeuvre, the SCM is used to a greater extent than during the maximum RM manoeuvre. This interpretation supports the hypothesis that the SCM is the primary muscle used during HL, and the other neck muscles are minor muscles which only help the SCM to perform the movement. As a respiratory muscle, the SCM is a minor muscle. Most of the load is taken by the other respiratory muscles: Diaphragm, external intercostal muscles, and scalene muscles. From Table 6.3, the mean ratio  $EMG(HL(max))$  over  $EMG(Pmusc(max))$  was calculated for every head height: (a) for 3cm, the EMG ratio was 3.31, and (b) for 10cm, the EMG ratio was 3.88. These results show that for both head heights the SCM is at least 3 times less used to perform a maximum inspiratory pressure than to perform maximum head lift. This confirms that the SCM muscle is not used to its full capacity to perform an inspiratory pressure manoeuvre. In patients with a high cervical lesion, the SCM muscle becomes the main inspiratory muscle. An increase in EMG at a constant inspiratory pressure was noted when compared to normal subjects, and a hypertrophy of the muscle was noted (Danon 1979). It seems that in these patients the SCM muscle is used to its full capacity, or close to it.

#### 7.4.2 Force-EMG relationship

Considering all the highly complex physiological events that occur within the muscle structure during a contraction, and considering the viscoelastic properties of the muscle tissue,

a purely linear Force-EMG relationship is unlikely over the entire force range. However, for practical purposes, a linear model provides a satisfactory fit to the data observed during isometric contractions, providing that the head position and the electrode placement remain constant.

Theoretical studies (Moore 1967) have suggested that the EMG amplitude should increase as the square root of the number of active motor units and hence the tension, since the number of activated fibres is directly related to the force (Moore 1967). However, the theoretical model seems to be dependent on the assumption of asynchronous activity of motor units. Zuniga (1969) showed that when synchronization occurs during an isometric contraction, linearity may be reached. Moore (1967) showed that synchronization increases the rms value of the EMG. Such a shift would make the muscle's rms value rise more nearly linearly with force, when otherwise it would rise less fast.

The Force-EMG relationship is primarily determined by the muscle under investigation. Each muscle has unique physiological properties and anatomical structure such as the relative amount of red and white fibres in the muscle (Woods 1978). Woods, working on the biceps, triceps, and adductor pollicis muscles, reported that the linearity in the red muscle Force-EMG relationships may reflect the relative uniformity of the fibre composition (80%-90% red fibres in the muscle) or, alternatively, a uniform distribution. Meanwhile, the non-linear relationships, observed in the two brachial muscles of roughly equal fibre representations, may reflect more a dif-

ferential distribution of the two fibre types. Specifically, if the higher-threshold pale fibres are more superficially located, then they would contribute more to the surface EMG as exerted force increases.

The Force-EMG relationship depends also on the experimental conditions; and in particular whether the muscle is fatigued. Fatigue can give rise to any type of relationship from linear to highly non-linear (Kuroda 1970). Furthermore, fatigue is likely to exert an increasing effect as it becomes more severe.

Additional variables that may be important in the shape of the Force-EMG relationship include:

- 1) electrode arrangement (parallel or perpendicular to the muscle fibres)
- 2) the type of movement executed during the experiment (continuous vs interrupted serial movements)
- 3) the physical conditioning level of the subject.

These variables can produce any type of change to the shape of the Force-EMG relationship.

In addition, the degree of contribution of other muscle groups and the varying amounts of cocontraction among antagonist muscle groups may alter the force contribution of the muscle under investigation to the measured net force (Lawrence 1983). The negative intercepts found in the head lift manoeuvre may be due to the activation of the platysma muscle whose action would be to stabilize the inferior jaw just before and during the head lift manoeuvre. It also can be due to the activation of the sternohyoid muscle whose action would be to

stabilize the hyoid bone just before and during the head lift manoeuvre. These two muscles are very close to the SCM muscle and to the recording site. There is a strong probability that their EMG signals were captured by the recording electrodes. The action of these muscles, however, does not seem to be very important because, according to Table 6.4, the negative intercepts are close to zero. The positive intercepts are due to synergist muscles whose EMG signals could not be recorded because the muscles were too far away from the recording site. For the head lift manoeuvre, the synergist muscles are: the medial and posterior scalenes, the longus colli, and the longus capitis. These muscles are located very deeply in the neck and no EMG could be recorded from the recording site. For the respiratory manoeuvre, the synergist muscles are: the diaphragm, the external intercostal muscles, and the scalene muscles. The first two sets of muscles are not located in the neck and they are the most important muscles of the manoeuvre. They are responsible for the first part of the curve where there is a large increase of  $P_{\text{musc}}$  with a very small increase in MRE (Figure 7.1). According to Lynn (1978), who worked out a mathematical model showing the effect of the muscle-electrodes geometry (bipolar surface electrodes) using the dipole theory, when a muscle lies close to the skin surface, most of the energy in the surface EMG is derived from fibres lying within one length unit of the electrodes, i.e., the distance between the two recording electrodes. The decrease in signal energy with fibre distance is so rapid that any active fibres within about 0.4 length unit of the electrodes will tend to do-

3cm

10cm

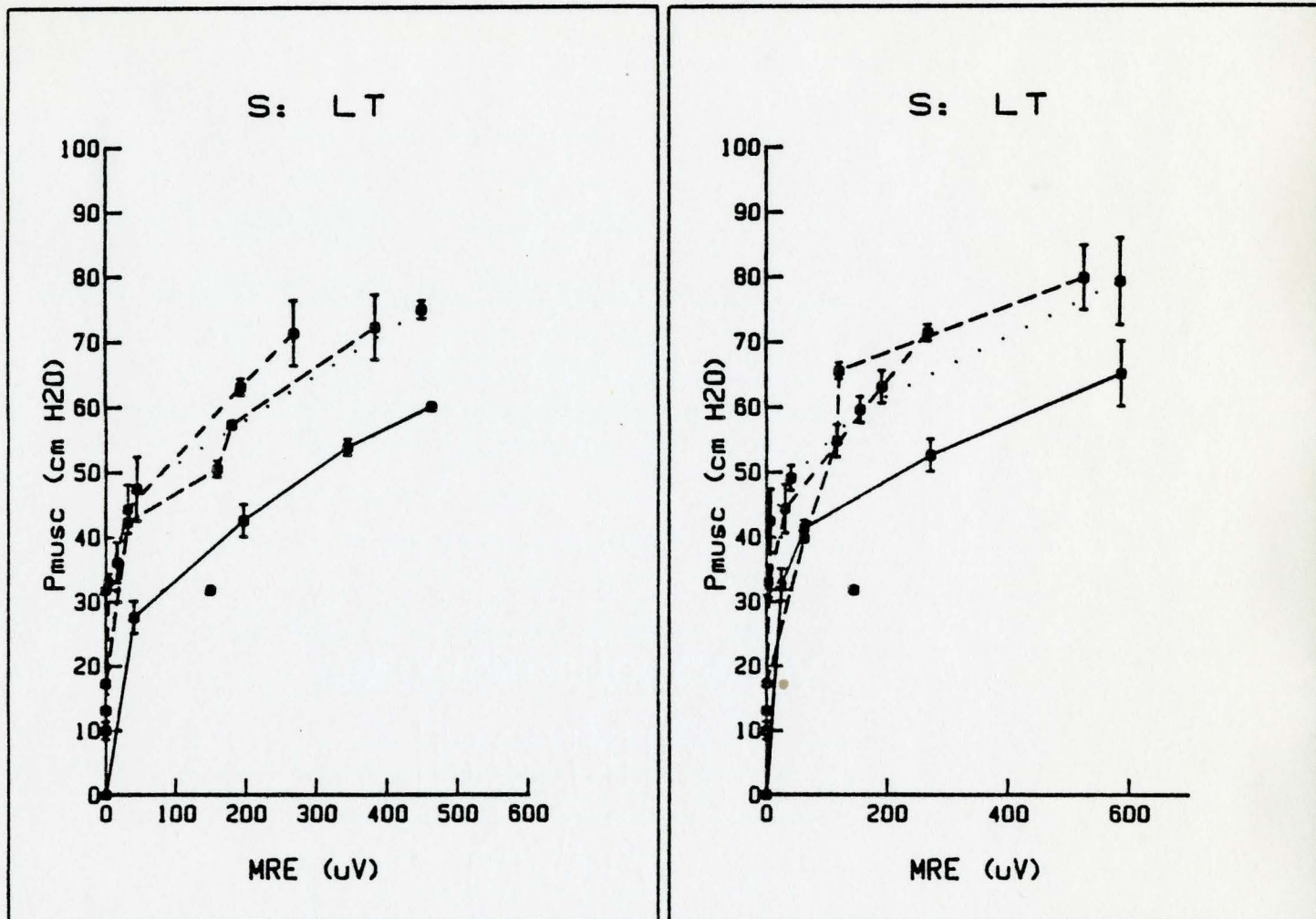


Figure 7.1: Respiratory Manoeuvre

Lung Volume	Symbol
FRC	—————
FRC+.5L	.....
FRC+1L	- - - - -
FRC+2L	- . - . -
TLC	- - - - -



minate the record, and any attempt to record from fibres more than about 1.5 length units below the skin surface will probably be foiled by an inadequate signal/noise ratio. It also seems that recording from a muscle lying below another one which is even slightly active will present great difficulties. According to this theory, the greatest effect would be due to the platysma muscle because it is located between the electrodes and the SCM muscle. The sternohyoid muscle, being further away, would have much less effect on the recorded EMG.

The other component of the Force-EMG relationship, the slope, was found to be positive in every subject, lung volume, head height above the bed, and type of manoeuvre. For an increase of force, a proportional increase in EMG was recorded. Many investigators tried to explain this phenomenon. Milner-Brown (1973), working on the first dorsal interosseous muscle, reported that among the two ways of increasing the force level of contraction, the recruitment of more muscle fibres and the increase in firing frequency, recruitment was the major mechanism at low levels of force (Milner-Brown 1973a), while the firing rate was the major mechanism at intermediate and high levels of force (Milner-Brown 1973b). Meanwhile, over the whole physiological force range, the firing rate is the major mechanism of increasing force output for more than two third of the force range. As explained in Chapter IV, the size principle is very important in recruiting more muscle fibres. More recent studies (Lawrence 1983) showed that large motoneurons increase their firing rate more rapidly with increasing stimulation and attain higher firing rate. At high force levels,

in absence of recruitment, the growth of the motor unit firing frequency and consequently the IEMG might increase more rapidly than would be expected, thus providing a strong possibility of straightening out of the quadratic relationship suggested on theoretical bases for the asynchronous model. Moreover, as mentioned before, synchronization contribute to linearity in the relationship (Moore 1967). The degree of recruitment and discharge frequency used by a muscle during an isometric contraction is highly dependent on the muscle under investigation. A review of the literature leads us to assume that the Force-EMG relationship may be linear even at high force levels.

#### 7.4.3 Importance of the Force-Length curve

The change in length of a muscle modifies its geometry relative to the recording site, and consequently, changes the EMG recorded (Chapter V). When a muscle shortens, more EMG is recorded for the same generated force (Manns 1977, Bigland 1954, Close 1960, Druz 1979); the muscle fibres shorten and an apparent increase in the conduction velocity is noted by the electrodes. This phenomenon increases the amplitude of mean-rectified-EMG (MRE). The MRE ratios given in Table 6.12 agree with the literature. The change in head height from 3cm to 10cm decreases the SCM muscle length. More EMG was recorded at 10cm than at 3cm for the same mechanical output force, for both types of manoeuvre, HL or RM. Therefore, the muscle length when the head height is 3cm seems to be closer to the optimal length because the neuromuscular efficiency ratio (Force/EMG) is larger than it is at 10cm.

By modelling the neck system and by looking at the distribution of the forces involved during a manoeuvre, one found that the values in Table 6.12 might represent an underestimation of the reality. By assuming that the neck behaves like a hinge with the axis of rotation located in the middle of the neck (Appendix D), the force generated by the SCM muscle decreases as the head height increases, for the same mass lifted or the same  $P_{\text{muscle}}$  generated. This model supports the hypothesis saying that the muscle shortens as the head height increases.

The change in lung volume, from FRC to TLC, may not affect much the force generated by the muscle since the cephalad displacement of the sternum may be very small, which gives rise to a very small increase of the angle  $\alpha$  (Figure 1, Appendix D).

It has been mentioned before that the change in lung volume over the range of inspiratory capacity (IC) does not give rise to any particular pattern of change in the slope of the regression lines. The reasons for this are probably the non specific way the subjects were breathing to the specified lung volumes, the use of the abdominal muscles during HL, and the non specific way to perform inspiratory pressures. At the same time, we noticed that for the HL manoeuvres, the slope of the regression lines was decreasing with increasing lung volume over the range of tidal volume ( $V_t$ ). This indicates that for a constant mass lifted, more EMG was recorded at a lung volume of FRC+0.5L than at FRC. The reason is that the SCM muscle shortens when the lung volume increases by 0.5L. Table 7.1 shows the slope ratio (FRC/FRC+0.5L) for both types of manoeuvre. The slope ratios are all greater than 1 (except for subject LT at 10cm)

Subject	3cm above the bed		10cm above the bed	
	HL Man.	Res. Man	HL Man.	Res. Man
LT	1.352	0.962	0.546	0.763
PM	1.441	0.546	1.040	1.241
AS	1.221	0.634	1.264	0.683
CW	2.372	0.947	1.044	0.434

TABLE 7.1: Slope ratio for a change in lung volume from FRC to FRC + 0.5L.

for the HL manoeuvre. In general, the values are below 1.5 (except for CW at 3cm). This indicates that the change in muscle length is not considerable. However, the slope ratios at 3cm are larger than at 10cm. This means that at 10cm, the subject's rib cage kept a more uniform configuration during the breathing of the 0.5L; the change in muscle length is much less because the ratios are closer to one (except for subject LT). At 3cm, the subjects used more their rib cage to breathe the 0.5L than at 10cm. One can conclude that rib cage breathing changes the SCM length. One would predict that using a fixed chest breathing pattern, the effect of a change in SCM length could be more clearly demonstrated.

In contrast to the HL manoeuvre, the RM manoeuvre shows an increase in slope with increasing lung volume over the range of  $V_t$ . This is represented by a slope ratio less than 1 (Table 7.1), and could be explained by a lengthening of the SCM muscle due to a paradoxical movement of the rib cage during breathing or/and during the inspiratory pressure manoeuvre. Agostoni (1966) reported that during inspiratory efforts, with closed airways, the horizontal section of the rib cage (upright posture) becomes more elliptical, whereas during expiratory efforts, it becomes more circular. During these respiratory activities, the main change occurs on the lateral diameter over the expiratory reserve volume (ERV) and on the dorso-ventral diameter over the inspiratory capacity (IC). The above deformations imply that some muscles lengthen instead of shortening. During the inspiratory efforts, Agostoni lost the EMG of the parasternal external intercostal muscles at the second

intervertebral space. He concluded that the intercostal (IC) muscles were lengthening during the manoeuvre. From this finding, one can extrapolate the lengthening of all the upper rib cage muscles including the SCM and scalene muscles because of their attachment points. Furthermore, during tidal breathing, the rib cage expands more than the abdomen in the upright posture, while the reverse occurs in the recumbent position (Druz 1981). Most normal subjects are abdominal breathers when supine and rib cage breathers when sitting or standing (Druz 1981). The inspiratory action of the diaphragm is to cause an expansion of the rib cage by pulling cephalad at its insertions on the lower ribs and to raise the intra-abdominal pressure which pushes outward on the diaphragm's zone of apposition to the rib cage (Loring 1982). Moreover, the inspiratory action of the diaphragm on the rib cage is greatest at low lung volumes. In a study performed by Koepke (1958), on subjects in the supine position, the pattern of recruitment during inspiration began with the diaphragm. The intercostal muscles (IC) were then recruited in a pattern from the first to the eleventh IC muscle downward. During quiet breathing, the diaphragm was always active, the first IC muscle was usually active, the second IC muscle was occasionally active, and the remaining IC, never active. One can conclude that the rib cage inspiratory muscles lengthen mainly during the inspiratory pressure manoeuvres at low lung volumes and not during quiet breathing. For two subjects out of four (Table 7.1), the lengthening of the SCM muscle was greater at 10cm than at 3cm. It indicates that these subjects performed the manoeuvres using more their dia-

phragm than their rib cage, which induces a greater paradoxical movement of the rib cage, than the two other subjects. By imposing a specific rib cage breathing pattern on the subjects, this phenomenon could decrease a lot and could possibly disappear.

The change in lung volume did not affect significantly the Force-EMG relationship for every subject (except for AS) as shown in Table 6.7. It seems that the variability within the subjects themselves was fairly great, but this might be reduced by paying attention to some of the variables presented in section 7.2. The consequence of this would be to increase the F-values but it does not mean that lung volume would become a significant factor affecting the Force-EMG relationship. Sharp (1974) showed that the changes in muscle function were closely related to the increase in lung volume. He found that the decrease in length of the SCM muscle was 15% when lung volume increased from FRC to TLC. The measurements were made at only two lung volumes, FRC and TLC. Furthermore, he reported, on a study done on 6 normal males, that to generate a given pressure, much more EMG was required at large than at small lung volumes, supporting the conclusion that the inspiratory muscles (Diaphragm, IC, SCM, and Scalene) decrease their length. As shown in Table 6.9, for the pooled subjects, a net increase in slope occurred with increasing lung volume, supporting the conclusion that the SCM muscle increases its length due to the paradoxical movement of the rib cage during the inspiratory pressure manœuvres. These results are in contrast to Sharp's results. However, Sharp did not mention how his subjects were breathing and what was their body position, supine or upright. It appears that Sharp's

subjects breathed more with their rib cage and more uniformly during the experiment. In addition, Sharp did not say whether the change in slope (for the pooled subjects) was significant. For this thesis experiment, Table 6.9 shows that the greatest change in slope, for the RM manoeuvre, occurs at low lung volumes, i.e., below FRC + 1L, for both head heights. This supports the hypothesis that the inspiratory action of the diaphragm on the rib cage is greatest at low lung volumes.

#### 7.5 The SCM muscle function

The experiment described was performed primarily to understand the function of the sternocleidomastoid (SCM) muscle under specific conditions.

The experiment contrasted two functions of the SCM muscle: forward flexion of the neck, and inspiratory motion of the chest wall. It appears that, in normal subjects, the Sternocleidomastoid muscle has a more important role in forward flexion of the neck (or head lift in subjects in the supine position), than it has in breathing. It seems that the important function of the SCM, as a respiratory muscle, is, like all the rib cage muscles, to position the rib cage to allow optimal length-tension conditions to prevail for the function of the diaphragm, which is viewed as the prime inspiratory muscle.

The change in lung volume affects much less the SCM muscle physiology than the head position, which appears to be a very



important factor. The effect of lung volume decreases with increasing forward bending of the neck (head position) as shown in Table 6.11. It might indicate that as the neck bends, the SCM muscle may change its position on its length-tension curve toward a flatter region, or alternatively, that the changes in length produced by the changes in lung volume are much smaller than the changes in length produced by the alteration in head position.

Head lift is closely related to the Sternomastoid activation (Fig. 6.4a), and even more at 10cm than at 3cm. Since the intercept is positive and close to zero, for both head heights, there is no doubt that at zero head lift, there is no activation of the SCM muscle. As a skeletal muscle, the SCM activation is linearly related to the mass lifted with the head. The slope is close to 1 and the intercept is close to 0,0, especially at a head height of 10cm.

As an accessory inspiratory muscle, the SCM muscle starts to be activated only after 50% of the maximum muscle pressure has already been generated (Fig. 6.4b). That first 50% of the pressure was performed by the prime inspiratory muscles, i.e., Diaphragm and IC muscles. Here again, the activation of the SCM is linearly related to the force (muscle pressure ( $P_{\text{musc}}$ )) generated.

By relating the two mechanical outputs at a specific EMG value, one defines a new method of testing the SCM muscle while it behaves as an inspiratory muscle (Fig. 6.5). By only using the head lift meter, one can approximately know the maximum  $P_{\text{musc}}$  that the subject is able to generate by knowing the

maximum mass he/she is able to lift with his/her head. This method does not involve any sophisticated device, but only the small hand held head lift meter.

The HL-EMG relationship at 10cm of head height has much more impact than the one at 3cm because the slope of the HL-EMG relationship is very close to 1 (1.058) and the intercept is very close to 0,0 (0,0.089). This indicates that the mass lifted is a close correlate of the Sternomastoid muscle activation (EMG), and that the regression line equation of the HL-Pmusc relationship at 10cm (Fig 6.5) is approximately the same as the regression line equation of the EMG-Pmusc relationship (Fig. 6.4b).

#### 7.6 Future steps of this study

The study of the SCM muscle is far from being finished. Two different kinds of projects can be done to continue the study. The first project would be to perform the same experiment using weak subjects. Firstly, one could study weak ICU patients. These patients must have no history of any disease affecting the SCM physiology and anatomical structure. In other words, their SCM must be intact. Secondly, one could study normal subjects weakened with curare. The purpose of these two studies would be to see the shift in slope and intercept of the HL-Pmusc relationship and its significance relative to the relationship obtained from normal subjects.

The second project would be to determine the length-

tension relationship of the SCM in normal subjects in the supine position while the change in head position changes the length of the muscle. Sharp (1974) described the length-tension relationship of the SCM when the change in lung volume was changing the length of the muscle. It was not specified, but everything leads to the conclusion that his subjects were in the supine position. A formal study should be carried out, whose purpose would be to define the shape of the curve. This would be necessary to confirm the hypothesis that, as the neck bends, the SCM muscle changes its position on its length-tension curve toward a flatter region, thus decreasing the effect of the change in lung volume.

## CHAPTER VIII

### CONCLUSIONS

The SCM muscle is used primarily to change the position of the head while it is much less involved as an inspiratory muscle. By comparing the EMG generated for a maximum manoeuvre, for a single subject, head height, lung volume, and type of manoeuvre, it has been found that the EMG produced during maximum lifting is much higher than the EMG produced during maximum inspiratory pressure.

The linear relationship between Force (mass lifted or muscle pressure) and EMG was found to be a very adequate approximation ( $r^2 > 0.95$ ).

For the head lift manoeuvre, the decrease in slope with increasing lung volume over the range of tidal volume indicates a decrease in the SCM muscle length, while for the respiratory manoeuvre, the increase in slope with increasing lung volume over the same range indicates a lengthening of the SCM muscle probably due to a paradoxical movement of the rib cage during the inspiratory pressure manoeuvre. Furthermore, it was found that for

the production of the same mechanical output, for both HL and RM manœuvres, more EMG was observed at 10cm than at 3cm of head height. These phenomena can be attributed to the force-length characteristics of the muscle, to the motor-unit recruitment, and to the muscle geometry relative to the electrodes.

On the pooled subjects' data, the change in lung volume does not affect significantly the Force-EMG relationship. This may be attributed to the following :

- 1) the great variability in the data hide any real significant effect due to lung volume,
- 2) the position of the SCM muscle on the force-length curve does not change sufficiently,
- 3) the change in lung volume does not change sufficiently the position of the SCM muscle relative to the electrodes to notice any effect on the recorded EMG.

By relating the two mechanical output forces, one can determine a new method of defining the function of the SCM muscle when it is used as an inspiratory muscle. The results show that for a head height of 3cm above the bed, the same SCM EMG activation is necessary when a maximum inspiratory muscle pressure (MIMPS) is performed as when a mass of 4.5 times head mass is lifted with the head, while at a head height of 10cm, the same MIMPS requires as much SCM EMG as a head lift of 1.3 times head mass. Furthermore, 50% of the MIMPS can be done without using the SCM muscle in normal subjects.

The HL-Fmuscle relationship at 10cm of head height is the most important curve of this experiment because the only instrument the investigator needs, to do the measurement, is the small hand-held head lift meter. There is no need to load the forehead with weights since the range of mass is mainly between zero and the mass of the subject's head. This becomes crucial in testing the SCM muscle of ICU patients: No damage to the vertebral column is likely to be sustained by voluntary lifting of the weight of the head alone. It was argued that the pattern of breathing may have an important effect on the variability. Since it is too demanding to ask a weak ICU patient to breathe using a specific pattern, we let the normal subjects breathe their own way. Free breathing consistency will therefore be kept between the normal subjects' and the weak ICU patients' experiments.

APPENDIX A

## APPENDIX A

The main statistical parameters of the ME signal are very important in the formulation of the model because investigators use them in their research. The general model presented allows cross-correlation of the MUAPT's detected at the recording site. The process adds a new term which takes into account the dependence between MUAPT's.

Consider two MUAPT's  $u_i(t)$  and  $u_j(t)$  whose MUAP's fire at  $t_a$ , for  $u_i(t)$ , and at  $t_b$ , for  $u_j(t)$  (Fig. A-1). The time dependent correlation of the MUAPT's may be expressed as:

$$R_{u_i u_j}(t_a, t_b) = u_i(t_a) * u_j(t_b) \quad (A.1)$$

For two statistically independent MUAPT's in the same contraction, the correlation is expressed as:

$$R_{u_i u_j}(t_a, t_b) = \int_0^{\infty} \lambda_i(\hat{t}) h_i(t_a - \hat{t}) d\hat{t} \int_0^{\infty} \lambda_j(\hat{t}) h_j(t_b - \hat{t}) d\hat{t} \quad (A.2)$$

The lower limit is zero because the MUAPT is only present for positive time.

Let's consider two cases:

1) Two motor units (MU's) fire in unison with identical firing rate,  $\lambda_i(t) = \lambda_j(t)$ . If the MUAPT's have a relative displacement ( $T_{ij}$ ) greater than or equal to the time duration of  $h_i(t)$  or  $h_j(t)$ , then the cross-correlation can be expres-



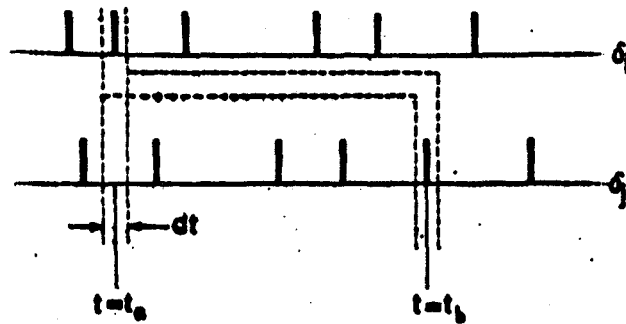


FIGURE A-1: Dirac Delta function impulse train graphically arranged to demonstrate autocorrelation and cross-correlation.

( de Luca 1975)

sed as:

$$Ru_i u_j(t_a, t_b) = \int_0^{\infty} \lambda_i(\hat{t}) h_i(t_a - \hat{t}) d\hat{t} \int_0^{\infty} \lambda_j(\hat{t}) h_j(t_b - \hat{t}) d\hat{t} \quad (A.3)$$

When  $T_{ij}$  is less than the time duration of  $h_i(t)$  or  $h_j(t)$ , then the cross-correlation is expressed as:

$$Ru_i u_j(t_a, t_b) = \int_0^{\infty} \lambda_i(\hat{t}) h_i(t_a - \hat{t}) d\hat{t} \int_0^{\infty} \lambda_j(\hat{t}) h_j(t_b - \hat{t}) d\hat{t} + \int_0^{\infty} \lambda_i(\hat{t}) h_i(t_a - \hat{t} \pm T_{ij}) h_j(t_b - \hat{t}) d\hat{t} \quad (A.4)$$

In such a case, the MUAPT's will be considered to be synchronized.

2) Two MU's fire in unison with identical firing rate,  $\lambda_i(t) = \lambda_j(t)$ , and both contain MUAP's with the same shape,  $h_i(t) = h_j(t)$ . In such a circumstance, the cross-correlation function will be identical to the auto-correlation function and can be expressed as:

$$Ru_i u_i(t_a, t_b) = \int_0^{\infty} \lambda_i(\hat{t}) h_i(t_a - \hat{t}) d\hat{t} \int_0^{\infty} \lambda_i(\hat{t}) h_i(t_b - \hat{t}) d\hat{t} + \int_0^{\infty} \lambda_i(\hat{t}) h_i(t_a - \hat{t}) h_i(t_b - \hat{t}) d\hat{t} \quad (A.5)$$

Let's go further in the analysis by giving more statistical dependence between the two MUAPT's, i.e., by putting  $t_a = t_b = t$ . Both mathematical expressions represent the same MUAPT. The cross-correlation function, being identical to the auto-correlation function, is now simplified as:

$$Ru_i u_i(t) = \left[ \int_0^{\infty} \lambda_i(\hat{t}) h_i(t - \hat{t}) d\hat{t} \right]^2 + \int_0^{\infty} \lambda_i(\hat{t}) h_i^2(t - \hat{t}) d\hat{t} \quad (A.6)$$

$$\begin{aligned}
&= [E(u_i(t))]^2 + \sigma_{u_i(t)}^2 \\
&= [\text{mean}]^2 + \text{Variance} \\
&= (\text{rms})^2
\end{aligned}$$

Disregarding the polarization of some recording electrodes, the ME signal has a mean value of zero. Therefore, the (rms)<sup>2</sup> value is equal to the variance  $\sigma_{u_i(t)}^2$ . One ends up with the main parameters of the MUAPT model presented in Chapter IV, section 4.3.

The ME model composed of two MUAPT's can be extended to many more, acting in the same contraction. The ME signal is represented as the spatial-temporal superposition of the individual MUAPT's that are active in the vicinity of the electrodes.

$$m(t) = \sum_{i=1}^S u_i(t) \quad (\text{de Luca \& Vandik 1975}) \quad (\text{A.7})$$

The above equation assumes that the number of active MUAPT's remain constant throughout the constant contraction. The auto-correlation of the ME signal allows us to find the expressions for the mean, the variance, and the rms value.

$$R_{mm}(t_a, t_b) = \sum_{i=1}^S \sum_{j=1}^S R_{u_i u_j}(t_a, t_b) \quad (\text{A.8})$$

Before summing the correlation functions, it is necessary to consider that some of the MUAPT's ( $v \leq S$ ) may be synchronized at some time throughout the contraction. Then, the auto-correlation function of the ME signal may be expressed as:

$$\begin{aligned}
R_{mm}(t_a, t_b) &= \sum_{i=1}^s \sum_{j=1}^s \int_0^{\infty} \lambda_i(\hat{t}) h_i(t_a - \hat{t}) d\hat{t} \int_0^{\infty} \lambda_j(\hat{t}) h_j(t_b - \hat{t}) d\hat{t} \\
&+ \sum_{i=1}^s \int_0^{\infty} \lambda_i(\hat{t}) h_i(t_a - \hat{t}) h_i(t_b - \hat{t}) d\hat{t} \\
&+ \sum_{i=1}^s \sum_{j=1}^s \int_0^{\infty} \lambda_i(\hat{t}) h_i(t_a - \hat{t} \pm T_{ij}) h_j(t_b - \hat{t}) d\hat{t} \quad (A.9)
\end{aligned}$$

(de Luca & Vandik 1975)

Restricting the analysis to the case where  $t_a = t_b = t$ , i.e., considering the auto-correlation of the ME signal when there is no relative shift, the above equation becomes:

$$\begin{aligned}
R_{mm}(t) &= \left[ \sum_{i=1}^s \int_0^{\infty} \lambda_i(\hat{t}) h_i(t - \hat{t}) d\hat{t} \right]^2 + \sum_{i=1}^s \int_0^{\infty} \lambda_i(\hat{t}) h_i^2(t - \hat{t}) d\hat{t} \\
&+ \sum_{i=1}^s \sum_{j=1}^s \int_0^{\infty} \lambda_i(\hat{t}) h_i(t - \hat{t} \pm T_{ij}) h_j(t - \hat{t}) d\hat{t} \quad (A.10) \\
&= [E(m(t))]^2 + \sigma_m^2(t) \\
&= (\text{mean})^2 + \text{Variance} \\
&= (\text{rms})^2
\end{aligned}$$

By approximating  $h_i(t)$  by  $K_i(t)$ , the above equation can be simplified as:

$$\begin{aligned}
R_{mm}(t) &= \left[ \sum_{i=1}^s \lambda_i(t) \frac{h_i(t)}{K_i(t)} \right]^2 + \sum_{i=1}^s \lambda_i(t) \frac{h_i^2(t)}{K_i^2(t)} \\
&+ \sum_{i=1}^s \sum_{j=1}^s \lambda_i(t) \frac{c_{ij}^2(t)}{K_i^2(t)} \quad (A.11)
\end{aligned}$$

This equation does not demonstrate the effect of the cancellation that results when positive and negative phases of different MUAP's superimpose. The cancellation will not affect the variance term, because of the  $h_i^2(t)$  term, but will affect only the mean term by reducing it. Consequently, a non positive function,  $J(t) \leq 0$ , must be added to the mean term to

give:

$$E[|m(t)|] = E\left[\sum_{i=1}^s |u_i(t)|\right] + J(t) \quad (\text{A.12})$$

Furthermore, the synchronization term,  $D(t)$ , reduces

$$D(t) = \sum_{i=1}^V \sum_{j=1}^V \int_0^{\infty} \lambda_i(\hat{t}) h_i(t-\hat{t} \pm T_{ij}) h_j(t-\hat{t}) d\hat{t} \quad (\text{A.13})$$

the mean-squared term because these MUAPT's do not correlate with each other. Thus, an extra term is added to the expression of the mean-squared value of the ME signal to give:

$$\text{MS}[m(t)] = \sum_{i=1}^s \text{MS}[u_i(t)] + D(t) \quad (\text{A.14})$$

where  $D(t) < 0$  or  $0 < D(t)$ .

Finally, the three main parameters of the ME signal can be expressed as:

1) Mean rectified value

$$E[|m(t)|] = \lambda(t) \sum_{i=1}^s |h_i(t)| + J(t) \quad (\text{A.15})$$

Full-wave rectification may be realized by taking the absolute value of  $h_i(t)$  and  $m(t)$ .

2) Mean integrated rectified value

$$\begin{aligned} E\left[\int_0^T |m(t)| dt\right] &= \int_0^T E[|m(t)|] dt \\ &= \int_0^T \lambda(t) \sum_{i=1}^s |h_i(t)| dt + \int_0^T J(t) dt \end{aligned} \quad (\text{A.16})$$

and if the value of  $h_i(t)$  remains constant during the contraction,

$$E \left[ \int_0^T |m(t)| dt \right] = \sum_{i=1}^S \frac{|h_i(t)|}{\lambda(t)} \int_0^T \lambda(t) dt + \int_0^T J(t) dt \quad (\text{A.17})$$

3) Root-mean-squared value

$$\text{rms}(m(t)) = \lambda(t)^{\frac{1}{2}} \left[ \sum_{i=1}^S h_i^2(t) + \sum_{i=1}^V \sum_{j=1}^V c_{ij}^2(t) \right]^{\frac{1}{2}} \quad (\text{A.18})$$

since the ME signal has zero mean.

APPENDIX B

## APPENDIX B-1

### Principle of Least Squares.

A simple illustration of the principle is as follow. Suppose  $x_i$  is the measurement of a quantity whose true value is  $T$ . Then  $\xi_i = x_i - T$  is the error in the measurement. If the measurement is repeated, one can end up with several errors. Let us call the sum of their square as:

$$E = \sum_{i=1}^n \xi_i^2 = \sum \{x_i - T\}^2 \quad (E.1)$$

where  $\sum_{i=1}^n$  is replaced by  $\sum$ .

According to the principle of least squares, the best choice for  $T$  is the one that makes  $E$  a minimum. At its minimum value,

$$\frac{\partial E}{\partial x} = 2 \sum (x_i - T) = 2 \sum x_i - 2nT = 0 \quad (E.2)$$

or  $T = \frac{\sum x_i}{n}$  which is nothing but the mean of  $n$  measurements.

Now suppose that one has two sets of data  $X$  and  $Y$  connected by a linear relationship  $Y = \alpha + \beta X$ , where  $\alpha$  and  $\beta$  are constants. The problem of determining the best line is nothing but evaluating and using the principle of least squares.



For example let us assume that X-values are fairly accurately known and error is associated with Y-values only. Suppose a and b are the least squares choices for  $\alpha$  and  $\beta$  respectively. Then  $a + bX_i$  is the calculated or the estimated Y whose actual value is  $Y_i$ . Therefore,

$$[ Y_i - (a + bX_i) ] = \epsilon_i \text{ is its error.} \quad (\text{B.3})$$

To satisfy the principle of least squares,

$$\sum [ Y_i - (a + bX_i) ]^2 = E \quad (\text{E.4})$$

must be minimum which means  $\partial E / \partial a = 0$  and  $\partial E / \partial b = 0$ .

Solving these equations, we get:

$$a = \frac{\sum Y_i \sum X_i^2 - \sum X_i \sum X_i Y_i}{n \sum X_i^2 - (\sum X_i)^2} \quad \text{and} \quad b = \frac{n \sum X_i Y_i - \sum X_i \sum Y_i}{n \sum X_i^2 - (\sum X_i)^2} \quad (\text{E.5})$$

a and b, as defined above, are known as REGRESSION COEFFICIENTS. They determine the so-called REGRESSION LINE :  $Y_c = a + bX$ .

The errors in a, b, and  $Y_c$  can be estimated. The regression line represents an average estimating line because it does not pass through all experimental points. Its overall reliability is measured by the so-called standard error of estimate,  $S_{y.x}$ , which is a measure of the scatter among  $Y_i$ 's around the average

$$S_{y.x} = \left[ \frac{\sum (Y_i - Y_c)^2}{(n - 2)} \right]^{\frac{1}{2}} \quad (\text{E.6})$$

line. By developing the equation L.6 and by replacing  $Y_0$  by its expression,  $a + bX_i$ ,  $S_{y.x}$  can take the following form:

$$S_{y.x} = \left[ \frac{\sum Y_i^2 - (a \sum Y_i + b \sum X_i Y_i)}{(n - 2)} \right]^{\frac{1}{2}} \quad (\text{B.7})$$

The errors in the coefficients  $a$  and  $b$  arise because of the errors in  $Y$ 's.  $X$ 's are assumed to be fairly accurately known. Going through a series of mathematical equations, the standard deviation of the coefficients can be expressed as:

$$S(a) = \left[ \frac{\sum X_i^2}{(n \sum X_i^2 - (\sum X_i)^2)} \right]^{\frac{1}{2}} S_{y.x} \quad (\text{L.8})$$

and

$$S(b) = \left[ \frac{n}{(n \sum X_i^2 - (\sum X_i)^2)} \right]^{\frac{1}{2}} S_{y.x} \quad (\text{L.9})$$

The method just described has been written under the form of a computer program. The computer language used is BASIC adapted for the Hp 87 microcomputer.

Once the regression line was found, the goodness of the fit had to be tested by calculating the coefficient of determination ( $r^2$ ). Its value is between zero and one. A  $r^2 = 1$  indicates that all the experimental points fall on the regression line (perfect fit). This coefficient is expressed as:

$$r^2 = \frac{\Sigma(Y_i - \bar{Y})^2}{\Sigma(Y_i - \bar{Y})^2} = \frac{\Sigma(X_i - \bar{X})(Y_i - \bar{Y})}{[\Sigma(X_i - \bar{X})^2 \Sigma(Y_i - \bar{Y})^2]} \quad (E.10)$$

where  $\bar{Y}$  is the mean value of  $Y$ 's.

Once the appropriate substitutions are made, the  $r^2$  value can be represented in a more useful expression:

$$r^2 = \left[ \frac{\Sigma X_i Y_i - (\Sigma X_i \Sigma Y_i)/n}{\Sigma X_i^2 - (\Sigma X_i)^2/n} \right] \left[ \frac{\Sigma X_i Y_i - \Sigma X_i \Sigma Y_i/n}{\Sigma Y_i^2 - (\Sigma Y_i)^2/n} \right] \quad (E.11)$$

The square root of  $r^2$ ,  $r$ , is called the coefficient of correlation. The value of  $r$  determines how closely the variables  $Y_i$  and  $Y_{ci}$  are associated. The value of  $r$  varies from -1 to +1. The sign of  $r$ , indicated by the sign of  $\Sigma(X_i - \bar{X})(Y_i - \bar{Y})$ , implies the sign of the slope of the regression line. Most investigators use the coefficient of determination,  $r^2$ , because it indicates that the regression equation accounts for  $(r^2 \times 100)\%$  of the variability of the data about  $\bar{X}$ .

APPENDIX B-1  
BEST FITTED STRAIGHT LINE

```

10 OPTION BASE 1
15 PRINTER IS 701
20 MASS STORAGE IS ":D701"
30 DISP "CURVE EQUATION PROGRAM NO.1 831031"
40 DISP "IT FINDS THE EQUATION Y=A+BX"
50 WAIT 2000
60 DIM X(50,2),Y(50,2),Z(50,2)
70 XX=0 @ YY=0 @ XY=0
80 XXS=0 @ YYS=0 @ XYSS=0
90 XM=0 @ YM=0 @ XSQ=0 @ YSQ=0
100 D=0 @ A=0 @ B=0
110 I=1 @ M=1
120 DISP "FILENAME";@ INPUT F$
130 ON ERROR GOTO 120
140 ASSIGN# 1 TO F$
150 READ# 1 ; N
160 FOR I=1 TO N
170 READ# 1 ; X(I,1),X(I,2)
180 DISP USING 220 ; I,X(I,1),X(I,2)
190 NEXT I
200 OFF ERROR
210 ASSIGN# 1 TO *
220 IMAGE "N=",2D.,2X,"X=",6D.3D,2X,"Y=",6D.3D
230 I=1
240 FOR I=1 TO N
250 XX=XX+X(I,1)
260 YY=YY+X(I,2)
270 XXS=XXS+X(I,1)^2
280 YYS=YYS+X(I,2)^2
290 XY=XY+X(I,1)*X(I,2)
300 NEXT I
310 XM=XX/N
320 YM=YY/N
330 XSQ=XXS-XM*XX
340 YSQ=YYS-YM*YY
350 XYSS=XY-XM*YM
360 B=XYSS/XSQ
370 A=YM-B*XM
380 D=XYSS^2/(XSQ*YSQ)
390 Syx=SQR ((YYS-(A*YY+B*XY))/(N-2))
400 SB=SQR (N/(N*XXS-XX^2))*Syx
410 SA=SQR (XXS/(N*XXS-XX^2))*Syx
420 DISP "ESTIMATING EQUATION YC=A+BX AND ITS STANDARD ERROR Syx ARE"
430 DISP USING 440 ; A,SA,B,SB,Syx
440 IMAGE "Yc =",3D.3D,2X,3D.3D," + ",3D.3D,2X,3D.3D,"X",5X,"Syx="3D.3
450 DISP USING 460 ; D

```

```

460 IMAGE "THE COEFFICIENT OF DETERMINATION ( R^2 ) IS :",1D.3D
465 PRINT " FOR THE INPUT FILENAME ";F$
470 PRINT "ESTIMATING EQUATION Yc=A+BX AND ITS STANDARD ERROR Syx AR
480 PRINT USING 440 ; A,SA,B,SB,Syx
490 PRINT USING 460 ; D
500 FOR I=1 TO N
510 Y(I,1)=X(I,1)
515 Y(I,2)=A+B*X(I,1)
520 NEXT I
522 Y(N+1,1)=(-A)/B
523 Y(N+1,2)=0
525 M=N+1
526 FOR I=1 TO M
527 Z(I,1)=Y(I,1) @ Z(I,2)=Y(I,2)
528 DISP USING 530 ; Z(I,1),Z(I,2)
529 NEXT I
530 IMAGE "X=",6D.3D,3X,"Y=",6D.3D
540 DISP "OUTPUT TO FILE, Y/N";
550 INPUT R$
560 IF UPC$(R$(1,1))="Y" THEN GOTO 590
570 IF UPC$(R$(1,1))#"N" THEN BEEP @ GOTO 540
580 GOTO 830
590 DISP "OUTPUT FILENAME";@ INPUT FO$
600 ON ERROR GOTO 620
610 GOTO 630
620 OFF ERROR @ IF ERRN =63 THEN GOTO 630 ELSE 670
630 DISP "FILE ALREADY EXISTS. STORE OVER IT";@ INPUT R$
640 IF UPC$(R$(1,1))="Y" THEN GOTO 800
650 IF UPC$(R$(1,1))#"N" THEN BEEP @ GOTO 630
660 GOTO 830
670 DISP "ERROR NO.",ERRN @ PAUSE
680 DISP "CREATE FILE, Y/N";
690 INPUT R$
700 IF UPC$(R$(1,1))="Y" THEN GOTO 730
710 IF UPC$(R$(1,1))#"N" THEN BEEP @ GOTO 680
720 GOTO 830
730 CREATE FO$,3
740 ASSIGN# 1 TO FO$
750 PRINT# 1 ; M
760 FOR I=1 TO M
770 PRINT# 1 ; Z(I,1),Z(I,2)
780 NEXT I
790 GOTO 810
800 PURGE F$ @ GOTO 680
810 OFF ERROR
820 ASSIGN# 1 TO *
830 DISP "DONE!"
840 END

```

APPENDIX E-2

E-2-1 Statistical analysis

The technique used will be entirely described for slopes. For the case of intercepts, only the final equations will be given because the technique is similar.

Suppose a series of  $n$  observations of pairs  $(X, Y)$  can be partitioned into  $r$  groups with  $n_i$  pairs in the  $i^{\text{th}}$  group such that  $n_1 + n_2 + \dots + n_r = n$ . Assume a simple linear regression model for each group of observations with a common error variance  $S^2$  for all groups (tested using the Bartlett's test). The hypothesis to test is:  $H_0: \beta_1 = \beta_2 = \dots = \beta_r$ , the equality of the  $r$  slopes of  $r$  regression lines. As defined before,  $b$  is the least squares best choice for  $\beta$ .

Considering the case  $r = 2$ , the variance of  $b_1 - b_2$  is  $S_{b_1}^2 + S_{b_2}^2$ . Since  $E(b_1 - b_2) = \beta_1 - \beta_2 = 0$  under  $H_0: \beta_1 = \beta_2$  and since  $b_1 - b_2$  has a normal distribution with mean  $\beta_1 - \beta_2$  and variance  $S_{b_1}^2 + S_{b_2}^2$ , then the statistic

$$T = \frac{b_1 - b_2}{\sqrt{\frac{S_{y \cdot x_1}^2}{\sum(x_{1j} - \bar{x}_1)^2} + \frac{S_{y \cdot x_2}^2}{\sum(x_{2j} - \bar{x}_2)^2}}} \quad (E-1)$$

has a  $t$ -distribution with  $n_1 + n_2 - 4$  degrees of freedom. To test the hypothesis  $H_0$ , the procedure is to use the statistic  $T$  with



rejection region  $T > t_{\nu, 1-\frac{\alpha}{2}}$  or  $T < t_{\nu, \frac{\alpha}{2}}$  where  $\nu = n_1 + n_2 - 4$ .

In the case  $r$  is greater than two, the general slope obtained by treating all the individual groups as one large group is  $b_p$  where

$$b_p = \frac{\sum_{i=1}^r \sum_{j=1}^{n_i} (X_{ij} - \bar{X})(Y_{ij} - \bar{Y})}{\sum_{i=1}^r \sum_{j=1}^{n_i} (X_{ij} - \bar{X})^2} \quad (E-2)$$

where  $\bar{X}$  and  $\bar{Y}$  denote the overall means using all  $n = \sum_{i=1}^r n_i$  values. The error sum of squares of the  $i^{\text{th}}$  group is  $S_{y \cdot x_i^2}$ , and the pooled error sum of squares is  $S_1 = \sum_{i=1}^r S_{y \cdot x_i^2}$ . The total sum of squares based on all  $r$  data sets collectively, can be partitioned as:

$$\begin{aligned} \sum_{i=1}^r \sum_{j=1}^{n_i} (Y_{ij} - \bar{Y})^2 &= \sum_{i=1}^r S_{y \cdot x_i^2} + \sum_{i=1}^r \sum_{j=1}^{n_i} (b_i - b_p)^2 (X_{ij} - \bar{X}_i)^2 \\ &\quad + b_p^2 \sum_{i=1}^r \sum_{j=1}^{n_i} (X_{ij} - \bar{X}_i)^2 \quad (E-3) \\ &= S_1 + S_2 + S_3 . \end{aligned}$$

The term  $S_1$  is the pooled error sum of squares of each regression curve,  $S_2$  is the sum of squares due to differences between group slopes, and  $S_3$  is the sum of squares due to the general slope  $b$ .

The statistic used is:

$$F = [S_2/(r-1)] / [S_1/(n-2r)] \quad (E-4)$$

has a  $F$ -distribution with  $(r-1)$  and  $(n-2r)$  degrees of freedom

if  $\beta_1 = \beta_2 = \dots = \beta_r = \beta$ . Thus the critical region for  $H_0: \beta_1 = \beta_2 = \dots = \beta_r$  is  $F > F_{v_1, v_2, 1-\alpha}$  where  $v_1 = r-1$ ,  $v_2 = n-2r$ , and  $\alpha$  is the significant level.

If  $H_0$  is accepted, then the slope of the pooled regression line is  $b_p$  and its variance,  $S_{b_p}^2$ , can be expressed as:

$$S_{b_p}^2 = \left[ \sum_{i=1}^r S_{y \cdot x_i}^2 / (n-2r) \right] / \left[ \sum_{i=1}^r \sum_{j=1}^{n_i} (X_{ij} - \bar{X}_i)^2 \right] \quad (E-5)$$

For the case of the intercepts, the same technique was used. For testing the homogeneity between the intercepts of  $r$  regression lines, the general intercept obtained by treating all the individual groups as one large group is  $a_p$ , where

$$a_p = \frac{\sum_{i=1}^r \sum_{j=1}^{n_i} X_{ij} (\bar{Y} - \bar{Y}_i)}{\sum_{i=1}^r \sum_{j=1}^{n_i} (X_{ij} - \bar{X}_i)^2} \quad (E-6)$$

where  $\bar{X}$  and  $\bar{Y}$  denote the overall means using all  $n$  values.

As before, the total sum of squares based on  $r$  data sets collectively can be expressed as:

$$\begin{aligned} \sum_{i=1}^r \sum_{j=1}^{n_i} (Y_{ij} - \bar{Y})^2 &= \sum_{i=1}^r S_{y \cdot x_i}^2 + \sum_{i=1}^r \sum_{j=1}^{n_i} (a_i - a_p)^2 (X_{ij} - \bar{X}_i)^2 / \sum_{i=1}^r \left( \sum_{j=1}^{n_i} X_{ij}^2 / n_i \right) \\ &\quad + a_p^2 \sum_{i=1}^r \sum_{j=1}^{n_i} (X_{ij} - \bar{X}_i)^2 / \sum_{i=1}^r \left( \sum_{j=1}^{n_i} X_{ij}^2 / n_i \right) \quad (B-7) \\ &= S1 + A2 + A3 \end{aligned}$$

similarly, the statistic is:

$$F = [A2/(r-1)] / [S1/(n-2r)] \quad (B-8)$$



If the hypothesis  $H_0: \alpha_1 = \alpha_2 = \dots = \alpha_r = \alpha$  is accepted, then the intercept of the pooled regression line is  $a_p$  and its variance  $S_{ap}^2$  can be expressed as:

$$S_{ap}^2 = \left[ \sum_{i=1}^r S_{y \cdot x_i}^2 / (n-2r) \right] / \left[ \sum_{i=1}^r \sum_{j=1}^{n_i} (X_{ij} - \bar{X}_i)^2 / \sum_{i=1}^r \left( \sum_{j=1}^{n_i} X_{ij}^2 / n_i \right) \right] \quad (E-9)$$

This technique turned out to be very useful for simplifying data manipulations. This analysis was performed by the Hp 87 microcomputer.

The whole technique can be used to test two or more regression lines. The t-test does not need to be used.

#### E-2-2 The Bartlett's test

The Bartlett's  $\chi^2$ -test was used to test the homogeneity of the variances.

Let  $S_1^2, S_2^2, \dots, S_k^2$  be  $k$  independent sample variances with degrees of freedom  $\nu_1, \nu_2, \dots, \nu_k; \nu_i (i = 1, 2, \dots, k)$  where  $\nu_i = n_i - 1$ . Here it is considered that a sample is represented by a set of data, and then  $S^2 = S_{y \cdot x}^2$ . Let's put  $\nu = \sum_{i=1}^k \nu_i$ ,  $S = \sum_{i=1}^k \nu_i S_i^2 / \nu$ , and  $C = 1 + \left[ \left( \sum_{i=1}^k \frac{1}{\nu_i} \right) - \frac{1}{\nu} \right] / (3(k-1))$ . As the test criterion, one uses the quantity

$$\chi = \left( \nu \ln S^2 - \sum_{i=1}^k \nu_i \ln S_i^2 \right) / C \quad (E-10)$$

The rejection region for testing  $H_0: S_1^2 = S_2^2 = \dots = S_k^2$  is  $\chi > \chi_{k-1}^2(1-\alpha)$  where  $\alpha$  represents the level of significance.

APPENDIX B-2  
STATISTICS ON THE STRAIGHT LINES

```

10  OPTION BASE 1
20  MASS STORAGE IS ":D701"
30  DISP "STAT PROGRAM 831126"
40  DISP "THIS PROGRAM COMPARES SEVERAL SETS OF DATA."
50  DISP "IT TESTS THE HOMOGENEITY OF THE INTERCEPTS AND SLOPES OF"
60  DISP "THE STRAIGHT LINES TESTED. IT TESTS THE PRECISION BY PERFORMING"
70  DISP "A F TEST. THE OUTPUT WILL TELL WHETHER THE CURVES ARE HOMOGENEOUS."
80  DISP "THE INPUT FILES MUST BE THE ONES USED TO GET THE CURVES EQUATION."
90  DIM X(100,50),Y(100,2),U(25,4),N(25),WBU(25),XMEAN(25),XX(25),WBOSIG(25)
100 DISP "THE FIRST OBJECTIVE IS TO SEE WHETHER THE CURVES VARIANCE (Vy.x)"
110 DISP "ARE HOMOGENEOUS, AND WHETHER THEY CAN BE REPLACED BY ONLY ONE"
120 DISP "VALUE (v). THEREFORE, A BARTLETT'S TEST IS PERFORMED."
130 DISP "      THE OPERATOR MUST MAKE THE ENTRY USING THE KEYBOARD."
140 DISP "THE A VALUE IS THE Sy.x OF EACH LINE, WHILE THE B VALUE CONTAINS"
150 DISP "THE NUMBER OF POINTS PER LINE; THE C VALUE IS THE SLOPE OF EACH"
160 DISP "LINE, AND THE D VALUE IS THE INTERCEPT OF EACH LINE."
170 DISP "HOW MANY LINES DO YOU HAVE TO TEST";@ INPUT NA
180 MU=0 @ VAR=0 @ C=0 @ VARR=0 @ SB1=0 @ SBU=0 @ T0=0 @ T1=0 @ M=0
190 INV=0 @ LOGV=0 @ T=0 @ BOB0=0 @ B1B1=0 @ WBA=0 @ VYX=0 @ AB=0
200 FOR I=1 TO NA
210 DISP "Sy.x(";I;")","N(";I;)","Slope(";I;)","Int(";I;)" ;
220 INPUT U(I,1),U(I,2),U(I,3),U(I,4)
230 NEXT I
235 FOR I=1 TO NA
240 U(I,1)=U(I,1)^2 @ U(I,2)=U(I,2)-1
250 MU=MU+U(I,2)
260 VAR=VAR+U(I,1)*U(I,2)
270 INV=INV+1/U(I,2)
280 LOGV=LOGV+LOG (U(I,1))*U(I,2)
290 NEXT I
300 C=1+(INV-1/MU)/(3*(NA-1))
310 VAR=VAR/MU
320 T=(MU*LOG (VAR)-LOGV)/C
330 DISP "THE OUTPUT (T) IS DISTRIBUTED AS CHI-SQUARE OF (NO. OF LINES-1)"
340 DISP "WE REJECT HOMOGENEITY AT THE SIGNIFICANCE LEVEL (alpha) IF THE"
350 DISP "REALIZATION OF (T), (t), IS SUCH THAT t >or= TO CHI-SQUARE(1-alpha)"
360 DISP "THE (1-alpha) QUANTILE OF THE DISTRIBUTION OF CHI-SQUARE(NO. OF"
370 DISP "LINES - 1)."

```

```

450 IF UPC$ (R$(1,1))# "N" THEN BEEP @ GOTO 430
460 GOTO 1180
465 I=1 @ J=1 @ WBOBO=0 @ WB=0 @ WB1B1=0 @ XINT=0 @ XSLO=0
470 FOR I=1 TO NA
480 DISP "INPUT FILENAME NO. "; I; ". ";
490 INPUT F$
500 ON ERROR GOTO 480
510 ASSIGN# 1 TO F$
520 READ# 1 ; N(I)
540 FOR J=1 TO N(I)
550 READ# 1 ; X(J,I), X(J,NA+I)
560 DISP USING 580 ; J, X(J,I), X(J,NA+I)
570 NEXT J
580 IMAGE "ROW NO. ", 2D, 2X, "X=" 6D.3D, 2X, "Y=" , 6D.3D
585 ASSIGN# 1 TO *
590 OFF ERROR
592 M=M+(N(I)-2)
595 NEXT I
597 I=1 @ K=1 @ L=1
600 FOR I=1 TO NA
605 XMEAN(I)=0 @ XX(I)=0 @ WBOSIG(I)=0 @ WBO=0
610 FOR K=1 TO N(I)
620 XMEAN(I)=XMEAN(I)+X(K,I)
630 XX(I)=XX(I)+X(K,I)^2
640 NEXT K
650 XMEAN(I)=XMEAN(I)/N(I)
655 FOR L=1 TO N(I)
660 WBOSIG(I)=WBOSIG(I)+(X(L,I)-XMEAN(I))^2
665 NEXT L
670 WBO(I)=N(I)*WBOSIG(I)/XX(I)
680 WBOBO=WBOBO+WBO(I)*U(I,4)
690 WB=WB+WBO(I)
700 WB1B1=WB1B1+WBOSIG(I)*U(I,J)
710 WBA=WBA+WBO(I)
720 VYX=VYX+U(I,1)
730 NEXT I
740 XINT=WBOBO/WB
750 XSLO=WB1B1/WBA
760 FOR I=1 TO NA
770 BOBO=BOBO+(U(I,4)-XINT)^2*WBO(I)
780 B1B1=B1B1+(U(I,3)-XSLO)^2*WBOSIG(I)
790 NEXT I
800 T0=BOBO/(NA-1)/VYX
810 T1=B1B1/(NA-1)/VYX
815 MB=NA-1
820 SBO=SQR (VYX/WB)
830 SBL=SQR (VYX/WBA)
831 DISP USING 835 ; MB,M
833 PRINT USING 835 ; MB,M
835 IMAGE "T IS DISTRIBUTED AS F(", 2D, ", ", 3D, ")"
840 DISP USING 850 ; T0,T1
850 IMAGE "FOR INTERCEPT T=", 4D.3D, 6X, "FOR SLOPE T=", 4D.3D
860 PRINT USING 850 ; T0,T1
870 DISP "HAS HOMOGENEITY BEEN PROVEN FOR SLOPE AND INTERCEPT Y/N" @ INPUT

```

```
880 IF UPC$ (R$(1,1))="Y" THEN GOTO 905
890 IF UPC$ (R$(1,1))#"N" THEN BEEP @ GOTO 870
900 GOTO 1180
905 VARR=SQR (VAR)
910 DISP USING 930 ; XINT,SB0,XSLO,SB1,VARR
920 PRINT USING 930 ; XINT,SB0,XSLO,SB1,VARR
930 IMAGE "Y=",4D.3D,2X,4D.3D,3X,"+",3X,4D.3D,2X,4D.3D,X,"X",3X,"Sy.x=",1D.
940 DISP "MINIMUM VALUE OF X" @ INPUT C
950 DISP "MAXIMUM VALUE OF X" @ INPUT D
960 DISP "STEP VALUE " @ INPUT E
970 J=0
980 FOR I=D TO C STEP -E
990 IF I<C THEN GOTO 1040
1000 J=J+1
1010 Y(J,1)=I
1020 Y(J,2)=XINT+XSLO*I
1030 NEXT I
1040 DISP "CREATE FILE " @ INPUT R$
1050 IF UPC$ (R$(1,1))="Y" THEN GOTO 1080
1060 IF UPC$ (R$(1,1))#"N" THEN BEEP @ GOTO 1040
1070 GOTO 1180
1080 DISP "OUTPUT FILENAME" @ INPUT FO$
1090 ON ERROR GOTO 1080
1095 GOTO 1100
1100 CREATE FO$,3
1110 ASSIGN# 1 TO FO$
1120 PRINT# 1 ; J
1130 FOR I=1 TO J
1140 PRINT# 1 ; Y(I,1),Y(I,2)
1150 DISP USING 580 ; I,Y(I,1),Y(I,2)
1155 NEXT I
1160 OFF ERROR
1170 ASSIGN# 1 TO *
1180 DISP "DONE!" @ END
```

APPENDIX C

**Note:**

In the graphs, every lung volume line has its own symbol. The following table gives the correspondence between the symbols and the lung volumes.

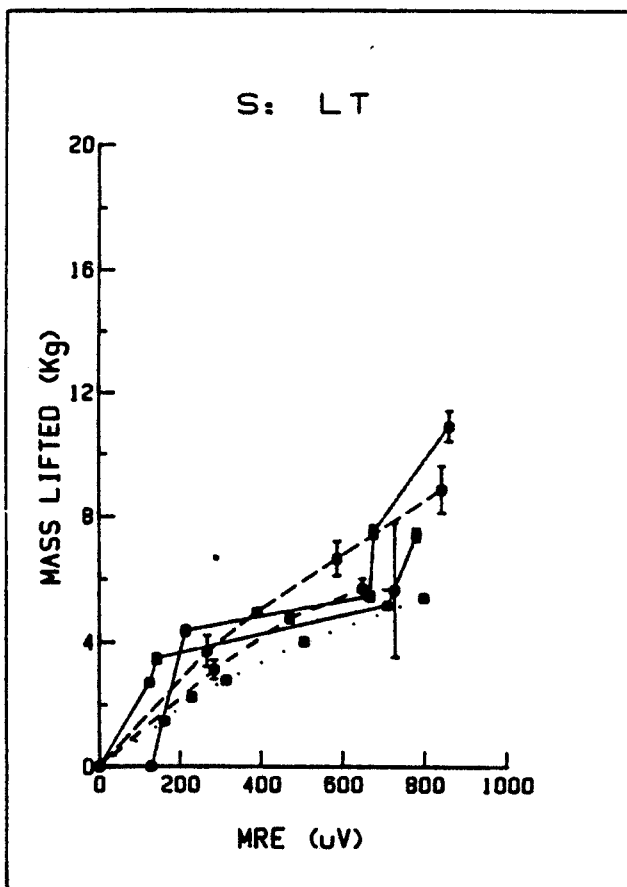
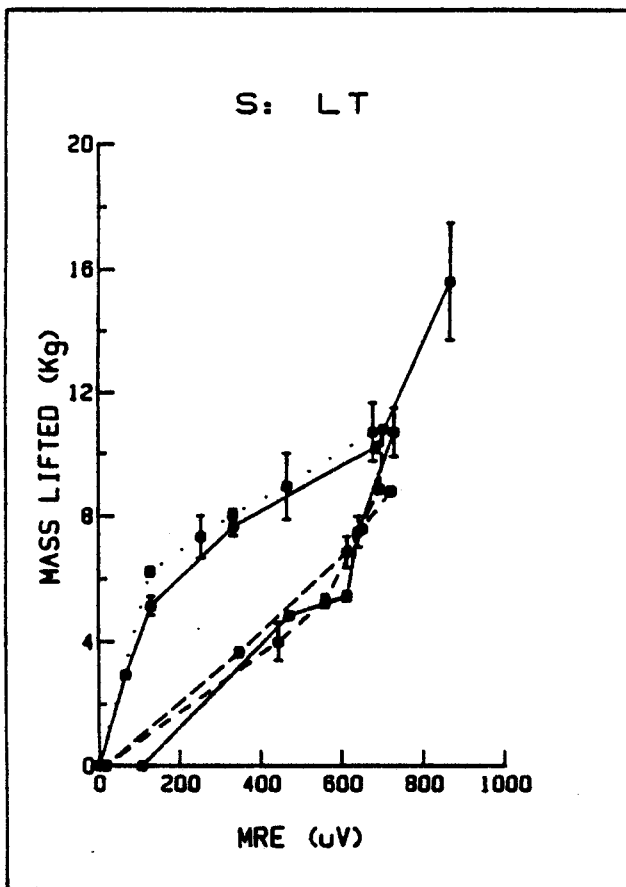
Lung Volume	Symbol
FRC	————
FRC+.5L	.....
FRC+1L	- - - -
FRC+2L	- - - -
TLC	-.....-

RAW DATA

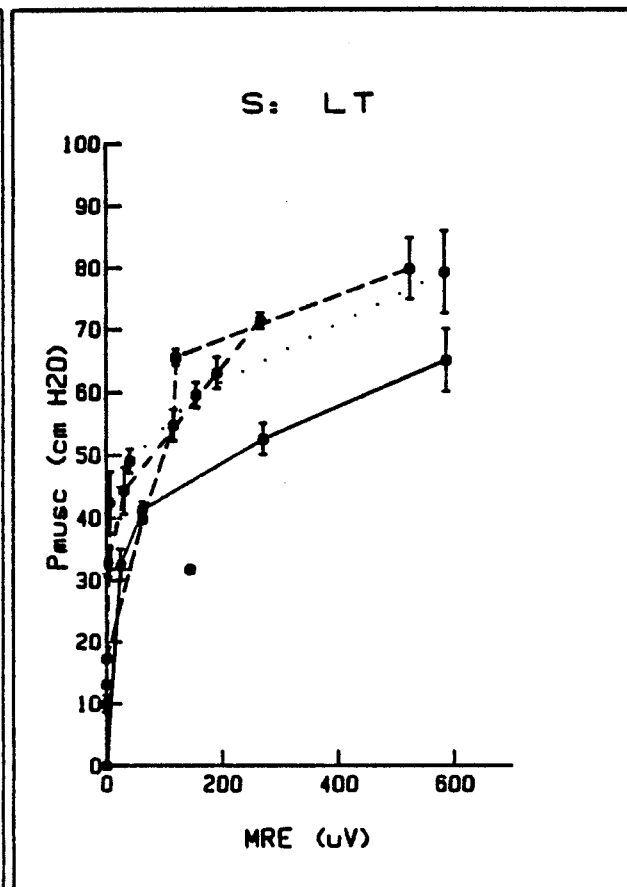
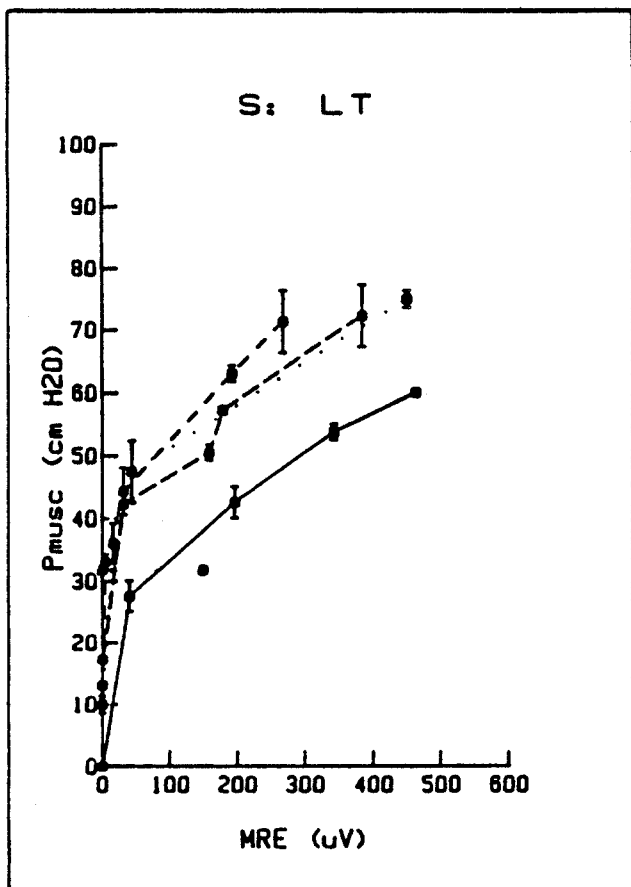
SUBJECT	LUNG VOLUME	HEAD LIFT MANOEUVRE				RESPIRATORY FUNCTION MANOEUVRE			
		EMG (uV)		HL (kg)		EMG (uV)		P <sub>musc</sub> (cm H <sub>2</sub> O)	
		VALUE ± S.D		VALUE ± S.D		VALUE ± S.D		VALUE ± S.D	
LT	FRC	865.454	51.426	15.600	1.900	462.220	0.000	60.000	.100
		682.910	91.538	10.188	.156	342.230	4.450	53.750	1.250
		333.331	8.568	7.659	.294	195.560	35.560	42.500	2.500
		129.455	18.513	5.133	.296	40.000	4.440	27.500	2.500
		66.364	9.000	2.928	.036	0.000	0.000	0.000	0.000
		0.000	0.000	0.000	0.000				
	FRC + 0.5L	676.364	10.285	10.700	.955	448.000	16.000	74.870	1.392
		465.455	29.091	8.947	1.058	44.000	12.000	47.370	4.928
		331.818	24.438	8.050	.177	16.000	0.000	35.995	3.160
		252.727	12.856	7.330	.674	0.000	0.000	9.870	1.392
		127.273	12.422	6.217	.141				
		0.000	0.000	0.000	0.000				
	FRC + 1L	720.000	8.890	8.800	0.000	435.560	0.000	88.025	5.000
		648.890	8.890	7.600	.100	346.670	44.450	74.275	1.250
		560.000	62.220	5.300	.200	102.200	4.530	49.275	3.750
		444.450	88.890	4.000	.600	26.670	8.890	39.275	1.250
		15.802	19.555	0.000	0.000	0.000	0.000	13.025	0.500
	FRC + 2L	702.220	8.890	10.800	.100	382.230	26.670	72.238	5.000
		693.330	0.000	8.850	.050	177.780	35.560	57.238	.100
		613.340	26.670	6.850	.500	157.780	2.220	50.488	1.250
		346.670	8.890	3.650	.150	31.120	4.450	42.238	.100
		15.556	17.480	0.000	0.000	0.000	0.000	17.238	0.100
TLC	728.890	17.780	10.700	.800	148.890	2.220	31.750	.500	
	640.000	0.000	7.500	.500					
	613.330	8.890	5.450	.150					
	471.110	8.890	4.830	.070					
	106.667	17.778	0.000	0.000					



SUBJECT	LUNG VOLUME	HEAD LIFT MANOEUVRE				RESPIRATORY FUNCTION MANOEUVRE			
		EMG (uV)		HL (Kg)		EMG (uV)		P <sub>musc</sub> (cm H <sub>2</sub> O)	
		VALUE ± S.D		VALUE ± S.D		VALUE ± S.D		VALUE ± S.D	
LT	FRC	782.220	.100	7.400	.200	586.670	.100	65.000	5.000
		711.110	71.110	5.150	.050	271.110	40.000	52.500	2.500
		142.220	0.500	3.450	.150	62.220	8.890	41.250	1.250
		124.450	17.780	2.700	0.000	24.450	2.230	32.500	2.500
		0.000	0.000	0.000	0.000	0.000	0.000	0.000	0.000
	FRC + 0.5L	800.000	52.460	5.400	.064	584.000	56.569	79.120	6.695
		505.491	4.415	4.001	.108	155.000	29.698	59.495	2.002
		314.023	34.981	2.768	.086	40.336	10.839	48.995	1.922
		228.871	6.929	2.236	.108	7.000	1.414	42.370	4.928
		162.145	6.598	1.453	.053	0.000	0.000	9.870	1.392
		0.000	0.000	0.000	0.000				
	FRC + 1L	728.890	17.780	5.650	2.150	266.670	.100	71.275	1.250
		648.890	8.890	5.700	.300	191.110	22.220	63.025	2.500
		471.110	8.890	4.750	.150	31.120	4.450	44.275	3.750
		284.450	7.780	3.100	.300	4.000	.440	33.025	2.500
		0.000	0.000	0.000	0.000	0.000	0.000	13.025	0.500
	FRC + 2L	844.450	44.450	8.850	.750	524.000	.100	79.738	5.000
		586.670	35.560	6.650	.550	120.000	13.330	65.488	1.250
		391.110	53.330	4.950	.050	115.530	26.700	54.738	2.500
		266.670	17.780	3.700	.500	62.220	8.890	39.738	.100
0.000		0.000	0.000	0.000	0.000	0.000	17.238	100	
TLC	862.220	8.890	10.900	.500	144.450	15.560	31.750	0.500	
	675.560	35.560	7.500	.200					
	666.670	44.450	5.450	.150					
	213.340	17.780	4.350	.150					
	128.000	17.778	0.000	0.000					



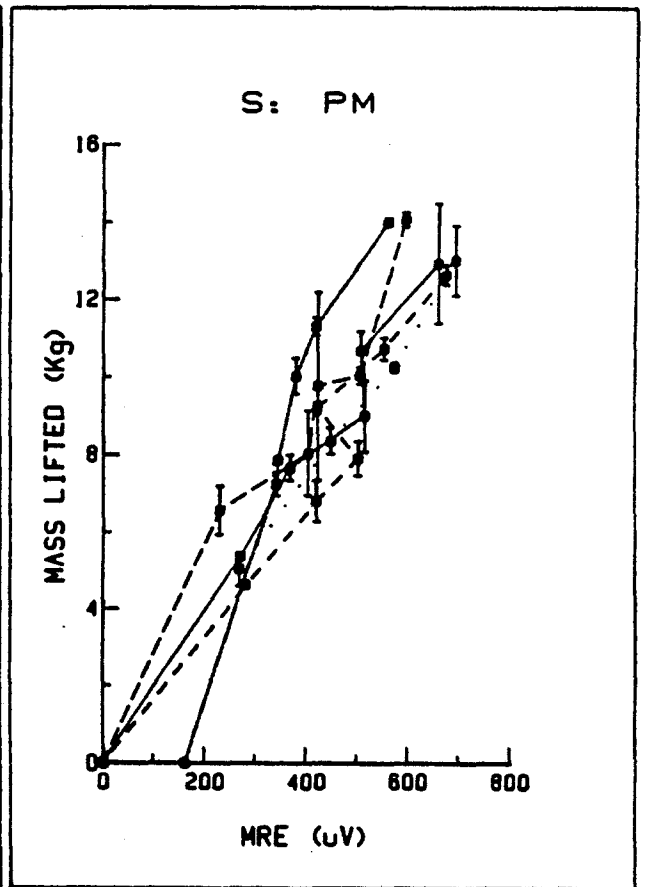
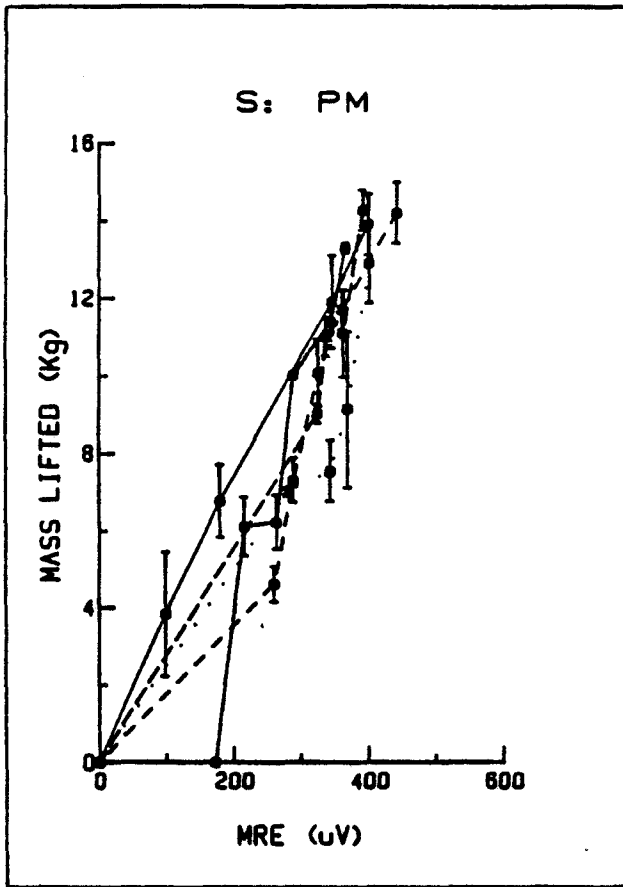
Head Lift Manoeuvre



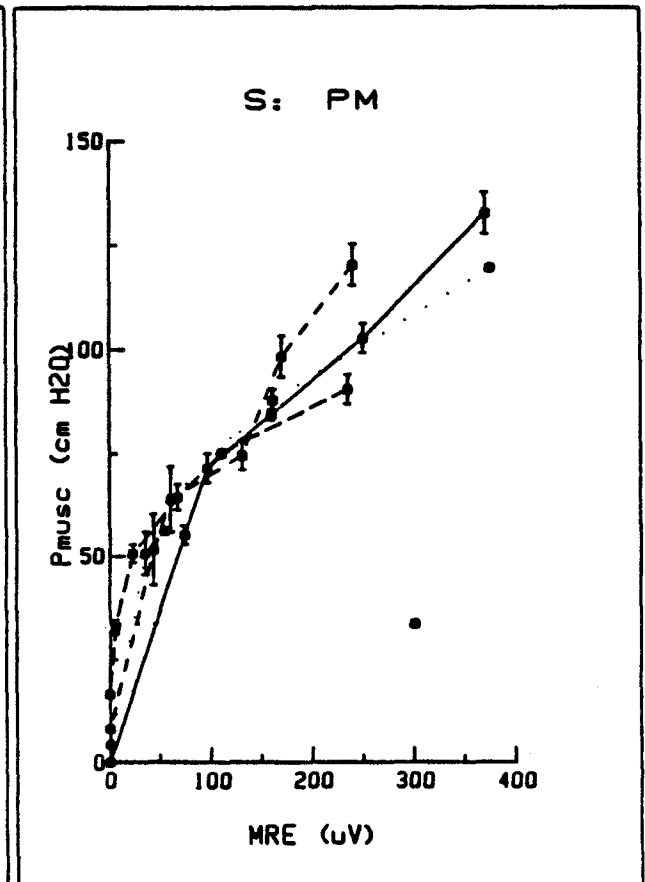
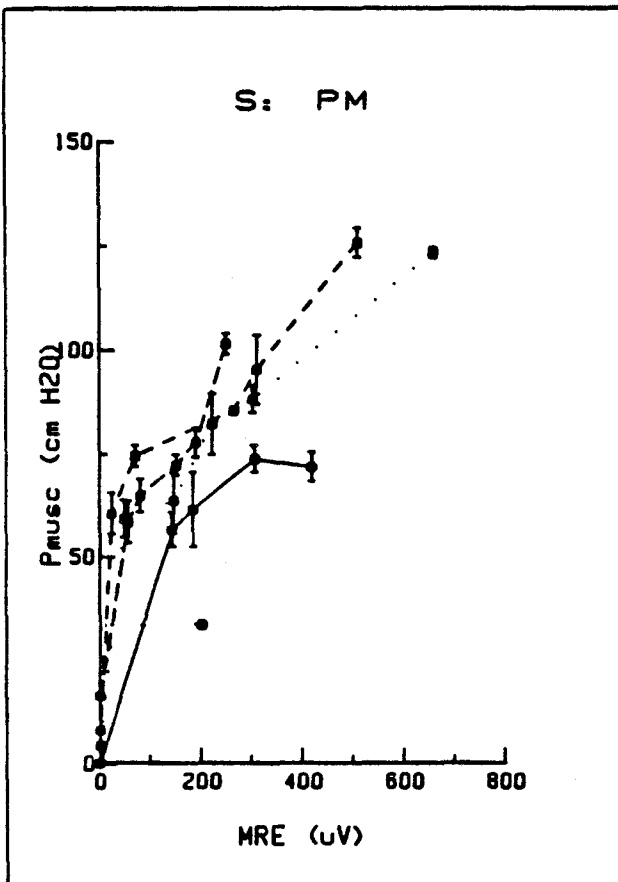
Respiratory Function Manoeuvre

SUBJECT	LUNG VOLUME	HEAD LIFT MANOEUVRE				RESPIRATORY FUNCTION MANOEUVRE			
		EMG (uv)		HL (kg)		EMG (uv)		P <sub>muscle</sub> (cm H <sub>2</sub> O)	
		VALUE ± S.D		VALUE ± S.D		VALUE ± S.D		VALUE ± S.D	
PM	FRC	398.400	31.200	13.900	.787	418.750	97.227	71.750	3.536
		345.000	41.480	11.900	1.198	305.830	83.674	73.714	3.233
		179.090	33.644	6.760	.943	183.630	59.928	61.458	9.133
		98.182	25.713	3.818	1.616	142.290	55.095	56.500	4.243
		0.000	0.000	0.000	0.000	0.000	0.000	0.000	0.000
	FRC + 0.5L	400.000	.100	12.900	1.032	660.000	20.000	123.082	1.250
		368.400	22.286	9.122	2.013	302.500	24.749	88.046	3.232
		342.500	28.723	7.543	.784	222.500	77.075	82.040	7.366
		280.000	30.000	7.000	.119	145.800	66.544	63.589	6.708
		0.000	0.000	0.000	0.000	48.750	22.127	59.228	4.567
	FRC + 1L	440.000	20.000	14.200	.789	510.000	56.569	125.564	3.536
		360.000	37.500	11.700	.509	310.000	70.711	95.189	8.309
		325.000	22.360	10.065	.875	265.000	2.357	85.356	.884
		288.330	36.938	7.300	.570	70.000	20.000	74.314	2.500
		260.000	52.786	4.600	.460	24.000	15.572	60.564	5.000
	FRC + 2L	0.000	0.000	0.000	0.000	0.000	0.000	8.064	.100
		390.000	25.820	14.272	.522	250.000	10.000	101.408	2.500
		362.000	10.860	11.085	1.130	190.000	70.000	77.658	3.536
		336.670	20.540	11.000	.500	150.000	50.000	72.158	2.475
		324.000	20.736	9.000	.243	80.000	10.000	64.846	3.977
TLC	0.000	0.000	0.000	0.000	56.667	13.611	58.387	5.156	
	365.000	15.000	13.287	.129	0.000	0.000	16.408	.100	
	344.000	32.863	11.400	.253	200.000	10.000	33.500	.500	
	288.000	22.804	10.000	.100					
	263.333	5.777	6.217	.704					
	215.000	25.981	6.100	.765					
	172.500	4.045	0.000	0.000					

SUBJECT	LUNG VOLUME	HEAD LIFT MANOEUVRE				RESPIRATORY FUNCTION MANOEUVRE			
		EMG (uV) VALUE $\pm$ S.D		HL (Kg) VALUE $\pm$ S.D		EMG (uV) VALUE $\pm$ S.D		P <sub>musc</sub> (cm H <sub>2</sub> O) VALUE $\pm$ S.D	
PM	FRC	660.000	40.000	12.900	1.548	370.000	20.000	132.500	5.000
		507.500	24.749	10.645	.500	250.000	98.995	102.500	3.536
		515.000	.313	8.966	.910	160.000	10.000	84.063	1.326
		369.000	66.468	7.652	.328	96.250	23.850	71.250	3.536
		271.670	91.924	5.328	.055	73.500	9.192	55.000	2.355
		0.000	0.000	0.000	0.000	0.000	0.000	0.000	0.000
		694.000	96.802	12.967	.903	375.000	35.360	119.332	.100
	FRC + 0.5L	573.170	21.449	10.215	.125	161.250	12.370	87.457	2.652
		448.340	134.355	8.330	.328	60.840	27.100	64.020	.442
		270.000	147.784	5.000	.441	54.170	10.610	56.082	.010
		281.670	40.065	4.600	.097	35.000	21.210	50.582	5.303
		0.000	0.000	0.000	0.000	0.000	0.000	4.332	.100
		675.000	35.355	12.600	.257	240.000	141.420	120.064	5.000
		554.050	10.438	10.700	.284	170.060	69.830	98.064	5.000
	FRC + 1L	422.000	25.456	9.170	.156	130.840	34.170	74.314	3.536
		501.430	42.426	7.890	.436	60.000	5.000	63.689	7.955
		420.380	16.440	6.784	.537	43.130	25.630	51.502	8.716
		0.000	0.000	0.000	0.000	0.000	0.000	8.064	.100
		595.000	7.071	14.031	.184	235.000	7.070	90.158	3.536
		505.750	16.617	10.010	.220	110.210	5.010	74.846	.442
		422.860	60.609	9.745	2.410	67.250	6.720	64.221	3.094
	FRC + 2L	404.000	8.485	8.024	1.082	22.500	5.900	50.471	2.210
		230.000	47.697	6.547	.635	5.000	.100	32.691	1.722
		0.000	0.000	0.000	0.000	0.000	0.000	16.408	.100
		560.000	84.853	13.968	.093	300.000	10.000	33.500	.500
		418.857	66.266	11.273	.228				
		379.196	17.046	9.995	.465				
		344.170	8.245	7.843	.034				
TLC	341.667	40.069	7.237	.308					
	160.000	10.000	0.000	0.000					



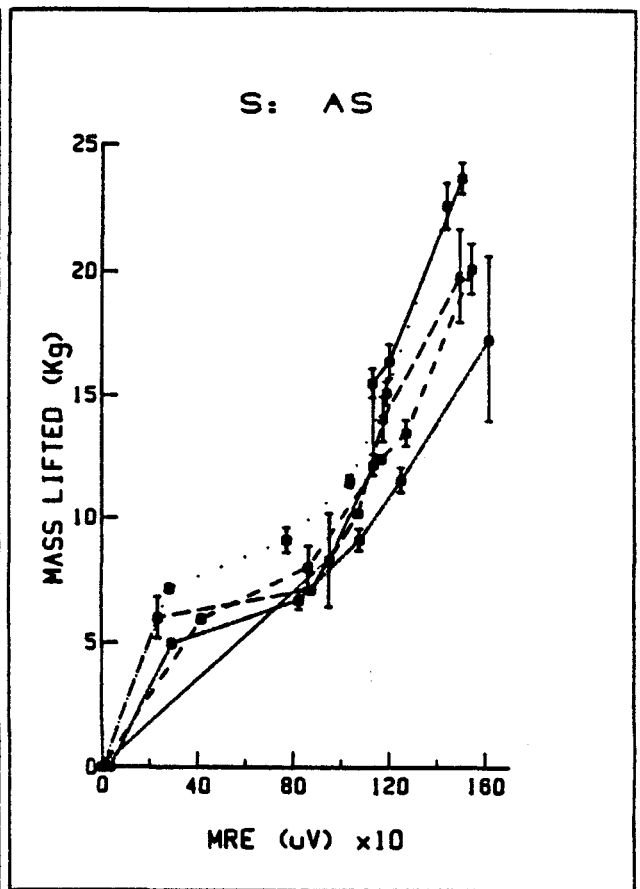
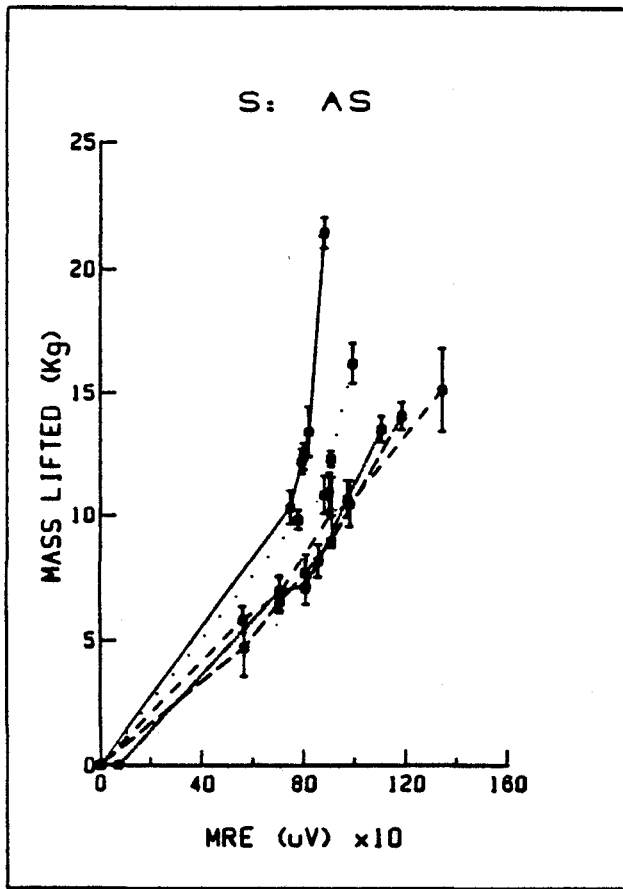
Head Lift Manoeuvre



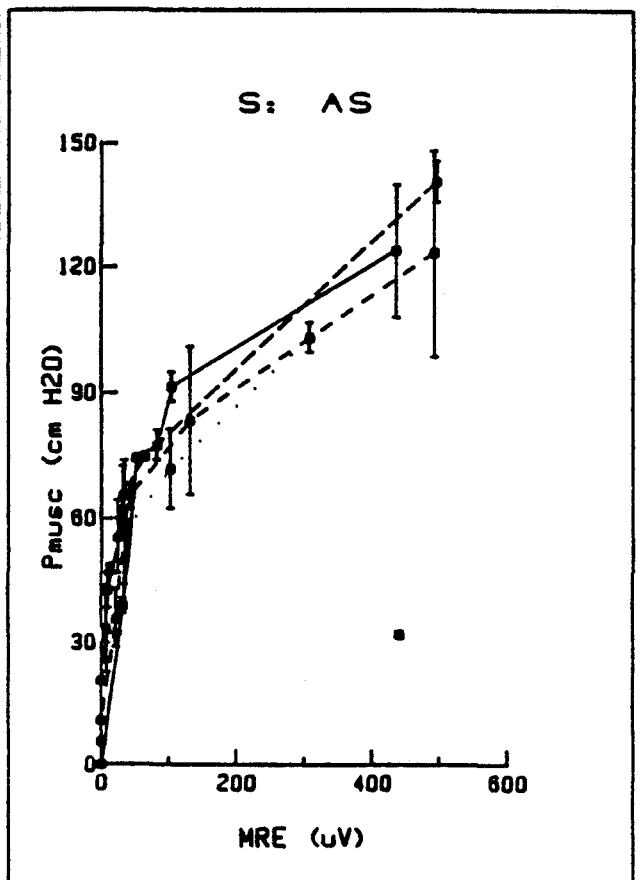
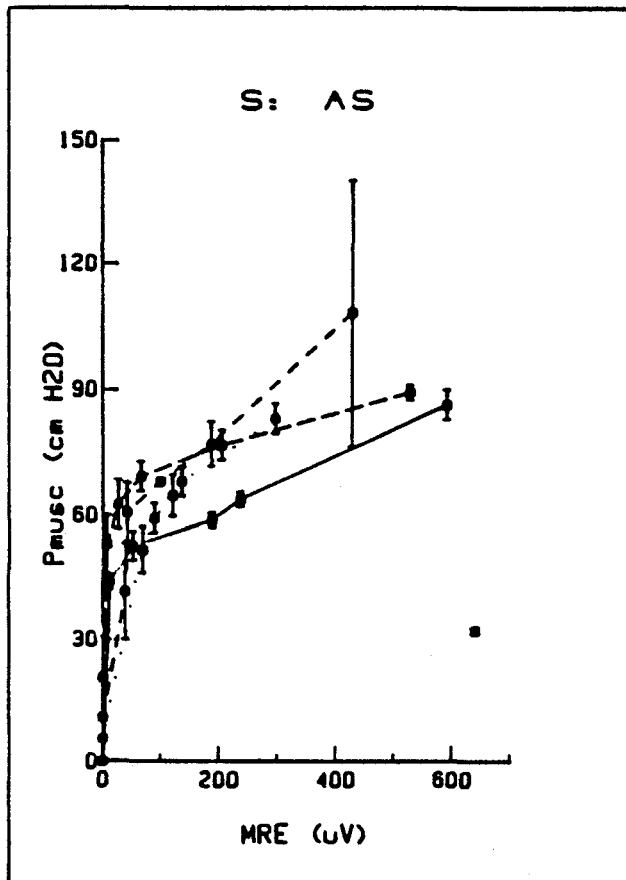
Respiratory Function Manoeuvre

SUBJECT	LUNG VOLUME	HEAD LIFT MANOEUVRE				RESPIRATORY FUNCTION MANOEUVRE			
		EMG (uV) VALUE ± S.D		HL (Kg) VALUE ± S.D		EMG (uV) VALUE ± S.D		P <sub>musc</sub> (cm H <sub>2</sub> O) VALUE ± S.D	
AS	FRC	880.000	80.000	21.400	.594	592.000	67.882	86.250	3.536
		820.000	32.800	13.410	1.009	236.000	39.598	63.750	1.768
		800.000	32.000	12.400	.542	188.000	39.598	58.750	1.768
		720.200	101.320	12.204	.497	52.000	16.971	52.500	3.536
		748.000	67.880	10.317	.683	12.000	5.657	43.750	1.768
		0.000	0.000	0.000	0.000	0.000	0.000	0.000	0.000
		0.000	0.000	0.000	0.000	0.000	0.000	0.000	0.000
	FRC+0.5L	992.000	32.000	16.200	.824	296.000	16.000	83.005	3.536
		906.400	93.900	12.300	.314	136.000	56.569	68.005	3.536
		900.000	84.850	10.938	.795	120.000	8.000	64.670	5.000
		880.000	99.600	10.834	.772	88.600	3.677	59.255	3.536
		778.670	75.420	9.813	.383	68.500	16.263	51.505	5.657
		0.000	0.000	0.000	0.000	0.000	0.000	5.505	.100
		0.000	0.000	0.000	0.000	0.000	0.000	0.000	0.000
	FRC+1L	1344.000	226.270	15.100	1.701	428.000	50.912	108.213	31.820
		981.330	18.850	10.465	.942	186.000	31.113	76.963	5.303
		910.400	246.640	10.120	1.442	98.676	37.726	67.963	.707
		706.130	57.320	6.824	.721	42.000	.125	60.713	7.071
		559.250	104.520	5.819	.519	39.000	.633	41.463	11.667
		0.000	0.000	0.000	0.000	0.000	0.000	10.713	.100
		0.000	0.000	0.000	0.000	0.000	0.000	0.000	0.000
	FRC+2L	1184.000	32.000	14.031	.556	528.000	22.627	89.209	1.768
		906.430	72.950	8.929	.101	204.000	28.284	76.709	3.536
		807.870	166.667	7.648	.739	65.200	7.354	69.209	3.536
		707.700	153.870	6.543	.348	26.000	5.657	62.542	5.890
		564.340	70.800	4.705	1.158	6.000	1.500	52.959	7.071
		0.000	0.000	0.000	0.000	0.000	0.000	20.459	.100
		0.000	0.000	0.000	0.000	0.000	0.000	0.000	0.000
TLC	1104.000	67.880	13.500	.519	640.000	.100	32.000	.500	
	970.670	75.420	10.658	.763					
	857.600	9.050	8.133	.645					
	809.810	158.690	7.120	.697					
	705.330	54.690	6.982	.502					
	70.730	13.570	0.000	0.000					
	0.000	0.000	0.000	0.000					

SUBJECT	LUNG VOLUME	HEAD LIFT MANOEUVRE				RESPIRATORY FUNCTION MANOEUVRE			
		EMG ( $\mu$ V) VALUE $\pm$ S.D		HL (Kg) VALUE $\pm$ S.D		EMG ( $\mu$ V) VALUE $\pm$ S.D		P <sub>musc</sub> (cm H <sub>2</sub> O) VALUE $\pm$ S.D	
AS	FRC	1504.000	32.000	23.600	.621	436.000	130.108	123.750	15.910
		1200.400	23.560	16.345	.692	103.500	21.920	91.250	3.536
		1129.300	133.890	15.461	.607	82.000	8.485	77.500	3.536
		1133.100	75.150	12.128	.421	51.332	.020	74.500	.707
		948.800	33.940	8.279	1.866	32.000	11.314	38.750	1.768
		0.000	0.000	0.000	0.000	0.000	0.000	0.000	0.000
	FRC+0.5L	1440.000	28.890	22.500	.910	308.000	5.657	103.005	3.536
		1189.200	5.200	15.045	.487	102.000	42.426	71.755	9.546
		1035.000	125.000	11.473	.252	36.000	5.657	56.755	5.303
		770.000	183.360	9.069	.513	12.000	5.657	47.505	1.414
		282.800	1.200	7.131	.111	8.000	8.000	33.005	10.607
		0.000	0.000	0.000	0.000	0.000	0.000	5.505	.100
	FRC+1L	1544.000	33.940	20.040	.987	492.000	16.971	123.213	24.749
		1270.000	77.320	13.421	.531	131.000	32.527	83.213	17.678
		1164.600	50.100	12.375	.015	42.688	18.854	65.401	3.094
		861.330	64.100	7.981	.842	34.000	5.657	58.838	15.026
		416.000	.100	5.935	.131	22.000	8.485	35.713	7.071
		0.000	0.000	0.000	0.000	0.000	0.000	10.713	.100
	FRC+2L	1496.000	33.940	19.744	1.834	496.000	16.000	140.459	5.000
		1172.800	65.620	13.993	.917	63.532	.662	74.834	.884
		1067.900	125.420	10.150	.071	31.500	16.263	65.459	7.071
		872.960	39.060	7.094	.075	24.000	11.314	55.459	8.839
		233.600	4.530	5.983	.829	10.000	10.000	42.459	4.243
		0.000	0.000	0.000	0.000	0.000	0.000	20.459	.100
TLC	1616.000	158.390	17.238	3.315	440.000	.100	32.000	.500	
	1249.420	7.670	11.506	.508					
	1073.150	50.100	9.073	.477					
	823.780	115.080	6.688	.375					
	292.000	28.280	4.945	.163					
	32.000	5.820	0.000	0.000					



Head Lift Manoeuvre



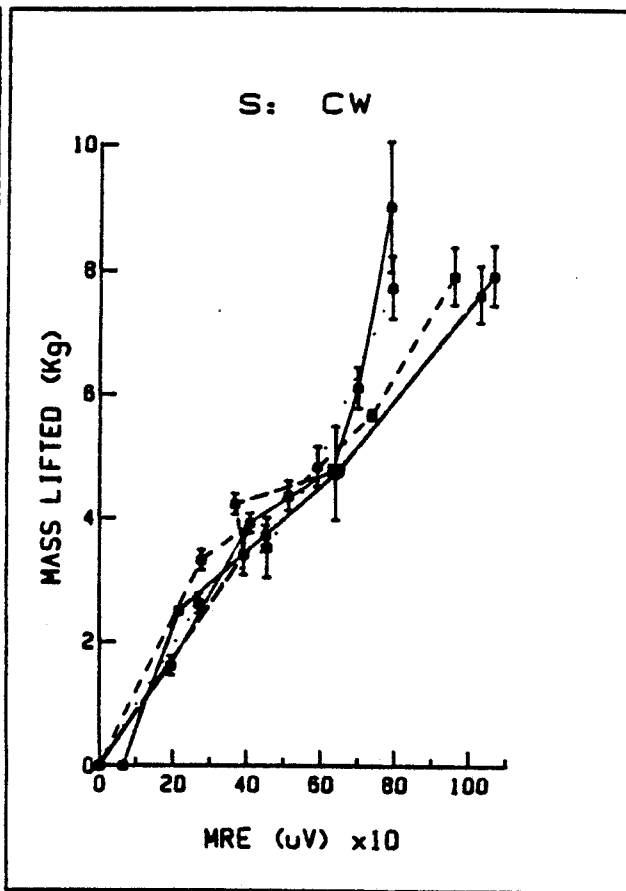
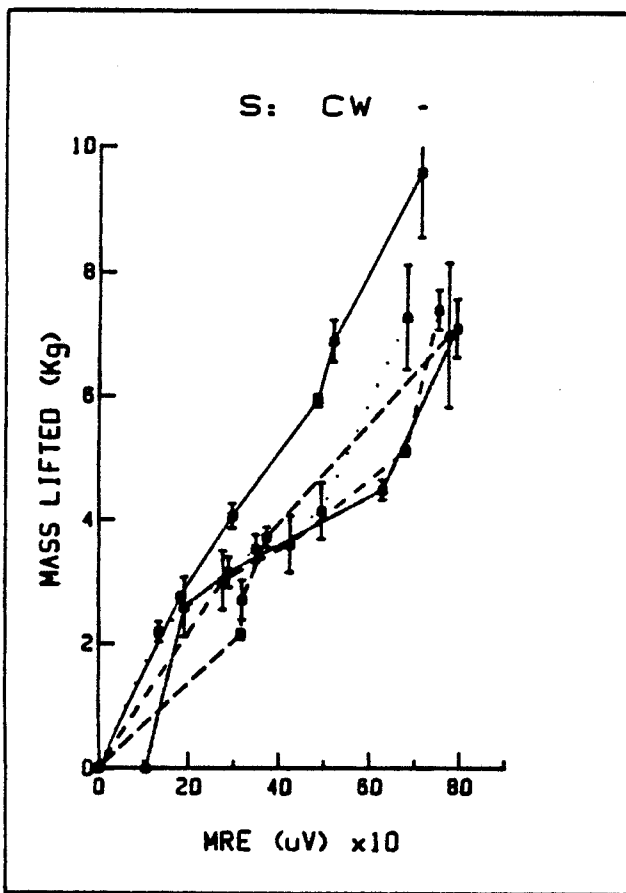
Respiratory Function Manoeuvre



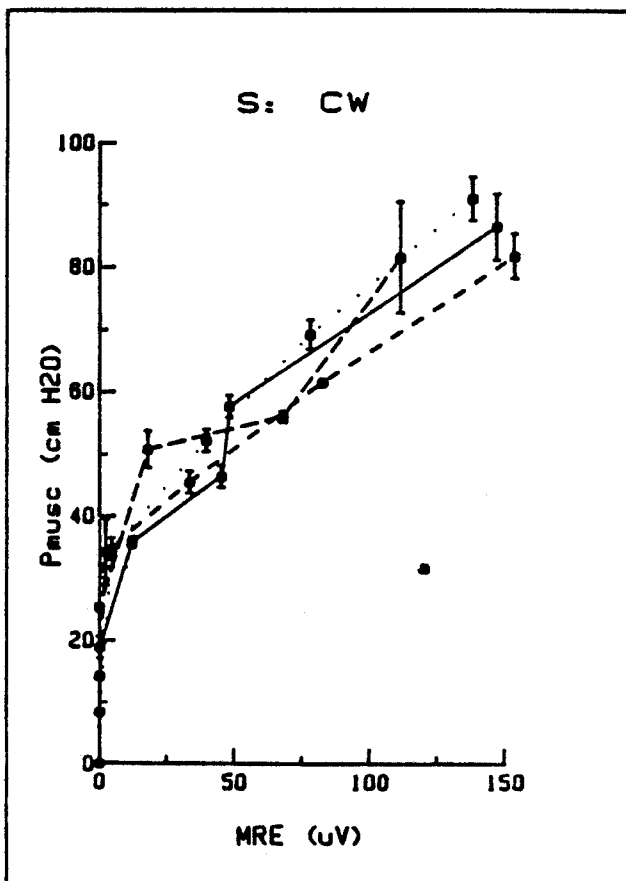
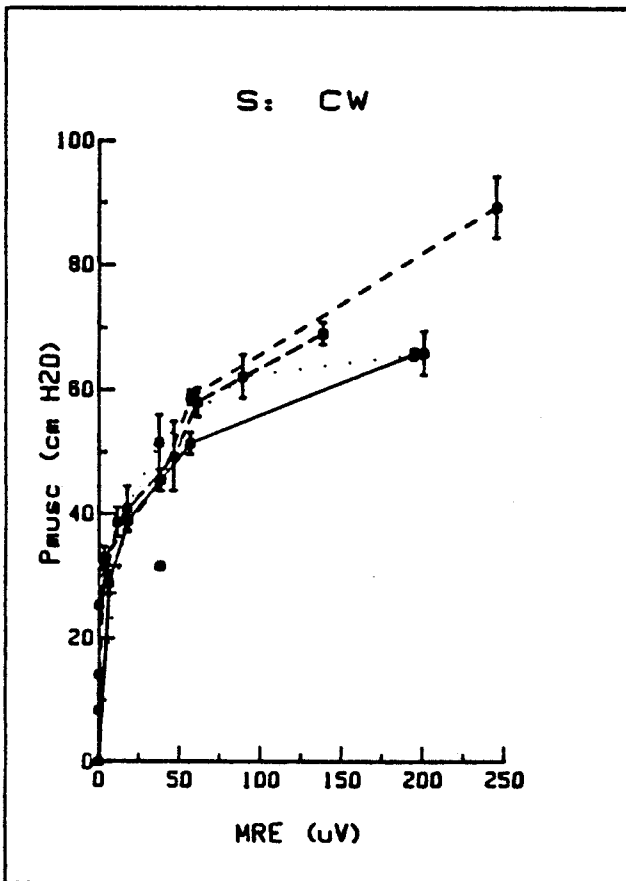
3cm

SUBJECT	LUNG VOLUME	HEAD LIFT MANOEUVRE				RESPIRATORY FUNCTION MANOEUVRE			
		EMG ( $\mu$ V) VALUE $\pm$ S.D		HL (Kg) VALUE $\pm$ S.D		EMG ( $\mu$ V) VALUE $\pm$ S.D		P <sub>musc</sub> (cm H <sub>2</sub> O) VALUE $\pm$ S.D	
CW	FRC	711.110	77.360	9.600	1.044	193.900	32.860	65.625	.884
		518.930	25.560	6.900	.336	56.000	8.800	51.250	1.768
		484.440	18.860	5.931	.098	17.788	6.285	38.750	1.768
		294.820	10.470	4.054	.203	6.111	2.357	28.750	1.765
		181.330	20.110	2.760	.100	0.000	0.000	0.000	0.000
		0.000	0.000	0.000	0.000	0.000			
	FRC+0.5L	680.000	6.290	7.281	.845	200.000	43.998	65.796	3.536
		492.540	14.600	4.140	.460	88.444	11.942	62.046	3.536
		346.670	6.290	3.519	.228	37.036	20.949	51.421	4.419
		133.330	12.570	2.185	.163	17.409	3.664	40.796	3.536
		0.000	0.000	0.000	0.000	0.000	0.000	8.296	.100
	FRC+1L	751.110	31.430	7.400	.325	244.440	94.281	89.091	5.000
		677.330	17.780	5.118	.081	56.520	25.877	58.674	1.177
		423.110	17.780	3.600	.460	37.778	16.971	45.341	1.768
		274.440	64.430	3.012	.473	3.333	1.571	32.841	1.768
		0.000	0.000	0.000	0.000	0.000	0.000	14.091	.100
	FRC+2L	773.330	17.780	6.982	1.171	137.780	43.998	68.977	1.768
		371.110	15.710	3.713	.159	60.520	7.649	57.870	2.323
		317.330	3.770	2.700	.318	46.000	36.770	49.185	5.597
		317.070	67.040	2.145	.078	11.111	3.143	38.560	2.358
0.000		0.000	0.000	0.000	0.000	0.000	25.227	.100	
TLC	791.110	37.710	7.100	.473	37.778	21.999	31.500	.100	
	626.670	103.710	4.485	.163					
	287.400	14.670	3.143	.242					
	189.630	71.240	2.588	.477					
	104.440	37.910	0.000	0.000					

SUBJECT	LUNG VOLUME	HEAD LIFT MANOEUVRE				RESPIRATORY FUNCTION MANOEUVRE			
		EMG (uV) VALUE $\pm$ S.D		HL (Kg) VALUE $\pm$ S.D		EMG (uV) VALUE $\pm$ S.D		P <sub>musc</sub> (cm H <sub>2</sub> O) VALUE $\pm$ S.D	
CW	FRC	786.670	31.430	9.000	1.032	146.667	6.285	86.250	5.303
		697.780	81.710	6.100	.332	47.964	3.143	57.500	1.768
		629.930	119.840	4.773	.081	45.036	3.143	46.250	1.768
		406.670	47.140	3.912	.158	11.853	1.571	35.625	.884
		192.890	33.940	1.607	.152	0.000	3.143	18.750	1.768
	0.000	0.000	0.000	0.000	0.000	0.000	0.000	0.000	
	FRC+0.5L	791.110	37.710	7.719	.504	137.780	18.856	90.796	3.536
		589.310	77.070	4.830	.325	77.778	6.285	69.129	2.358
		453.330	6.290	3.513	.481	39.409	3.350	52.046	1.768
		268.890	15.710	2.614	.161	4.444	4.444	34.546	1.768
		0.000	0.000	0.000	0.000	0.000	0.000	8.296	.100
	FRC+1L	960.000	35.560	7.900	.460	153.330	9.428	81.591	3.536
		734.810	46.090	5.658	.082	82.418	8.448	61.384	.293
		511.110	94.280	4.357	.240	33.333	3.143	45.341	1.768
		275.560	17.780	3.314	.162	2.222	2.222	34.091	5.303
		0.000	0.000	0.000	0.000	0.000	0.000	14.091	.100
	FRC+2L	1066.700	35.560	7.900	.479	111.110	18.856	81.477	8.839
		648.370	142.580	4.773	.081	67.778	7.857	55.852	.884
		366.670	59.710	4.221	.171	17.778	8.889	50.645	2.945
		391.110	17.780	3.400	.321	0.000	0.000	25.227	.100
0.000		0.000	0.000	0.000					
TLC	1031.110	35.560	7.600	.460	120.000	43.998	31.500	.100	
	637.880	111.960	4.715	.759					
	449.630	49.240	3.713	.159					
	214.820	2.100	2.500	.100					
	64.000	30.150	0.000	0.000					



Head Lift Manoeuvre

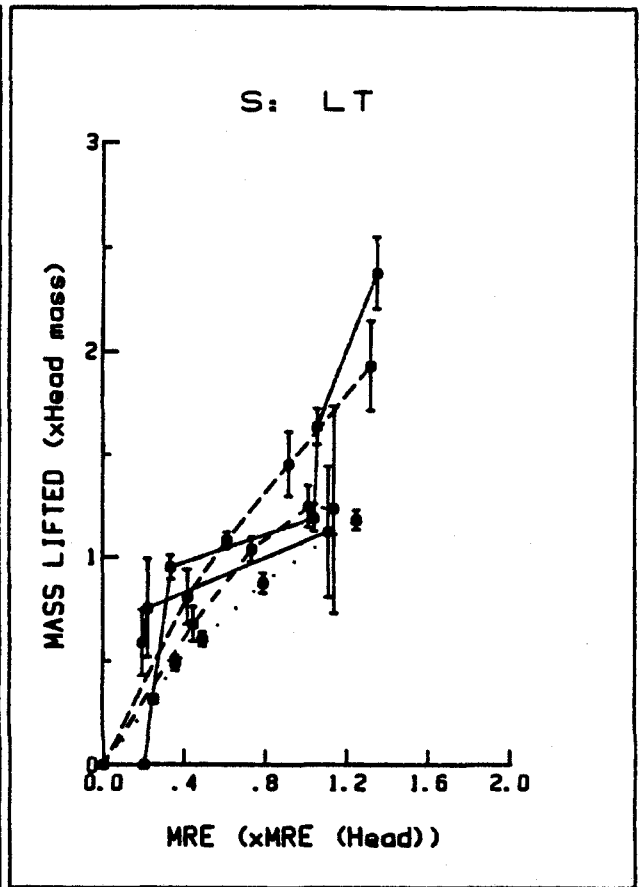
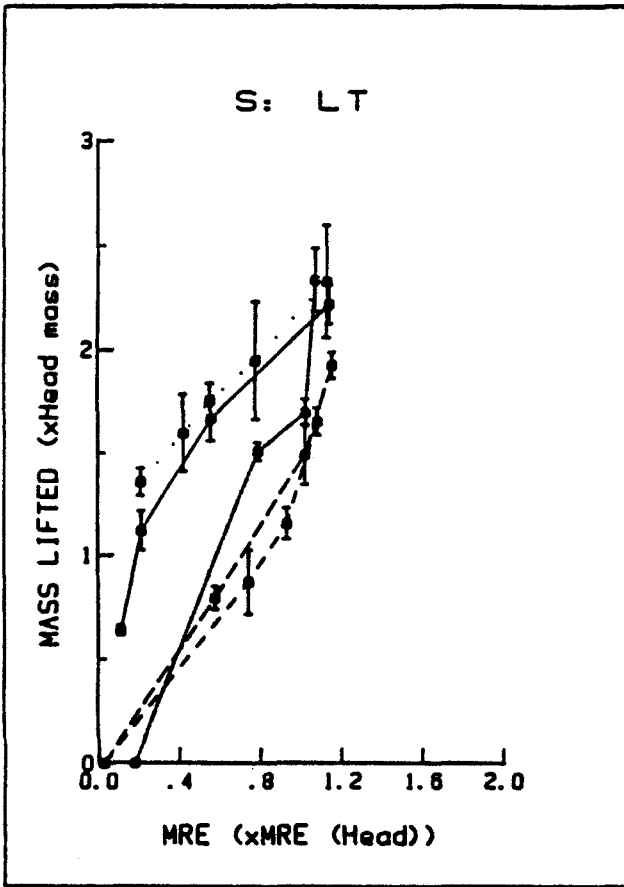


Respiratory Function Manoeuvre

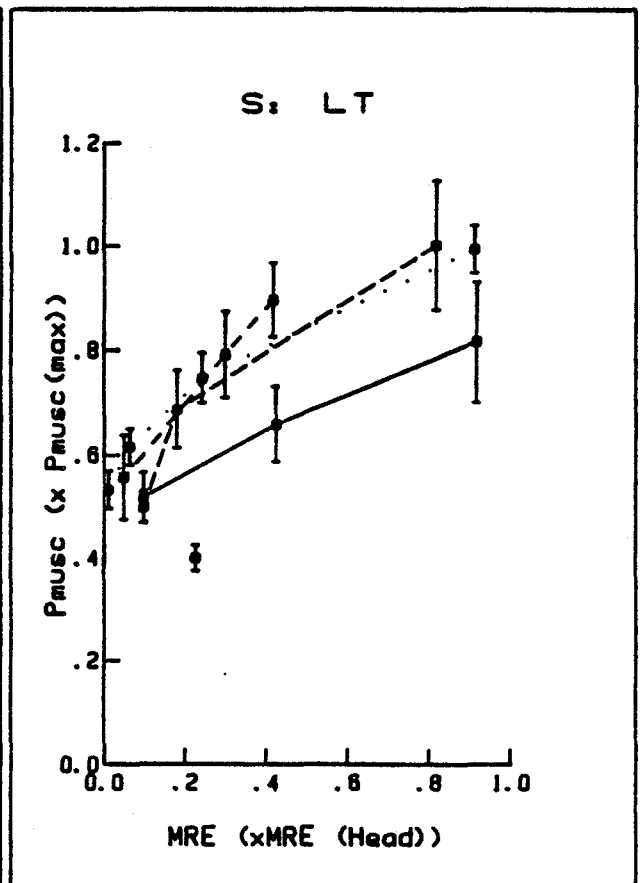
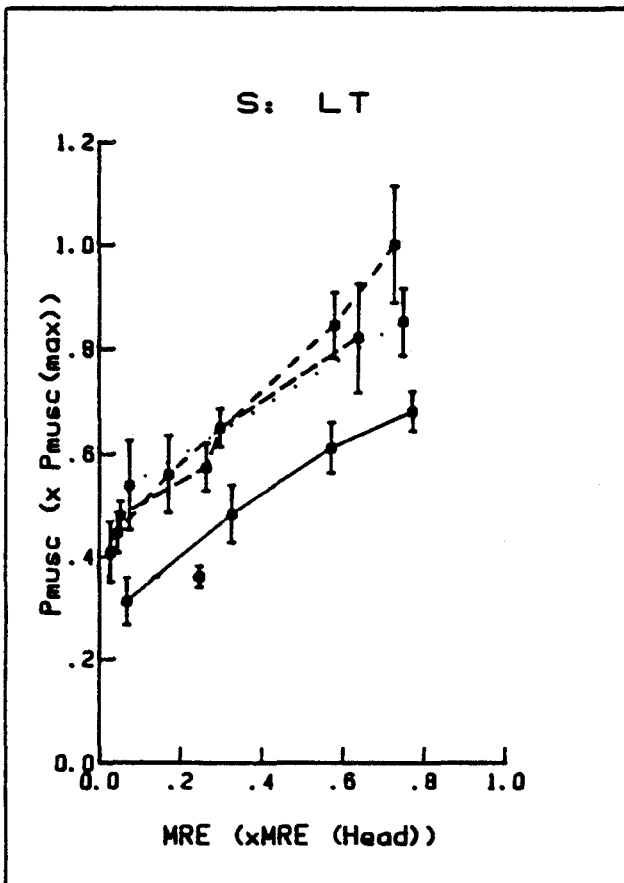
NORMALIZED DATA

SUBJECT	LUNG VOLUME	HEAD LIFT MANOEUVRE				RESPIRATORY FUNCTION MANOEUVRE			
		EMG (xEMG head mass) VALUE $\pm$ S.D		HL (xHead Mass) VALUE $\pm$ S.D		EMG (xEMG head mass) VALUE $\pm$ S.D		Pmusc (xPmusc max) VALUE $\pm$ S.D	
LT	FRC	1.137	.247	2.215	.094	.770	.009	.682	.039
		.555	.061	1.665	.109	.570	.014	.611	.049
		.216	.049	1.116	.095	.326	.063	.483	.056
		.111	.024	.637	.025	.067	.008	.312	.046
	FRC+.5L	1.126	.111	2.326	.271	.746	.036	.851	.064
		.775	.113	1.945	.283	.073	.021	.538	.087
		.553	.087	1.750	.086	.027	.000	.409	.059
		.421	.056	1.593	.190				
		.212	.038	1.352	.067				
	FRC+1L	1.081	.105	1.652	.067	.726	.009	1.000	.114
		.933	.181	1.152	.075	.578	.081	.844	.062
		.740	.210	.870	.154	.170	.010	.560	.074
		.026	.035	0.000	0.000	.044	.015	.446	.040
	FRC+2L	1.155	.096	1.924	.063	.637	.052	.821	.103
		1.021	.130	1.489	.149	.296	.063	.650	.037
		.577	.063	.793	.054	.263	.007	.574	.047
		.026	.031	0.000	0.000	.052	.008	.480	.027
	TLC	1.070	.089	1.333	.153	.248	.007	.361	.020
		1.025	.100	1.696	.065				
		.787	.080	1.503	.044				
.178		.044	0.000	0.000					

SUBJECT	LUNG VOLUME	HEAD LIPT MANOEUVRE				RESPIRATORY FUNCTION MANOEUVRE			
		EMG (xEMG head mass) VALUE ± S.D		HL (xHead Mass) VALUE ± S.D		EMG (xEMG head mass) VALUE ± S.D		Pmusc (xPmusc max) VALUE ± S.D	
LT	FRC	1.111	.127	1.120	.315	.917	.013	.815	.114
		.222	.003	.750	.236	.424	.068	.658	.073
		.194	.030	.587	.159	.097	.015	.517	.048
	FRC+.5L	1.250	.099	1.174	.046	.912	.101	.992	.146
		.790	.018	.870	.047	.242	.050	.746	.072
		.491	.061	.602	.035	.063	.018	.614	.063
		.358	.016	.486	.037	.011	.002	.531	.095
		.253	.014	.316	.020				
	0.000	0.000	0.000	0.000					
	FRC+1L	1.139	.044	1.228	.501	.417	.006	.894	.072
		1.014	.028	1.239	.099	.299	.039	.790	.081
		.736	.024	1.033	.061	.049	.008	.555	.082
		.444	.018	.674	.084				
		0.000	0.000	0.000	0.000				
	FRC+2L	1.319	.088	1.924	.215	.819	.011	1.000	.125
		.917	.068	1.446	.159	.181	.044	.686	.074
		.611	.092	1.076	.040	.097	.015	.498	.031
		.417	.034	.804	.131				
		0.000	0.000	0.000	0.000				
	TLC	1.347	.033	2.370	.173	.226	.027	.398	.025
1.056		.070	1.630	.088					
1.042		.084	1.185	.065					
.333		.032	.946	.058					
.200		.031	0.000	0.000					



Head Lift Manoeuvre

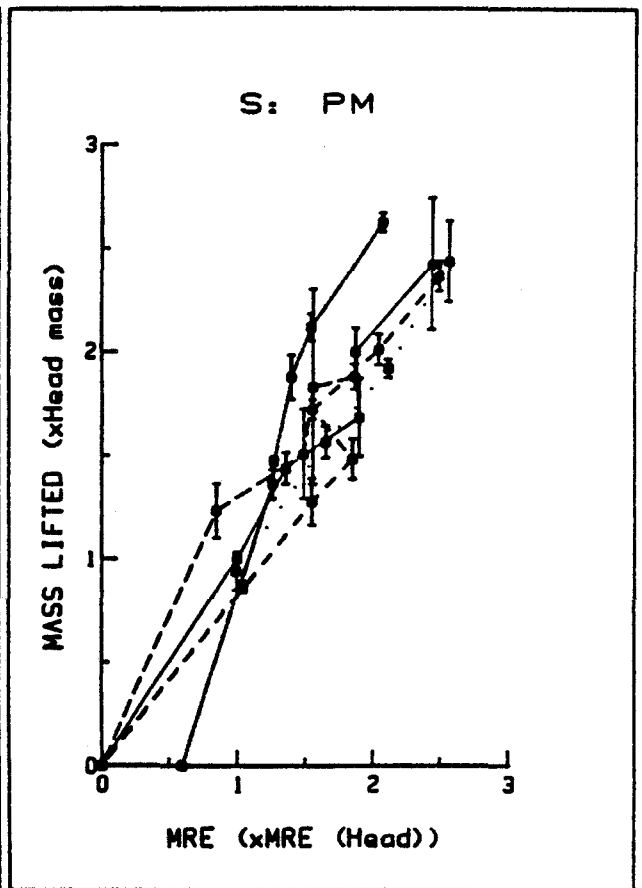
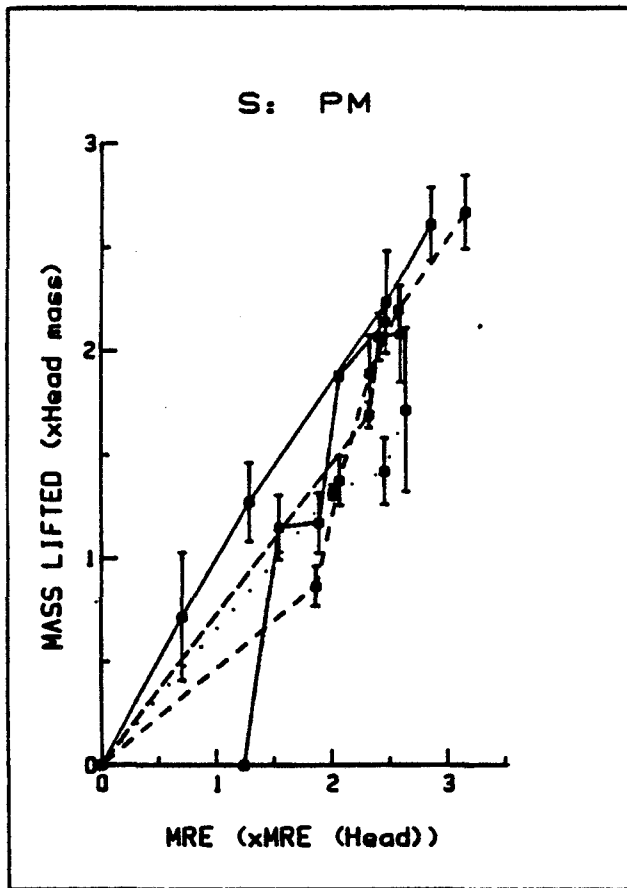


Respiratory Function Manoeuvre

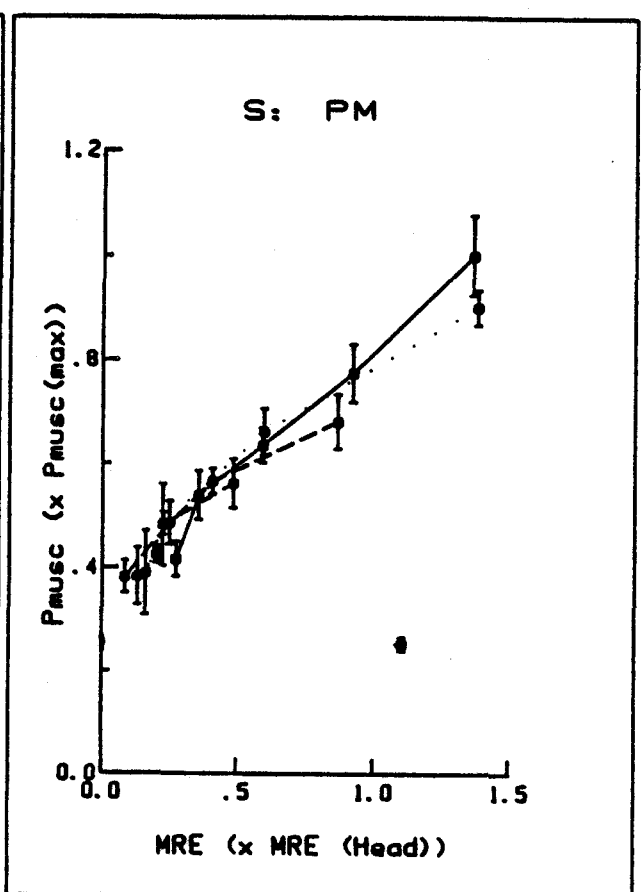
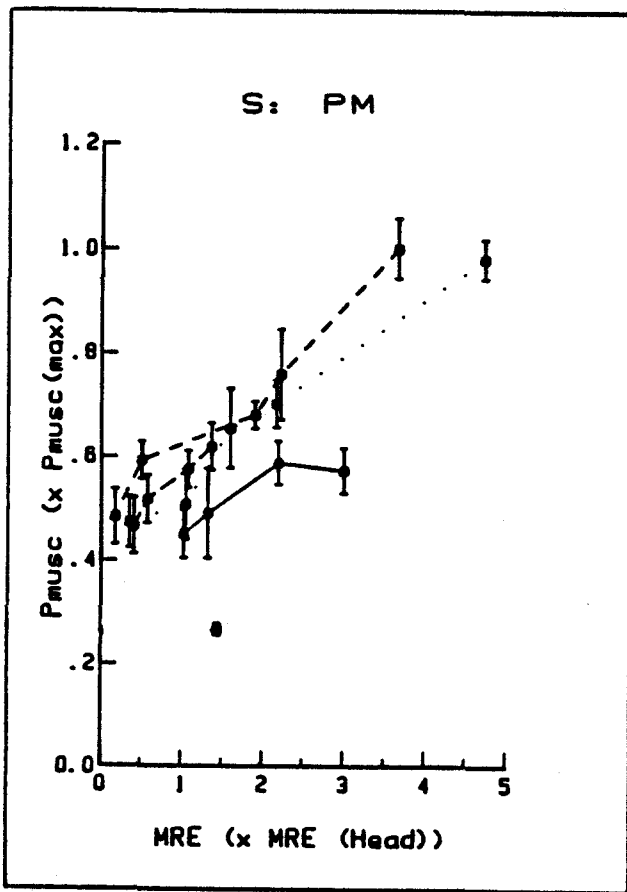
SUBJECT	LUNG VOLUME	HEAD LIFT MANOEUVRE				RESPIRATORY FUNCTION MANOEUVRE			
		EMG (xEMG head mass) VALUE ± S.D		HL (xHead Mass) VALUE ± S.D		EMG (xEMG head mass) VALUE ± S.D		P <sub>musc</sub> (xP <sub>musc</sub> max) VALUE ± S.D	
PM	FRC	2.846	.426	2.609	.175	2.991	.908	.571	.044
		2.464	.472	2.233	.248	2.185	.754	.587	.042
		1.279	.332	1.269	.190	1.312	.522	.489	.087
		.701	.324	.717	.311	1.016	.466	.450	.046
		0.000	0.000	0.000	0.000				
	FRC+.5L	2.631	.347	1.712	.395	4.714	.480	.980	.038
		2.446	.380	1.416	.162	2.161	.331	.701	.045
		2.000	.357	1.314	.036	1.589	.664	.653	.077
		0.000	0.000	0.000	0.000	1.041	.550	.506	.068
						.348	.183	.472	.050
	FRC+1L	3.143	.367	2.655	.176	3.643	.664	1.000	.056
		2.571	.452	2.196	.118	2.214	.663	.758	.088
		2.321	.326	1.889	.184	1.893	.152	.680	.026
		1.060	.411	1.370	.121	.500	.179	.592	.037
		1.857	.510	.863	.095	.171	.123	.482	.053
		0.000	0.000	0.000	0.000				
	FRC+2L	2.586	.262	2.081	.234	1.357	.597	.618	.046
		2.405	.318	1.065	.115	1.071	.434	.575	.036
		2.314	.313	1.689	.063	.571	.112	.516	.046
		0.000	0.000	0.000	0.000	.405	.126	.465	.054
TLC	2.457	.410	2.140	.070	1.429	.173	.267	.011	
	2.057	.310	1.877	.019					
	1.881	.176	1.167	.144					
	1.536	.295	1.145	.155					
	1.232	.117	0.000	0.000					



SUBJECT	LUNG VOLUME	HEAD LIFT MANOEUVRE				RESPIRATORY FUNCTION MANOEUVRE			
		EMG (xEMG head mass) VALUE ± S.D		HL (xHead Mass) VALUE ± S.D		EMG (xEMG head mass) VALUE ± S.D		P <sub>musc</sub> (xP <sub>musc</sub> max) VALUE ± S.D	
PM	FRC	2.429	.969	2.421	.316	1.362	.534	1.000	.075
		1.868	.723	1.998	.114	.920	.676	.774	.056
		1.896	.643	1.683	.188	.589	.236	.634	.034
		1.358	.704	1.436	.076	.354	.208	.538	.047
		1.000	.677	1.000	.021	.271	.125	.415	.033
		0.000	0.000	0.000	0.000				
	FRC+.5L	2.555	1.221	2.434	.195	1.380	.597	.901	.034
		2.110	.793	1.917	.043	.594	.246	.660	.045
		1.650	1.053	1.563	.078	.224	.176	.483	.022
		.994	.880	.938	.092	.199	.107	.423	.016
		1.037	.498	.863	.027	.129	.122	.382	.054
		0.000	0.000	0.000	0.000				
	FRC+1L	2.485	.971	2.365	.073	.482	.289	.561	.048
		2.039	.729	2.008	.074	.221	.093	.481	.078
		1.553	.619	1.721	.047	.159	.148	.389	.080
		1.846	.781	1.481	.097				
		1.547	.584	1.273	.114				
		0.000	0.000	0.000	0.000				
	FRC+2L	1.862	.691	1.879	.061	.865	.319	.680	.052
		1.557	.750	1.829	.471	.406	.156	.565	.025
1.487		.534	1.506	.219	.248	.108	.485	.042	
.847		.462	1.229	.132	.083	.050	.381	.031	
0.000		0.000	0.000	0.000					
TLC	2.061	1.010	2.622	.045	1.104	.410	.253	.013	
	1.542	.766	2.116	.065					
	1.396	.535	1.876	.107					
	1.267	.459	1.472	.022					
	1.258	.573	1.358	.072					
	.589	.236	0.000	0.000					



Head Lift Manoeuvre

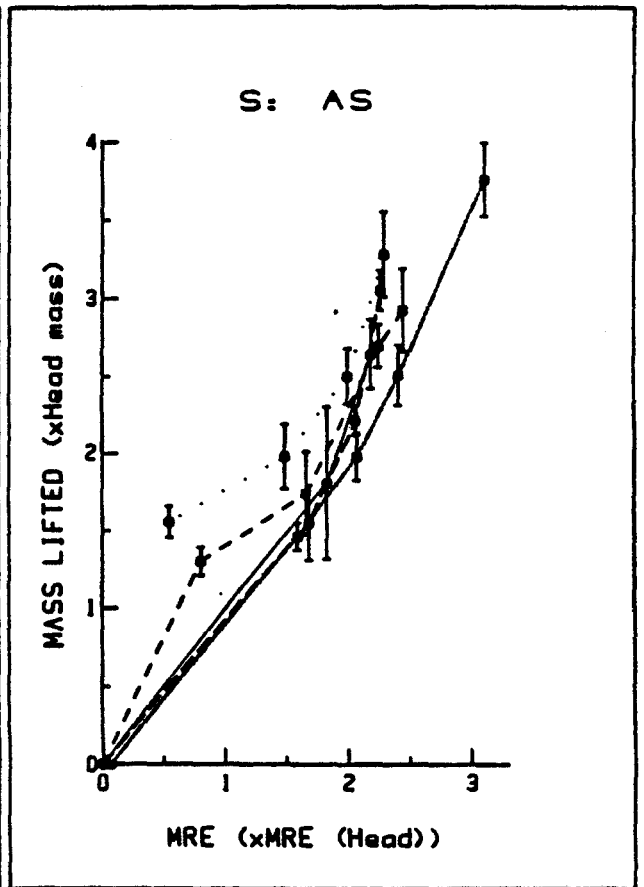
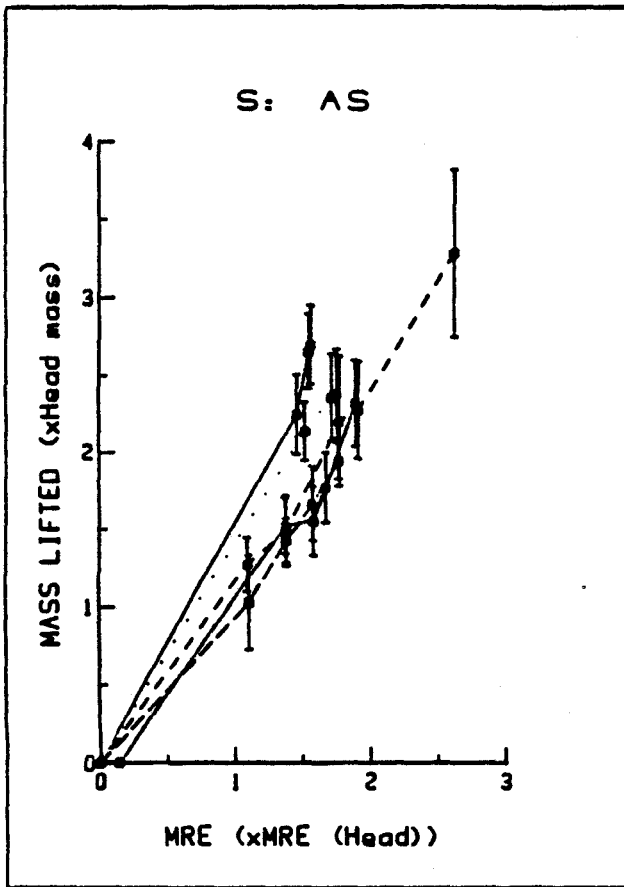


Respiratory Function Manoeuvre

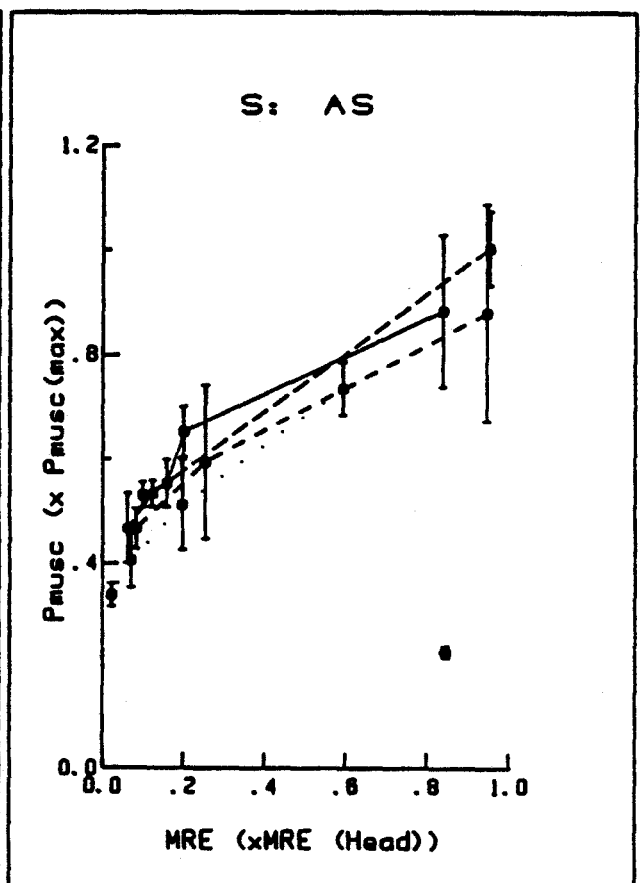
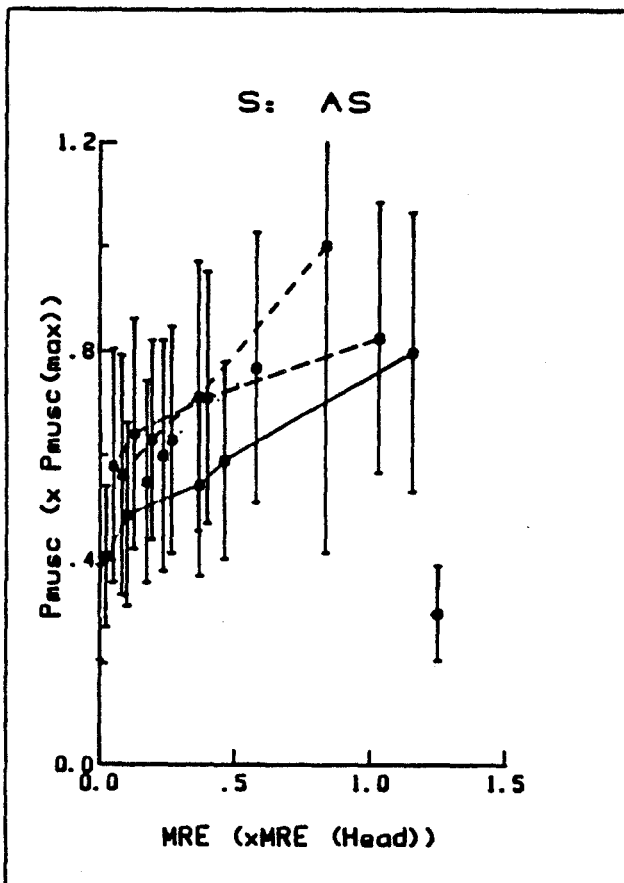
3cm

SUBJECT	LUNG VOLUME	HEAD LIFT MANOEUVRE				RESPIRATORY FUNCTION MANOEUVRE			
		EMG (xEMG head mass) VALUE $\pm$ S.D		HL (xHead Mass) VALUE $\pm$ S.D		EMG (xEMG head mass) VALUE $\pm$ S.D		Pmusc (xPmusc max) VALUE $\pm$ S.D	
AS	FRC	1.563	.111	2.696	.253	1.156	.169	.797	.267
		1.547	.246	2.653	.241	.461	.092	.589	.190
		1.461	.178	2.243	.261	.367	.089	.542	.176
		0.000	0.000	0.000	0.000	.102	.036	.485	.175
						.023	.012	.404	.135
	FRC+.5L	1.758	.221	2.378	.292	.578	.049	.767	.258
		1.719	.248	2.355	.286	.266	.119	.628	.217
		1.521	.195	2.133	.190	.234	.023	.598	.222
		0.000	0.000	0.000	0.000	.173	.013	.548	.194
	FRC+1L	2.625	.524	3.283	.534	.836	.126	1.000	.588
		1.917	.097	2.275	.319	.363	.072	.711	.258
		1.778	.537	2.200	.423	.193	.080	.628	.191
		1.379	.155	1.483	.231	.082	.003	.561	.230
		1.092	.238	1.265	.176				
	0.000	0.000	0.000	0.000					
	FRC+2L	1.770	.198	1.941	.119	1.031	.076	.824	.259
		1.578	.375	1.663	.244	.398	.068	.709	.241
		1.381	.344	1.422	.147	.127	.018	.640	.221
		1.102	.173	1.023	.303	.051	.013	.578	.224
0.000		0.000	0.000	0.000					
TLC	1.896	.207	2.317	.282	1.250	.039	.296	.092	
	1.675	.070	1.768	.229					
	1.582	.359	1.548	.229					
	1.378	.150	1.518	.185					
	.138	.031	0.000	0.000					

SUBJECT	LUNG VOLUME	HEAD LIFT MANOEUVRE				RESPIRATORY FUNCTION MANOEUVRE			
		EMG (xEMG head mass) VALUE $\pm$ S.D		HL (xHead Mass) VALUE $\pm$ S.D		EMG (xEMG head mass) VALUE $\pm$ S.D		P <sub>musc</sub> (xP <sub>musc</sub> max) VALUE $\pm$ S.D	
AS	FRC	2.176	.362	2.637	.223	.837	.278	.881	.145
		1.822	.247	1.800	.496	.199	.049	.650	.048
		0.000	0.000	0.000	0.000	.157	.022	.552	.045
						.099	.003	.530	.024
	FRC+.5L	2.284	.238	3.271	.269	.591	.031	.733	.051
		1.987	.439	2.494	.179	.196	.088	.511	.086
		1.479	.500	1.972	.210	.069	.013	.404	.052
		.543	.057	1.550	.102	.023	.012	.338	.022
	FRC+1L	2.439	.392	2.918	.261	.945	.065	.877	.207
		2.236	.320	2.690	.138	.252	.071	.592	.147
		1.654	.288	1.735	.270	.082	.039	.466	.039
		.799	.080	1.291	.093				
	FRC+2L	0.000	0.000	0.000	0.000				
		2.252	.446	3.042	.126	.952	.063	1.000	.071
		2.051	.243	2.207	.093	.122	.005	.533	.025
		1.676	.054	1.542	.245	.060	.033	.466	.067
	TLC	0.000	0.000	0.000	0.000				
		3.103	.255	3.747	.236	.845	.029	.228	.012
		2.399	.302	2.501	.196				
		2.061	.379	1.972	.154				
1.582		.110	1.454	.089					
	.061	.017	0.000	0.000					



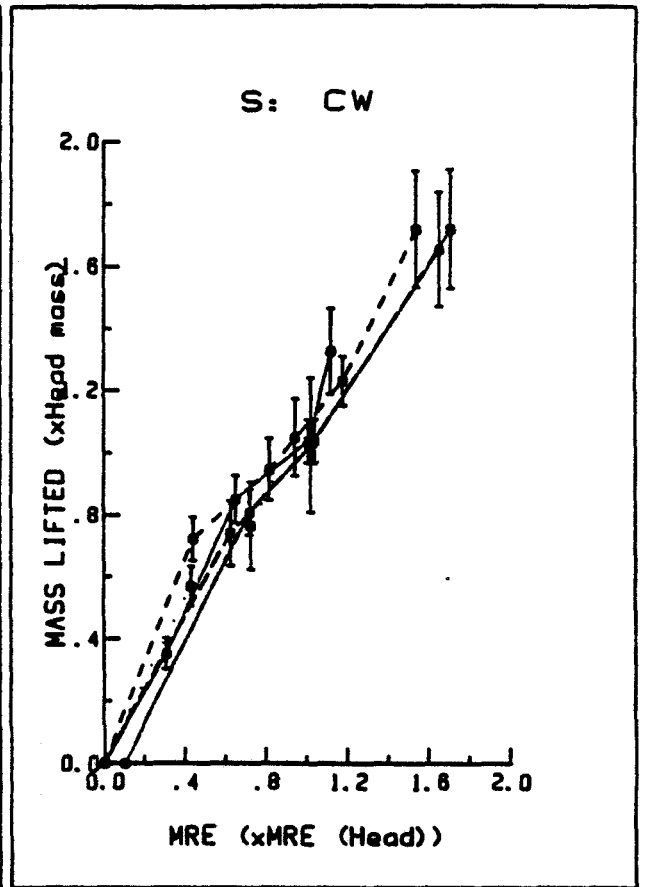
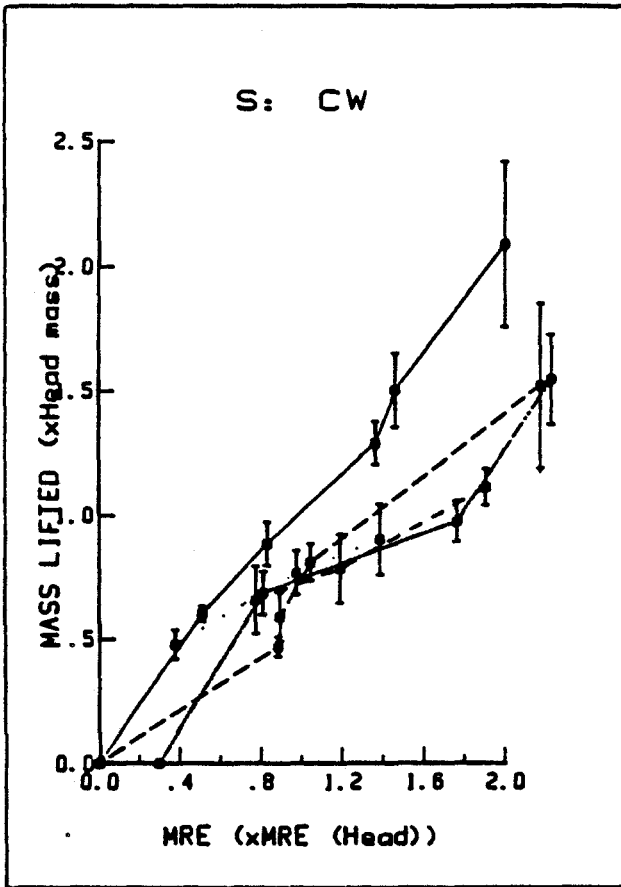
Head Lift Manoeuvre



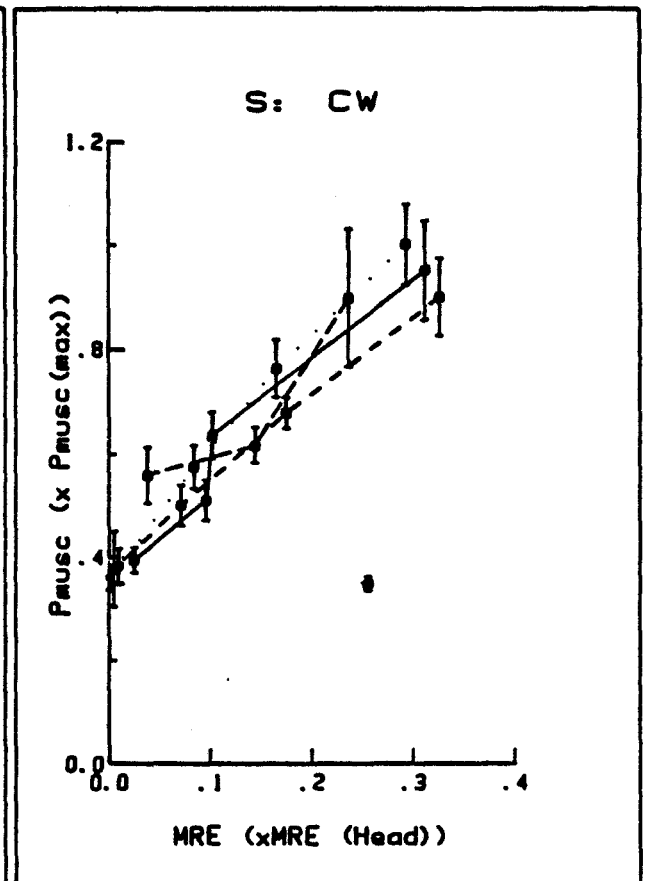
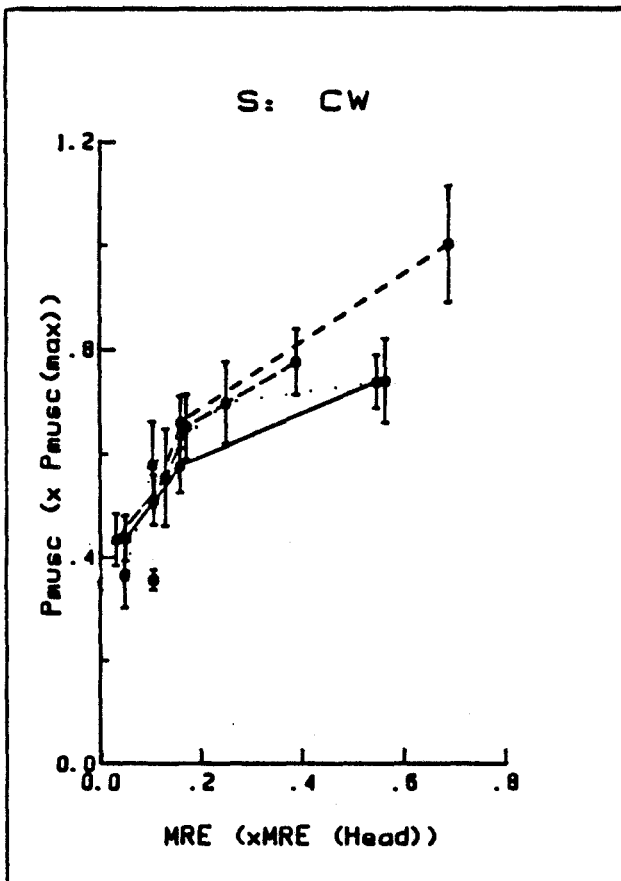
Respiratory Function Manoeuvre

SUBJECT	LUNG VOLUME	HEAD LIFT MANOEUVRE				RESPIRATORY FUNCTION MANOEUVRE			
		EMG (xEMG head mass) VALUE $\pm$ S.D		HL (xHead Mass) VALUE $\pm$ S.D		EMG (xEMG head mass) VALUE $\pm$ S.D		P <sub>muscle</sub> (xP <sub>muscle</sub> max) VALUE $\pm$ S.D	
CW	FRC	2.000	.318	2.087	.331	.545	.120	.737	.051
		1.459	.145	1.500	.148	.157	.033	.575	.052
		1.362	.121	1.289	.086	.050	.020	.435	.044
		.829	.071	.881	.088				
		.510	.082	.600	.030				
	0.000	0.000	0.000	0.000					
	FRC+.5L	1.385	.110	.900	.145	.562	.152	.739	.081
		.975	.066	.765	.088	.249	.046	.696	.079
		.375	.054	.475	.059	.104	.064	.577	.082
						.049	.013	.365	.065
	FRC+1L	1.905	.145	1.113	.073	.687	.300	1.000	.112
		1.190	.110	.783	.139	.159	.081	.659	.050
		.772	.220	.655	.136	.106	.053	.509	.048
	FRC+2L	2.175	.159	1.518	.330	.388	.143	.774	.063
		1.044	.096	.807	.075	.170	.030	.650	.063
		.892	.055	.587	.098	.129	.110	.552	.094
		.883	.233	.466	.040	.031	.010	.433	.051
		0.000	0.000	0.000	0.000				
	TLC	2.225	.217	1.543	.180	.106	.067	.354	.020
		1.763	.380	.975	.084				
.808		.082	.683	.087					
.294		.121	0.000	0.000					

SUBJECT	LUNG VOLUME	HEAD LIFT MANOEUVRE				RESPIRATORY FUNCTION MANOEUVRE			
		EMG (xEMG head mass) VALUE $\pm$ S.D		HL (xHead Mass) VALUE $\pm$ S.D		EMG (xEMG head mass) VALUE $\pm$ S.D		Pmusc (xPmusc max) VALUE $\pm$ S.D	
CW	FRC	1.116	.201	1.326	.138	.311	.019	.950	.095
		1.008	.280	1.038	.069	.102	.009	.633	.044
		.650	.116	.850	.077	.096	.008	.509	.039
		.309	.080	.349	.051	.025	.004	.392	.025
		0.000	0.000	0.000	0.000				
	FRC+.5L	.943	.187	1.050	.123	.292	.046	1.000	.078
		.725	.032	.764	.143	.165	.016	.761	.056
		.430	.044	.568	.063	.084	.009	.573	.042
		0.000	0.000	0.000	0.000	.009	.010	.380	.034
	FRC+1L	1.535	.114	1.717	.186	.325	.026	.899	.074
		1.175	.127	1.230	.079	.175	.021	.676	.030
		.817	.221	.947	.100	.071	.008	.499	.039
		.441	.049	.720	.071	.005	.005	.375	.073
		0.000	0.000	0.000	0.000				
	FRC+2L	1.706	.118	1.717	.190	.236	.044	.897	.132
		1.037	.329	1.038	.069	.144	.019	.615	.034
		.626	.053	.739	.107	.038	.020	.558	.054
		0.000	0.000	0.000	0.000				
TLC	1.649	.117	1.652	.183	.255	.098	.347	.014	
	1.020	.263	1.025	.216					
	.719	.123	.807	.075					
	.102	.067	0.000	0.000					



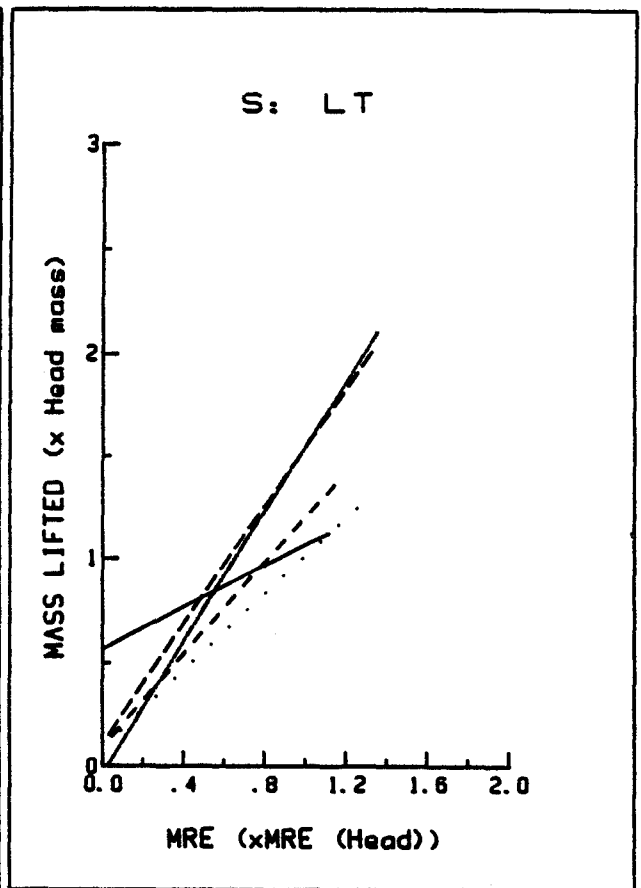
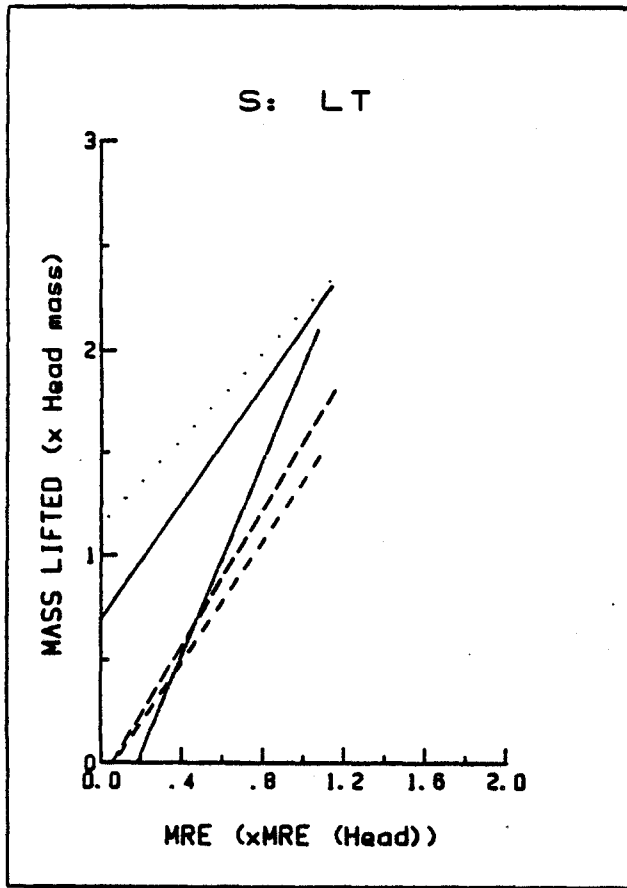
Head Lift Manoeuvre



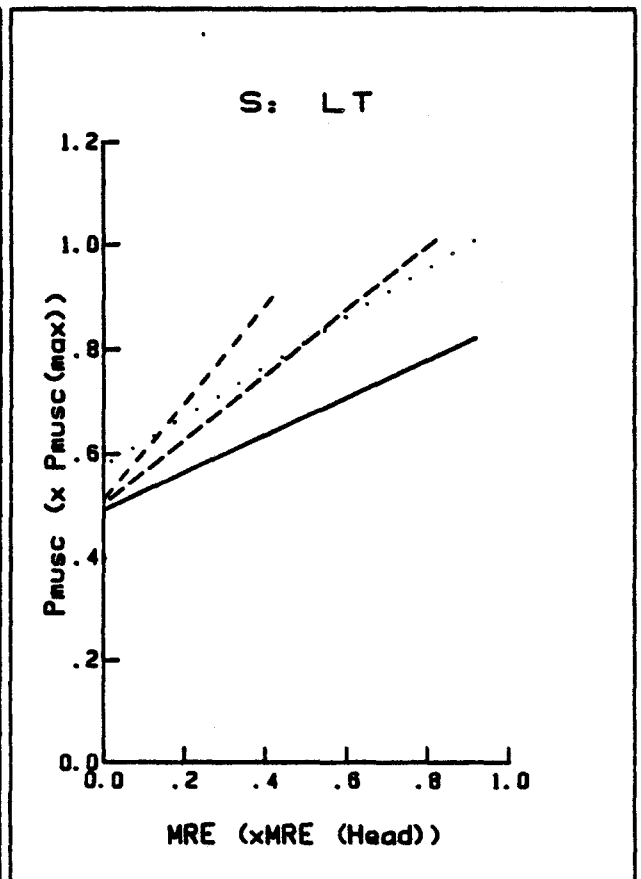
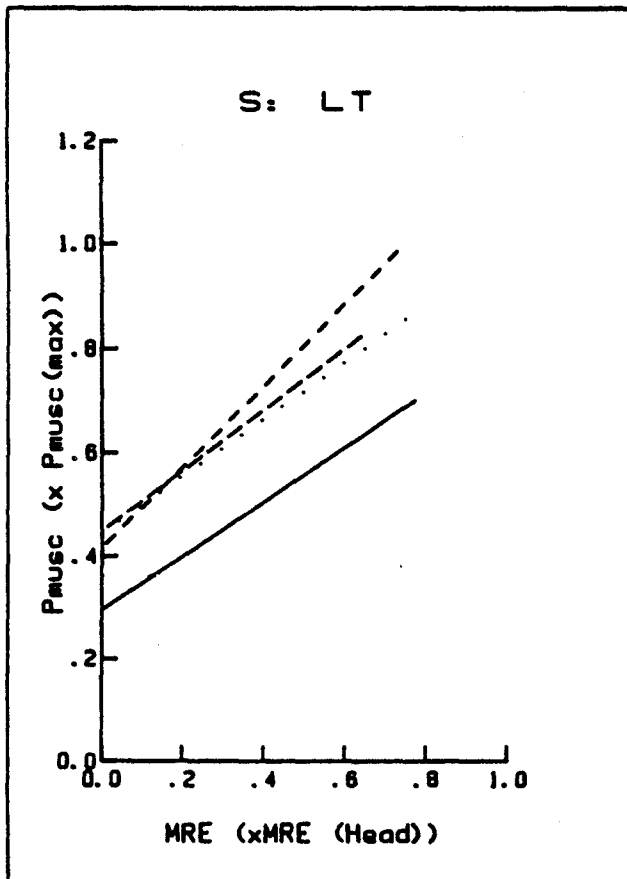
Respiratory Function Manoeuvre



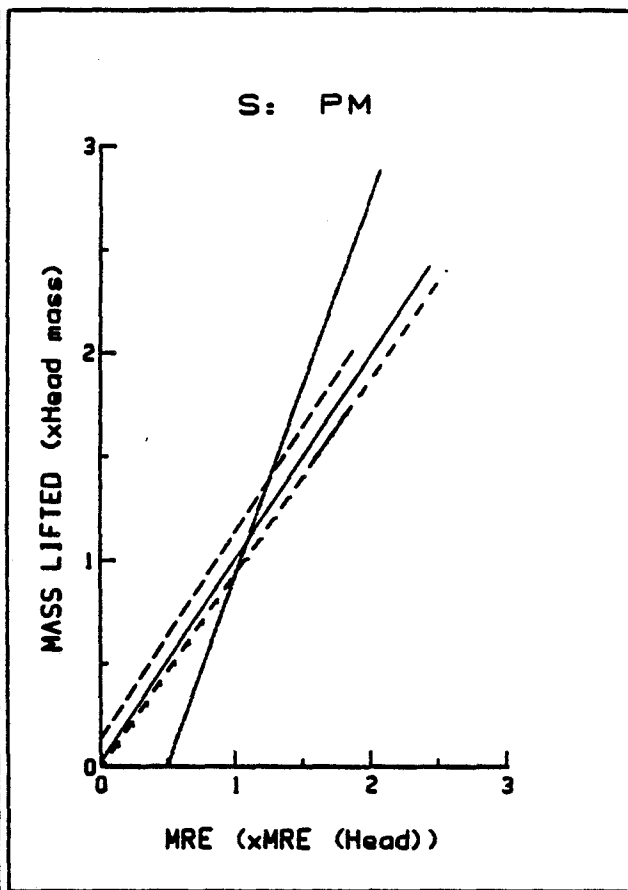
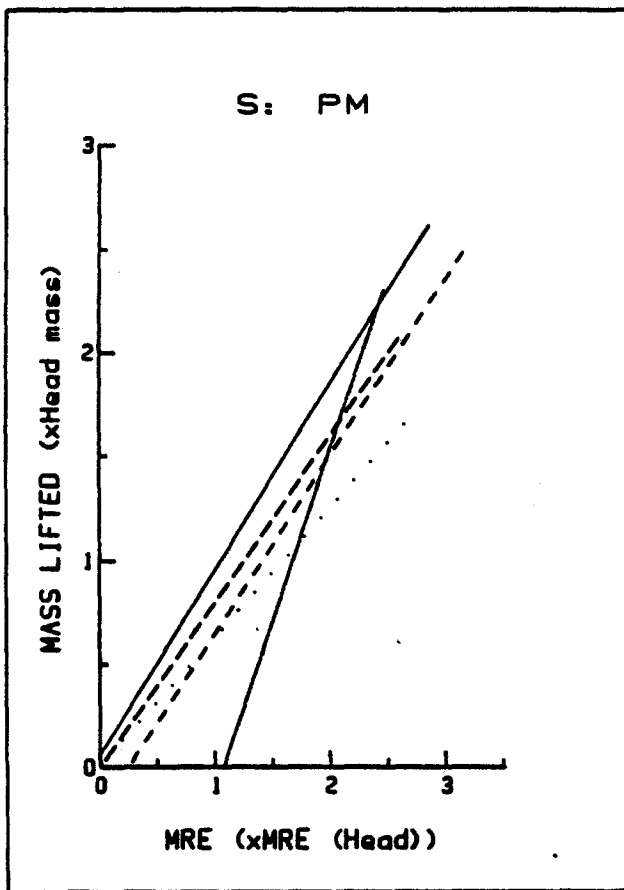
REGRESSION LINES  
FROM  
NORMALIZED DATA



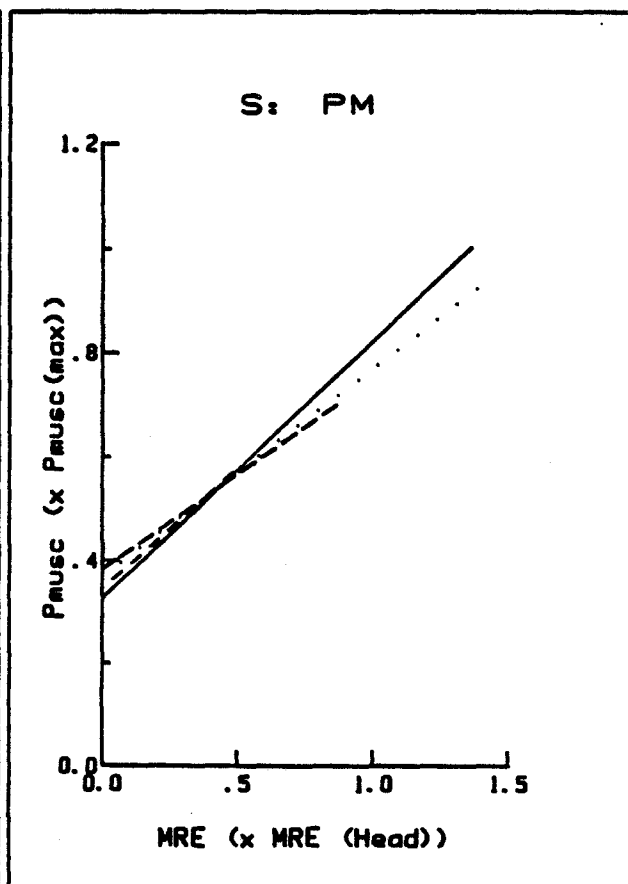
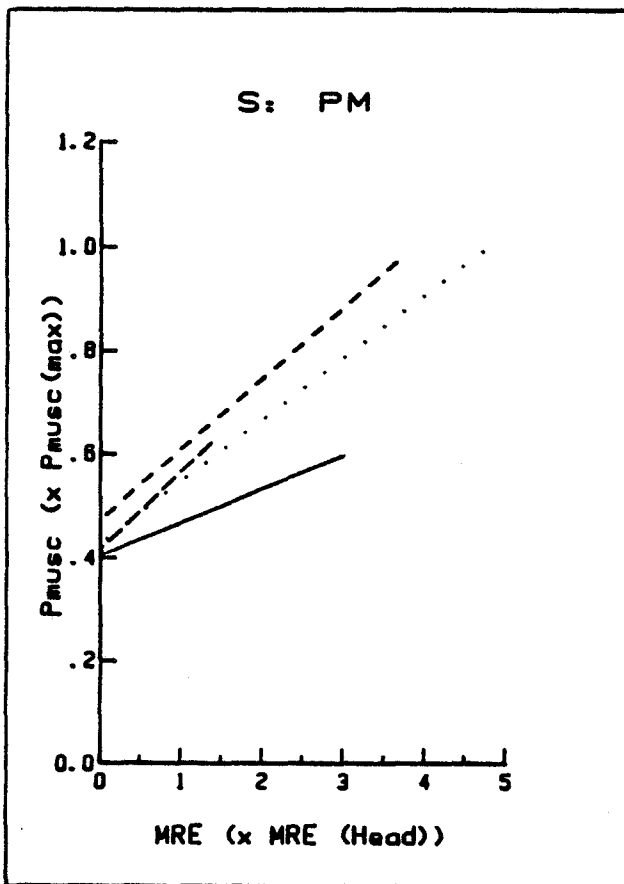
Head Lift Manoeuvre



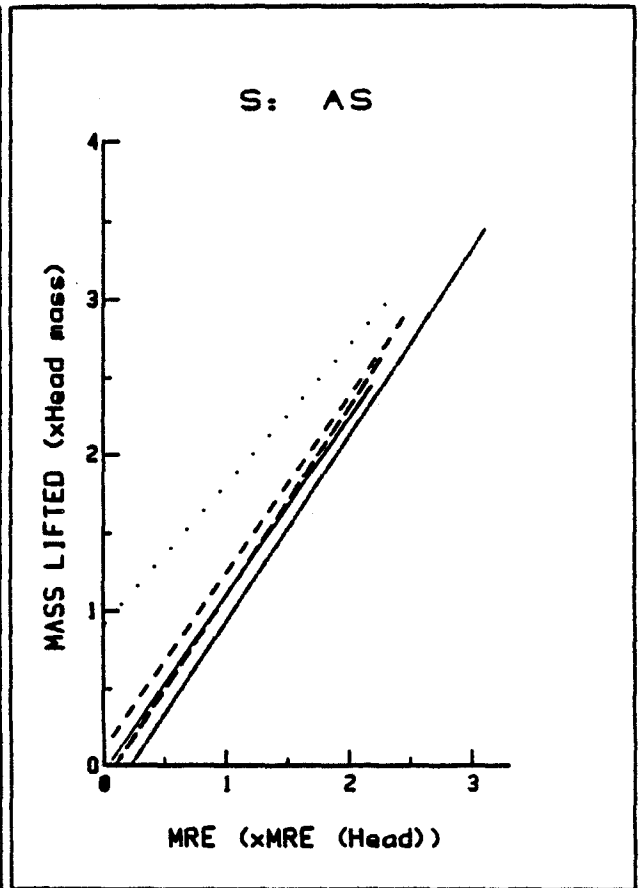
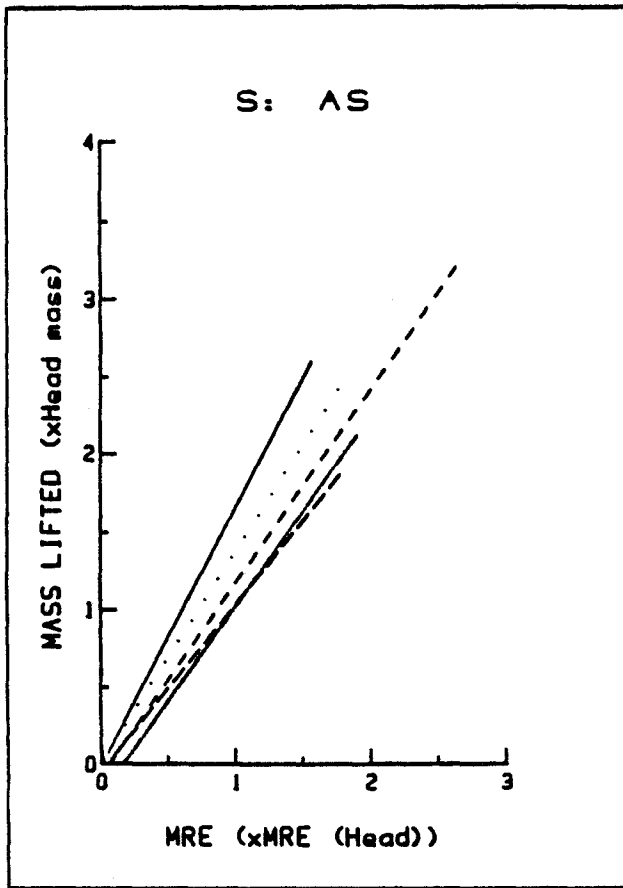
Respiratory Function Manoeuvre



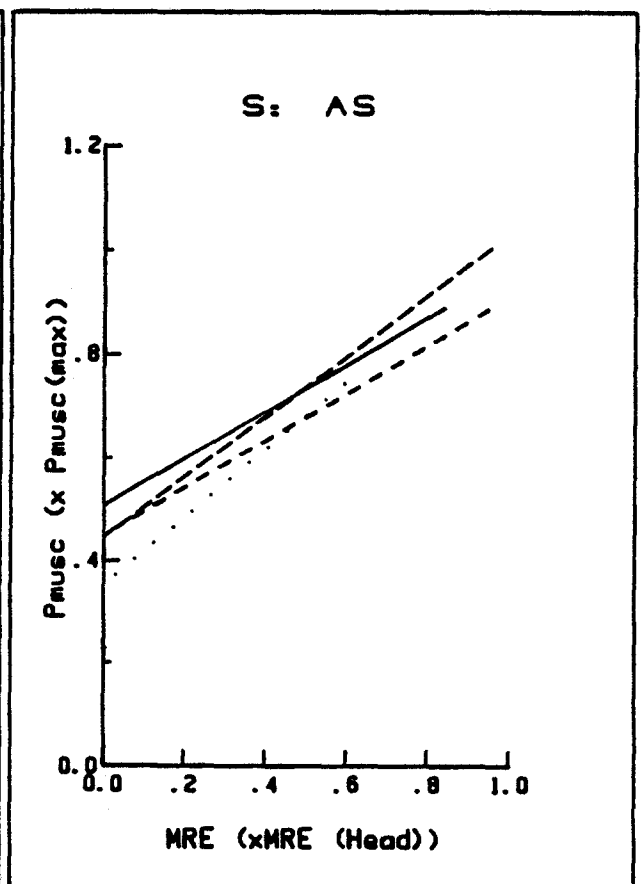
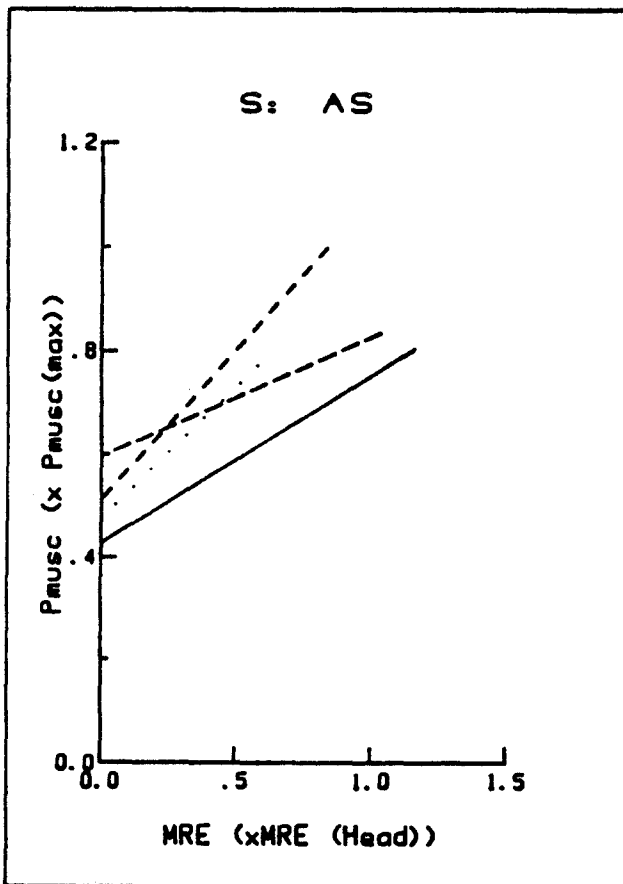
Head Lift Manoeuvre



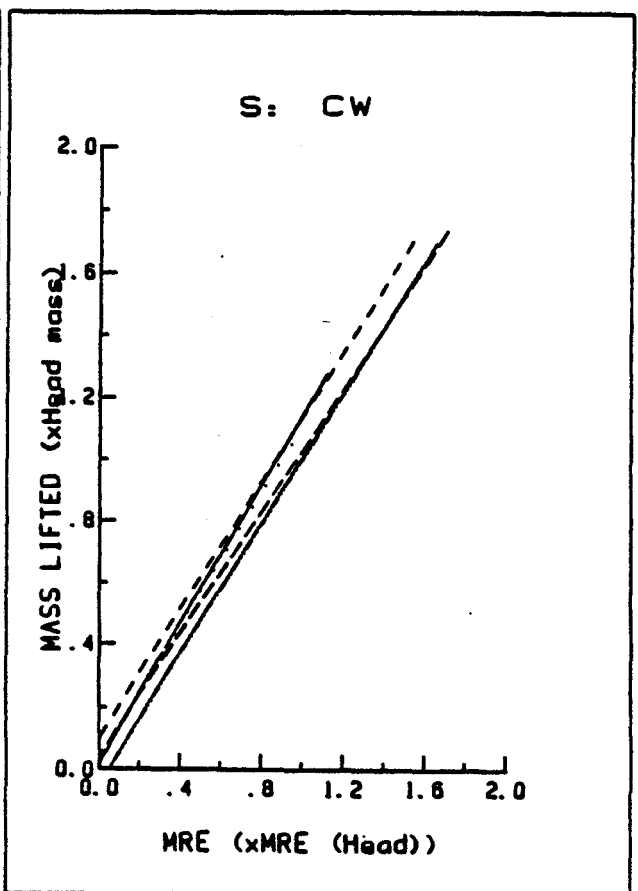
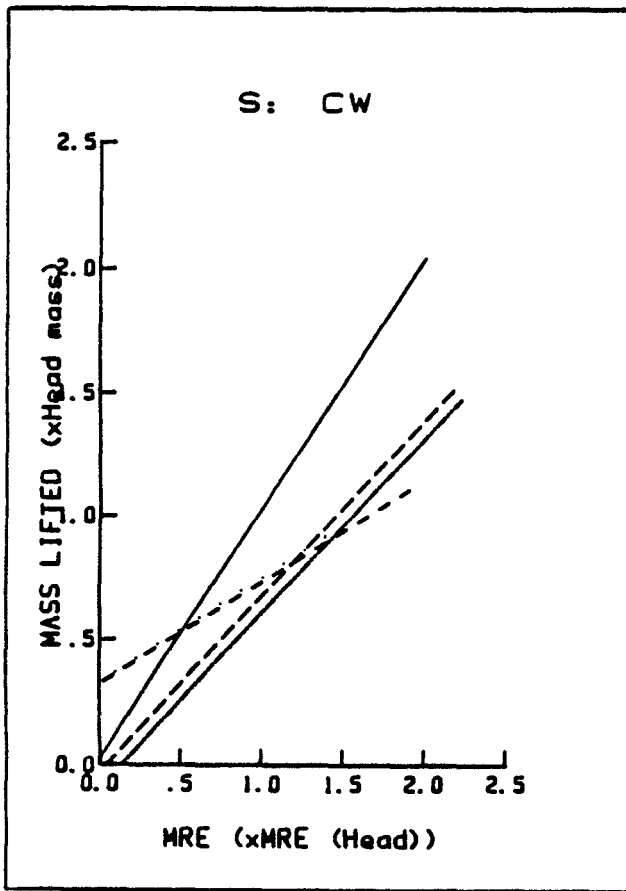
Respiratory Function Manoeuvre



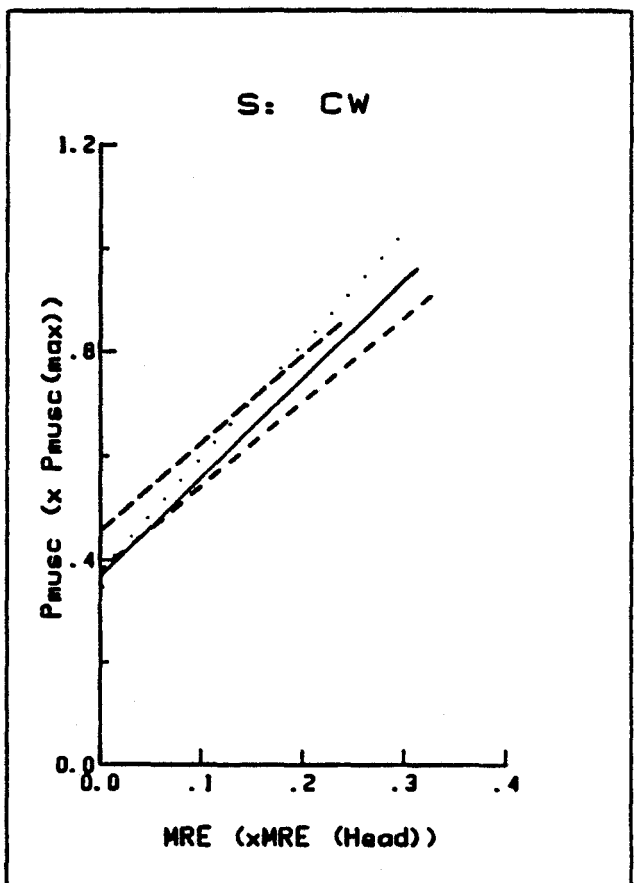
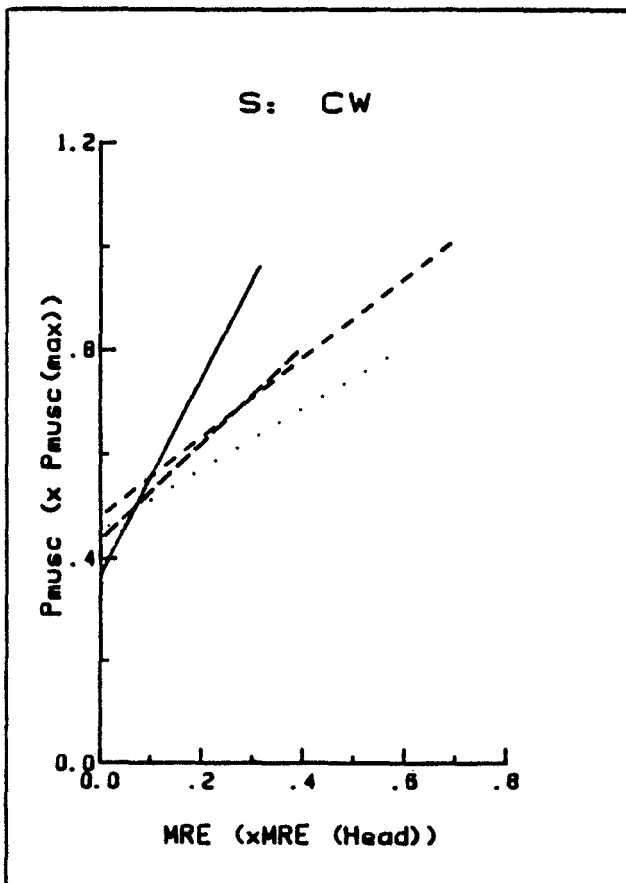
Head Lift Manoeuvre



Respiratory Function Manoeuvre

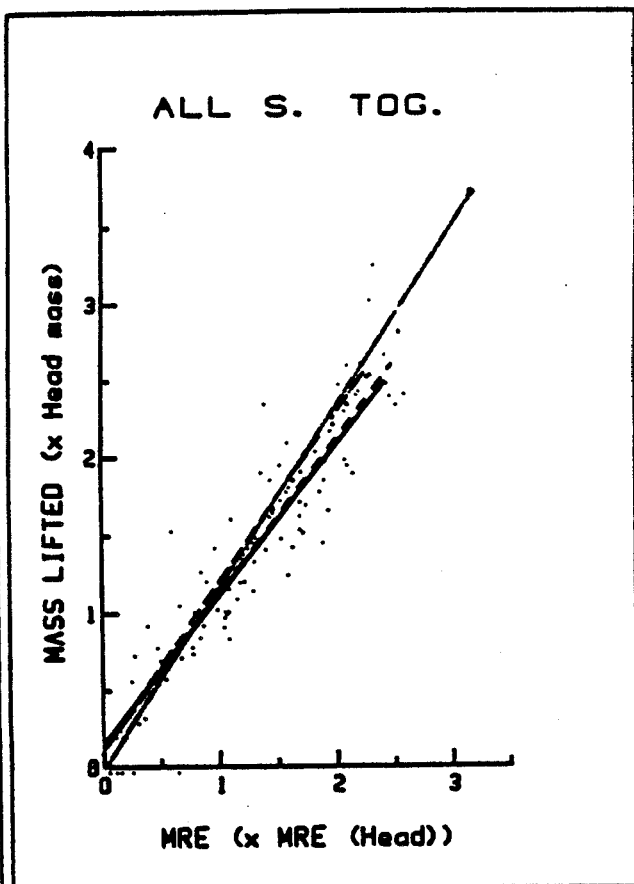
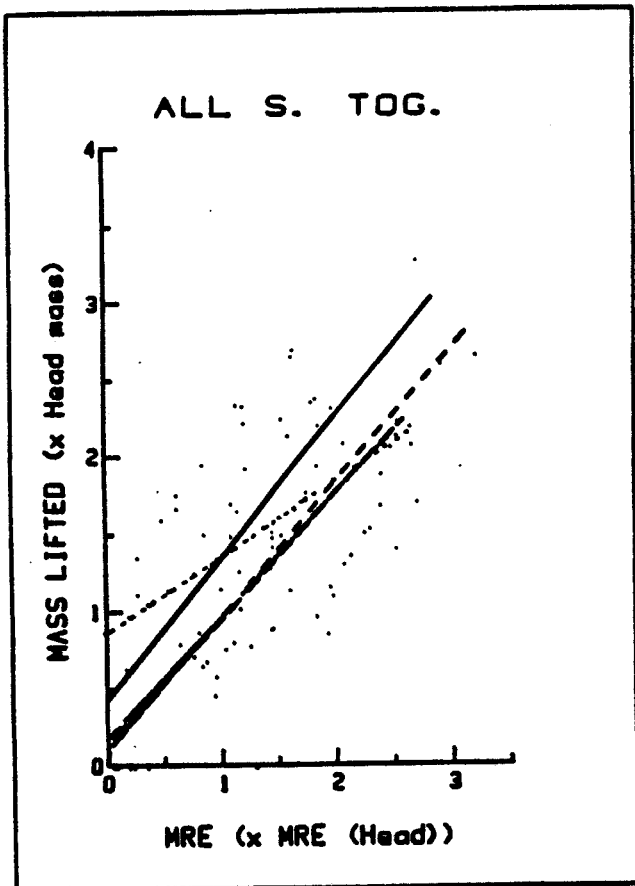


Head Lift Manoeuvre

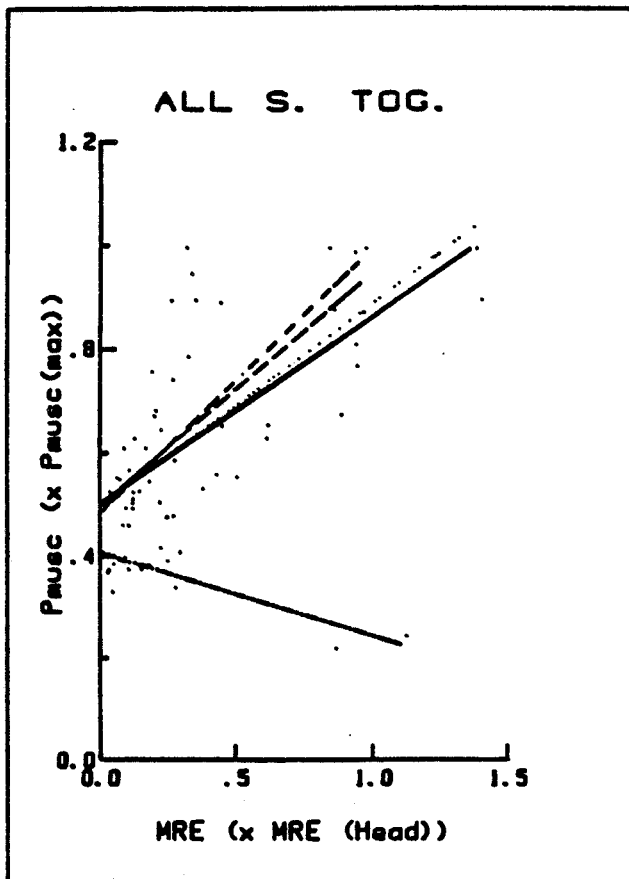
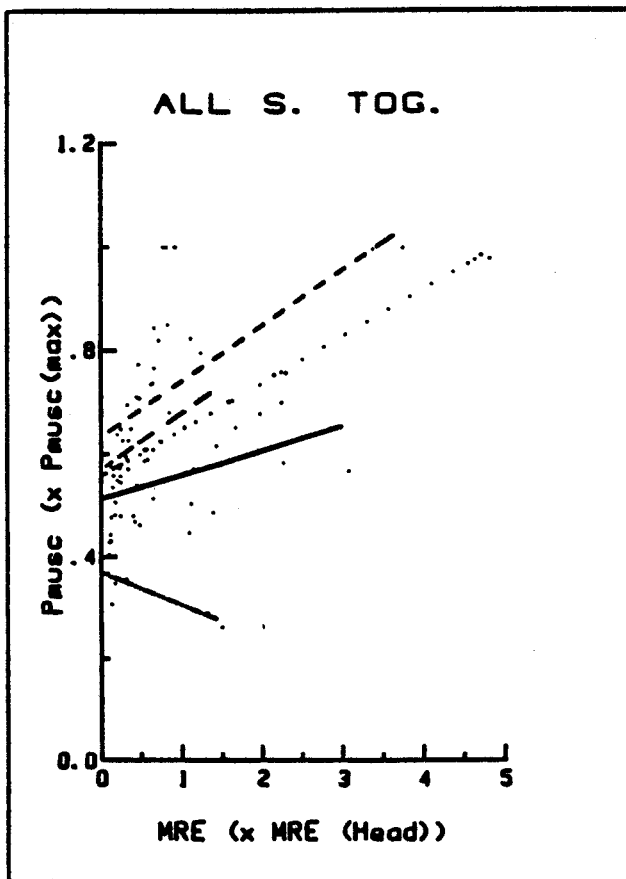


Respiratory Function Manoeuvre

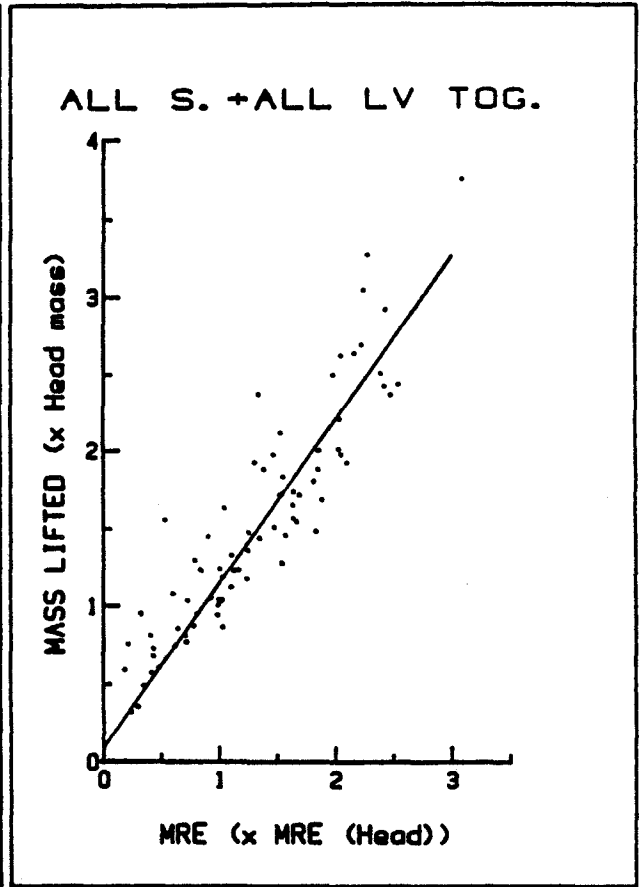
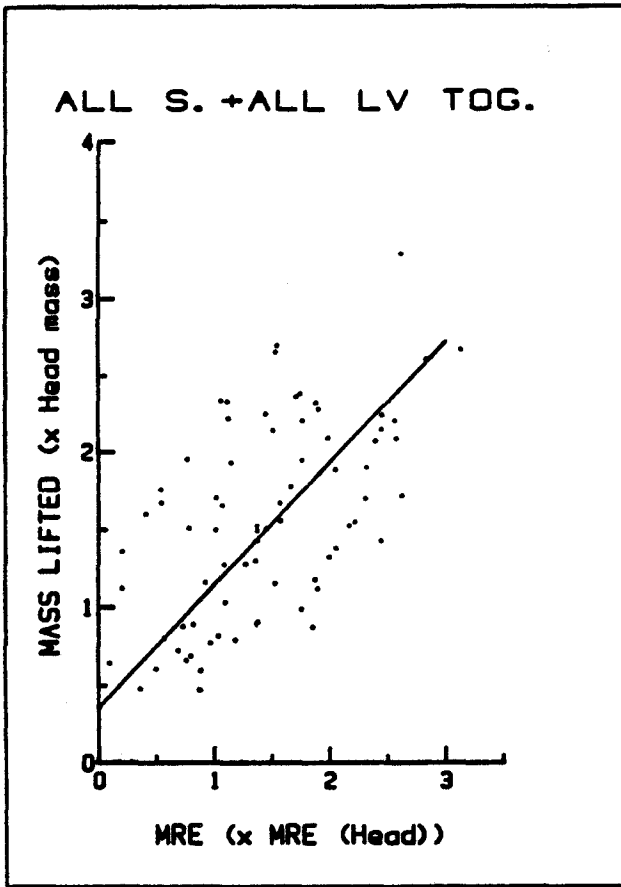
POOLED DATA  
[REFER TO  
CHAPTER VI.]



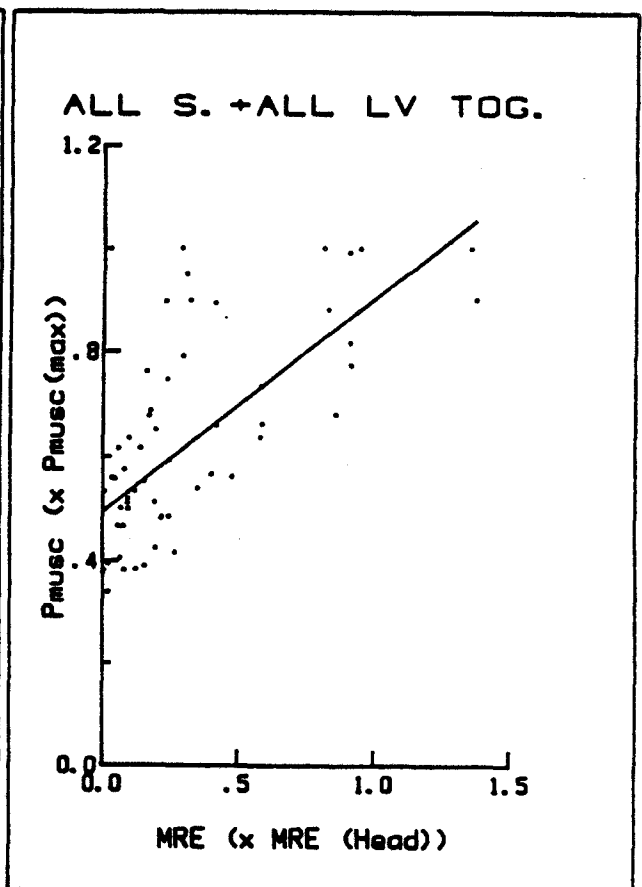
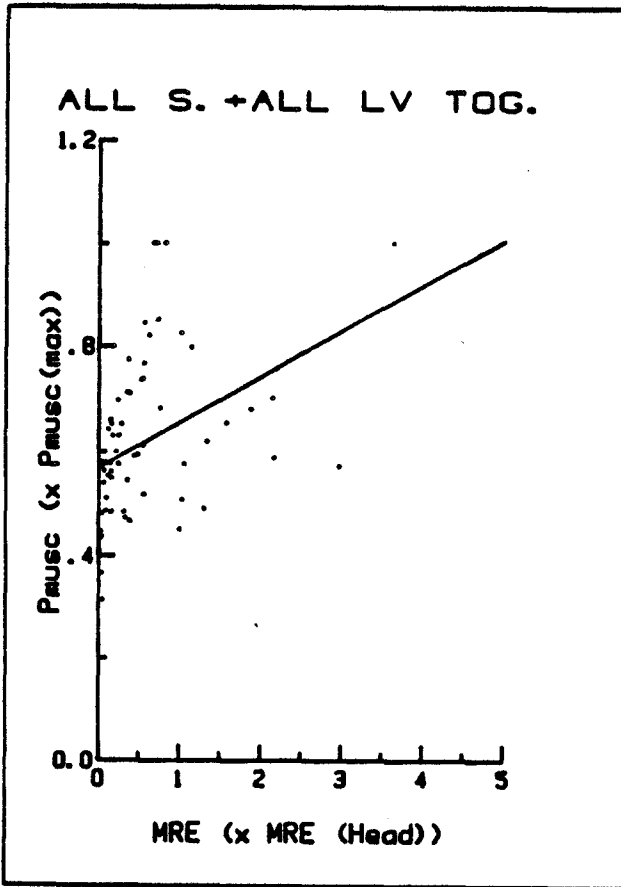
Head Lift Manoeuvre



Respiratory Function Manoeuvre



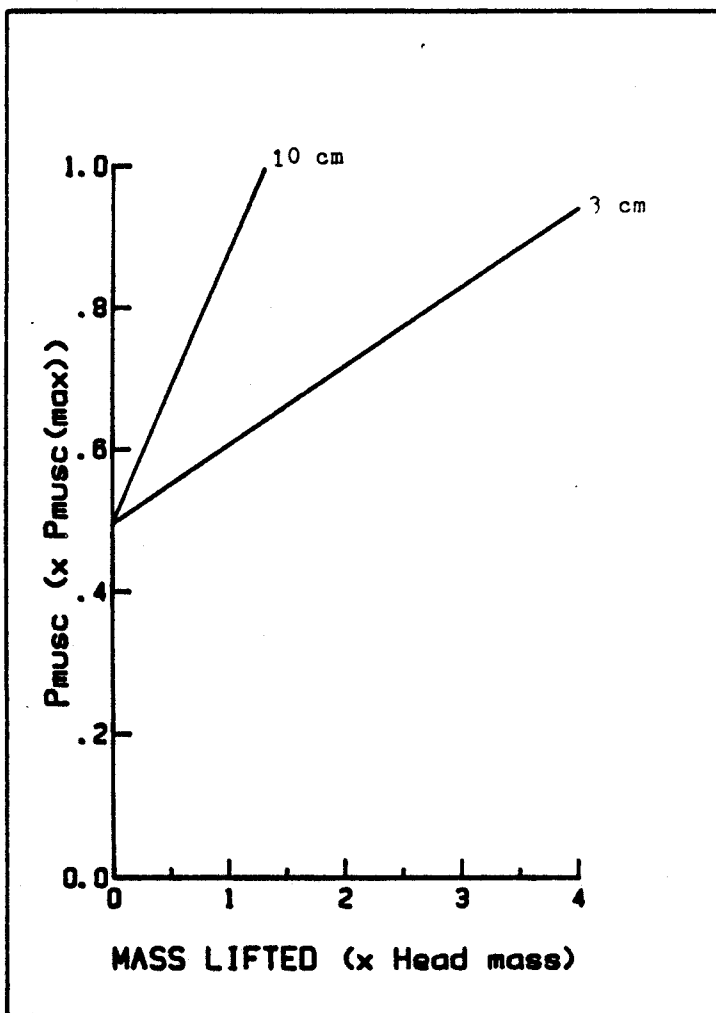
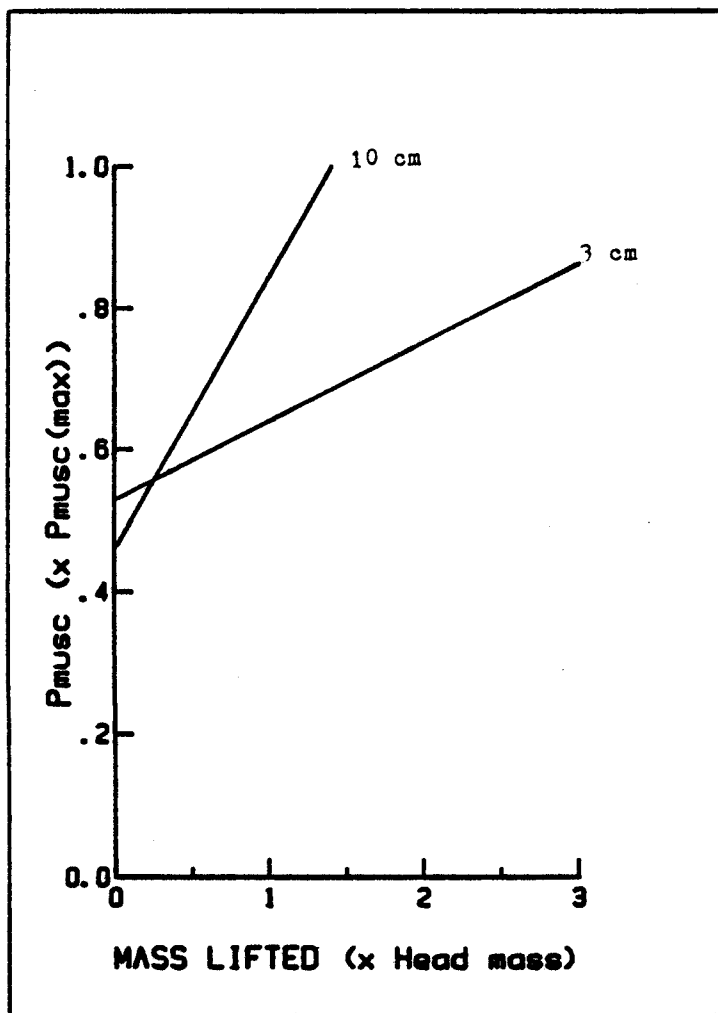
Head Lift Manoeuvre



Respiratory Function Manoeuvre



FINAL RELATIONSHIPS



For 3cm:  $P_{musc} = .528 + .112 \times HL$

For 3cm:  $P_{musc} = .494 + .112 \times HL$

For 10cm:  $P_{musc} = .459 + .386 \times HL$

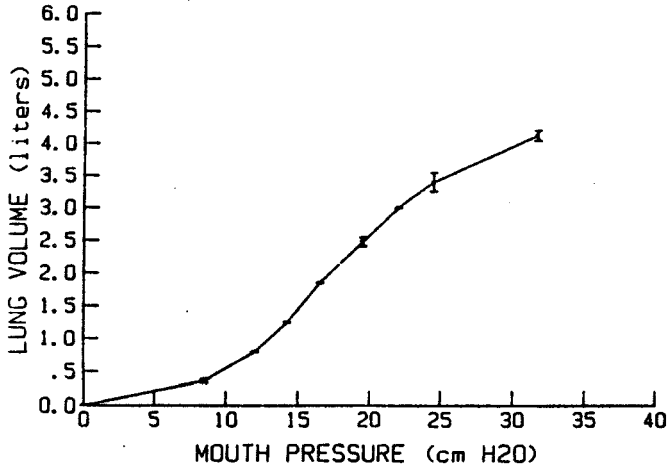
For 10cm:  $P_{musc} = .494 + .386 \times HL$

RELAXATION MANOEUVRE

LT				PM			
Mouth Pressure ( cm H2O ) Value $\pm$ S.D.		Lung Volume ( Liters ) Value $\pm$ S.D.		Mouth Pressure ( cm H2O ) Value $\pm$ S.D.		Lung Volume ( Liters ) Value $\pm$ S.D.	
31.750	2.250	4.125	0.125	33.500	0.500	3.525	0.075
24.500	0.500	3.395	0.150	28.000	0.000	3.350	0.000
22.000	0.000	2.995	0.000	23.750	0.250	2.800	0.100
19.500	0.500	2.475	0.070	20.000	0.000	2.550	0.000
16.500	0.000	1.845	0.000	17.750	0.750	2.125	0.025
14.250	1.250	1.245	0.000	14.000	0.000	1.800	0.000
12.000	0.500	0.795	0.000	12.500	1.500	1.475	0.075
8.500	0.500	0.365	0.030	11.000	0.000	1.100	0.000
0.000	0.000	0.000	0.000	7.000	0.000	1.000	0.000
				6.500	0.000	0.700	0.000
				0.000	0.000	0.000	0.000
AS				CW			
Mouth Pressure ( cm H2O ) Value $\pm$ S.D.		Lung Volume ( Liters ) Value $\pm$ S.D.		Mouth Pressure ( cm H2O ) Value $\pm$ S.D.		Lung Volume ( Liters ) Value $\pm$ S.D.	
32.000	0.500	3.325	0.050	31.500	0.000	2.550	0.025
30.000	0.000	3.100	0.000	29.250	1.250	2.375	0.025
29.000	0.000	2.950	0.000	26.500	0.000	2.100	0.000
27.000	0.000	2.750	0.000	21.000	0.000	1.725	0.125
25.000	0.000	2.500	0.000	15.500	0.000	1.125	0.125
21.000	0.000	2.150	0.100	9.500	0.000	0.600	0.000
18.000	0.000	1.650	0.000	8.000	1.000	0.225	0.025
15.000	0.000	1.500	0.000	0.000	0.000	0.000	0.000
12.000	0.000	1.150	0.000				
0.000	0.000	0.000	0.000				

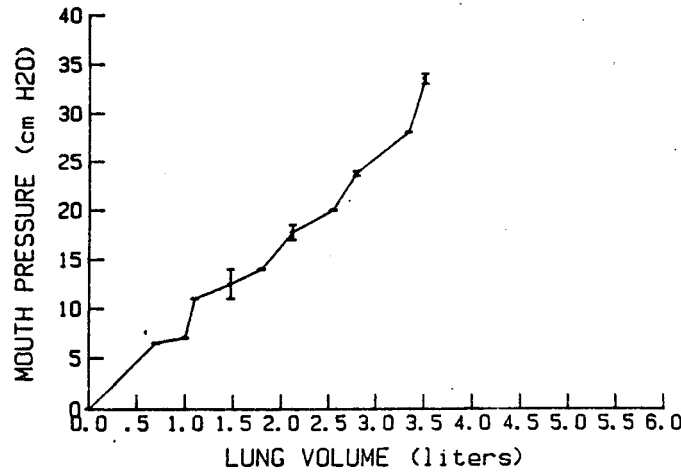
SUBJECT: L.T.

RELAXATION MAN.



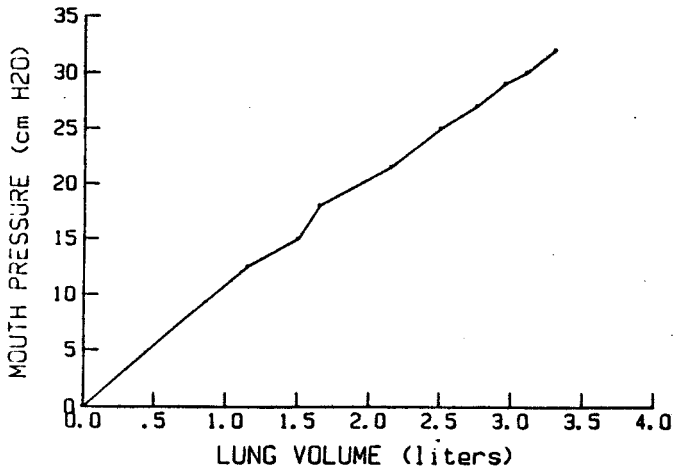
SUBJECT: P.M.

RELAXATION MAN.



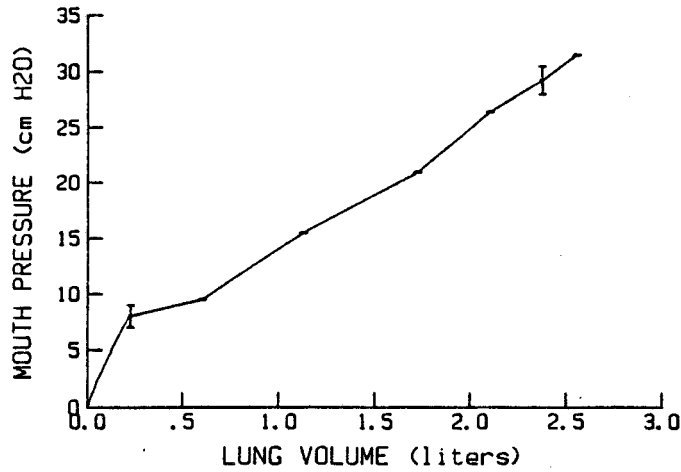
SUBJECT: A.S.

RELAXATION MAN.



SUBJECT: C.V.

RELAXATION MAN.



REPRODUCIBILITY

**Note:**

The following manoeuvres were performed at a head height of 3cm above the bed.

Manoeuvre	Symbol
Recording No. 1	—————
Recording No. 2	- - - - -

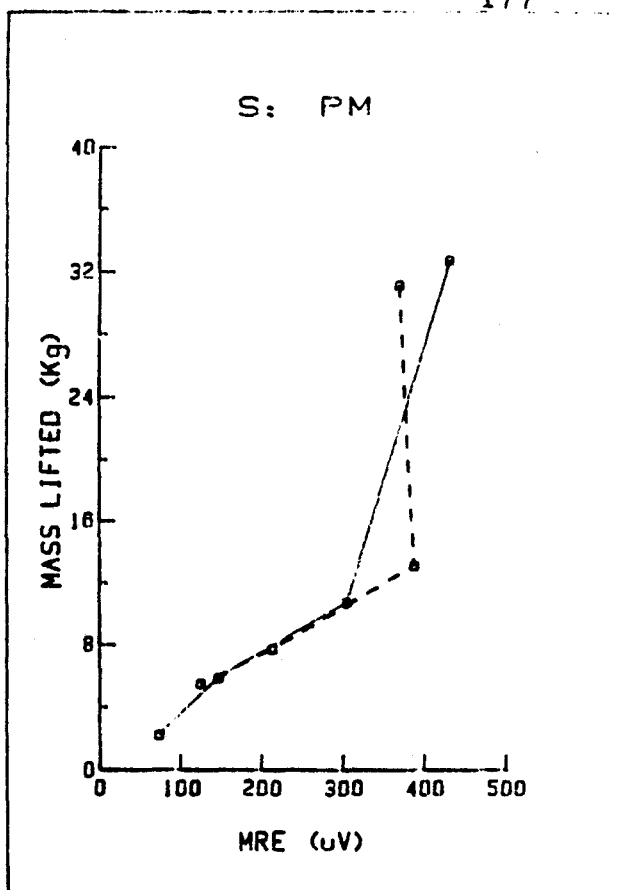
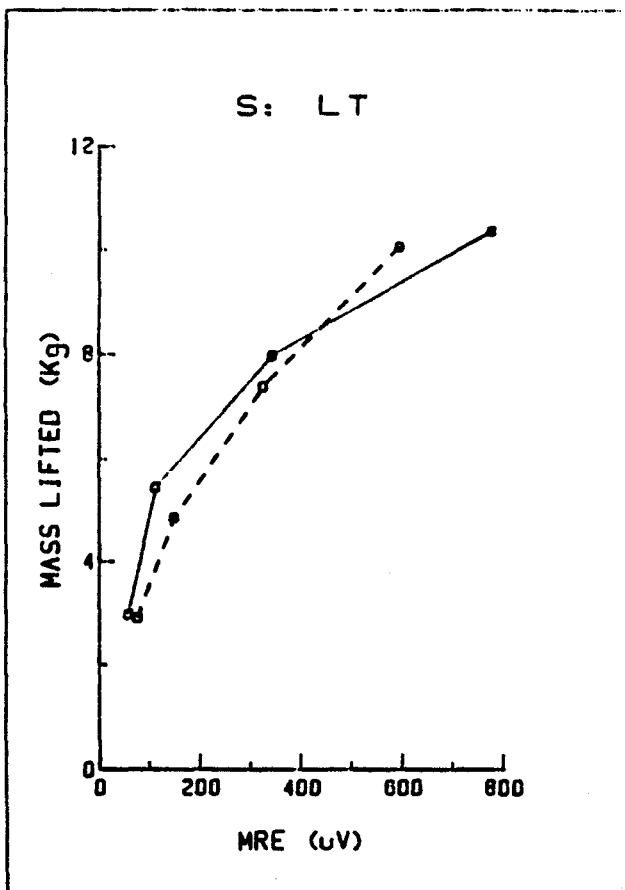
SUBJECT	LUNG VOLUME	MEASUREMENT No. 1		MEASUREMENT No. 2	
		EMG uV	MASS Kg	EMG uV	MASS Kg
LT	FRC	774.448	10.344	591.372	10.032
		341.899	7.953	324.763	7.365
		110.942	5.429	147.968	4.837
		57.364	2.964	75.364	2.892
	FRC+2L	693.330	8.900	693.330	8.800
		640.000	7.350	586.670	6.350
		355.560	3.800	337.780	3.500
		33.036	0.000	1.924	0.000
PM	FRC	429.600	32.687	367.200	31.113
		303.520	10.702	386.480	13.098
		145.446	5.817	212.734	7.703
		72.469	2.202	123.895	5.434
	FRC+2L	372.860	12.215	351.140	9.955
		316.130	6.000	357.210	16.000
		303.264	8.757	344.736	9.243

HL MANOEUVRE AT A HEAD HEIGHT OF 3cm ABOVE THE BED

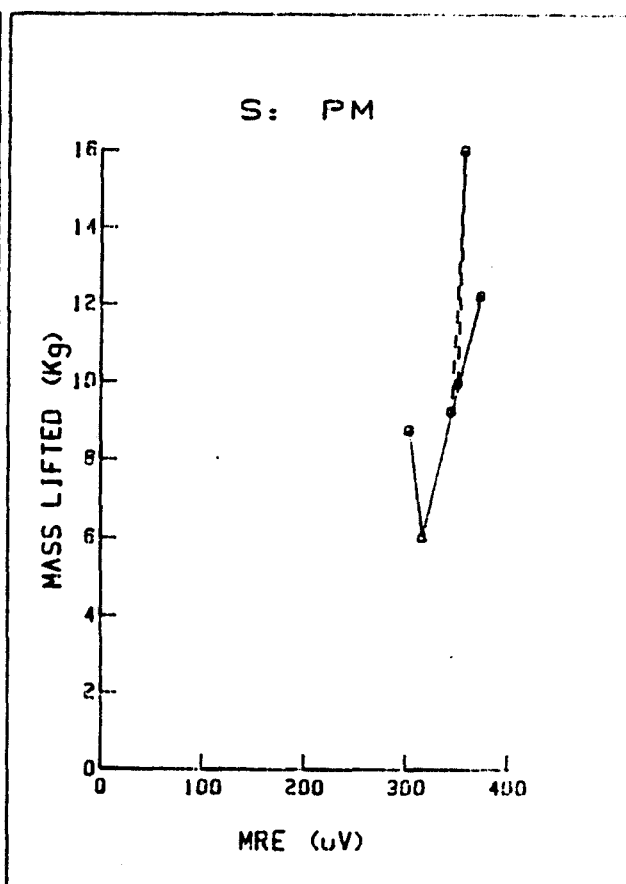
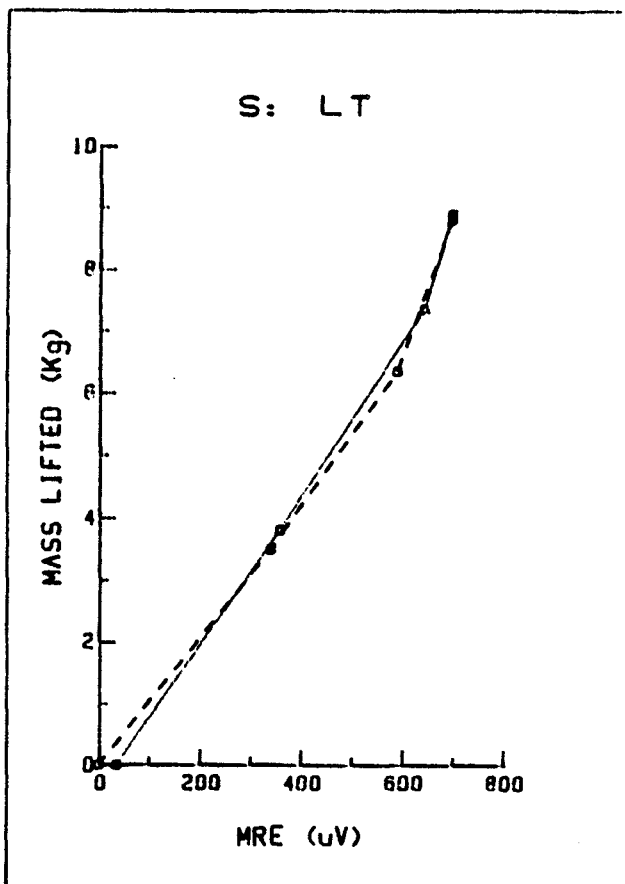


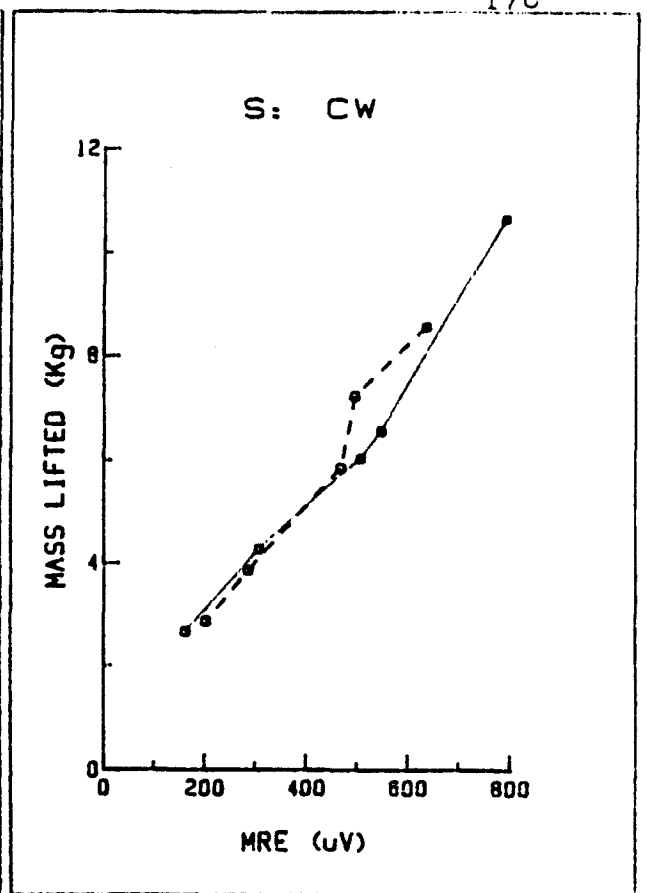
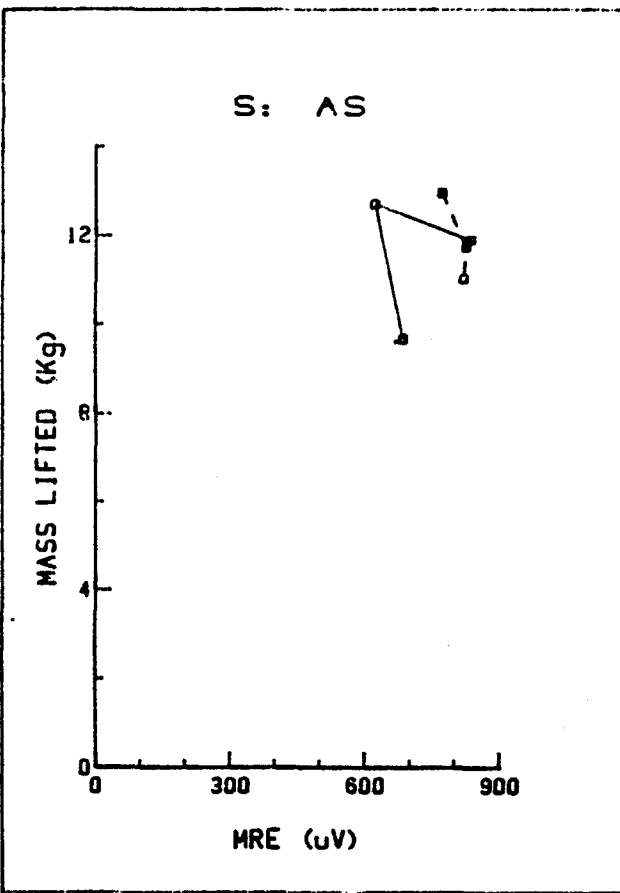
SUBJECT	LUNG VOLUME	MEASUREMENT No. 1		MEASUREMENT No. 2	
		EMG uV	MASS Kg	EMG uV	MASS Kg
AS	FRC	832.000	11.858	768.000	12.942
		618.680	12.701	821.520	11.707
		680.120	9.634	815.880	11.000
	FRC+2L	958.016	8.828	854.848	9.030
		925.728	8.387	690.016	6.909
		598.400	6.196	816.000	6.891
		514.272	3.547	614.000	5.863
	CW	FRC	788.470	10.644	633.750
544.490			6.564	493.370	7.236
503.300			6.029	465.580	5.833
305.290			4.257	284.350	3.851
161.220			2.660	201.440	2.860
FRC+2L		755.550	8.153	791.110	5.811
		386.820	3.554	355.400	3.872
		321.100	2.382	313.560	3.018
		384.110	2.223	250.130	2.067

HL MANOEUVRE AT A HEAD HEIGHT OF 3cm ABOVE THE BED

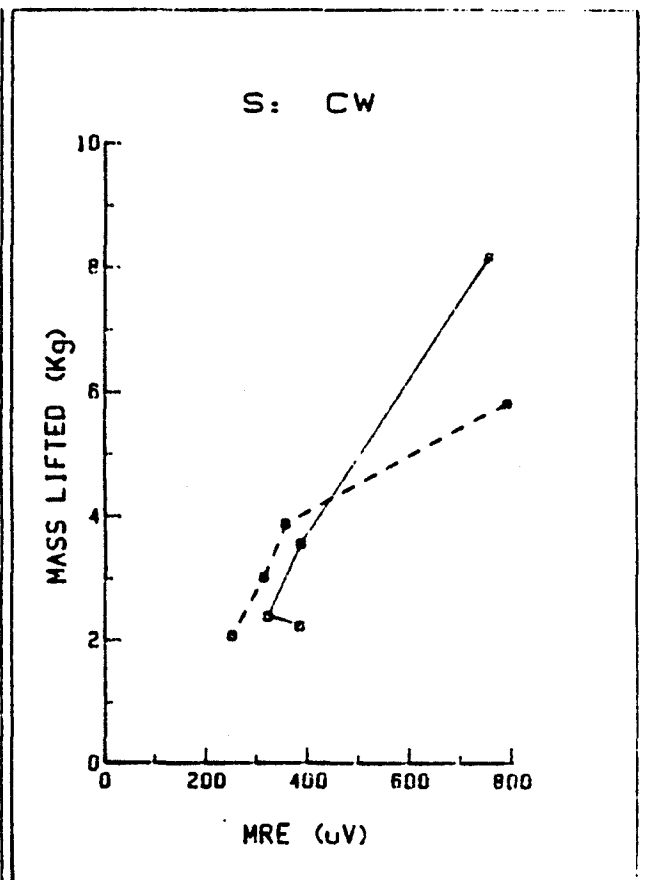
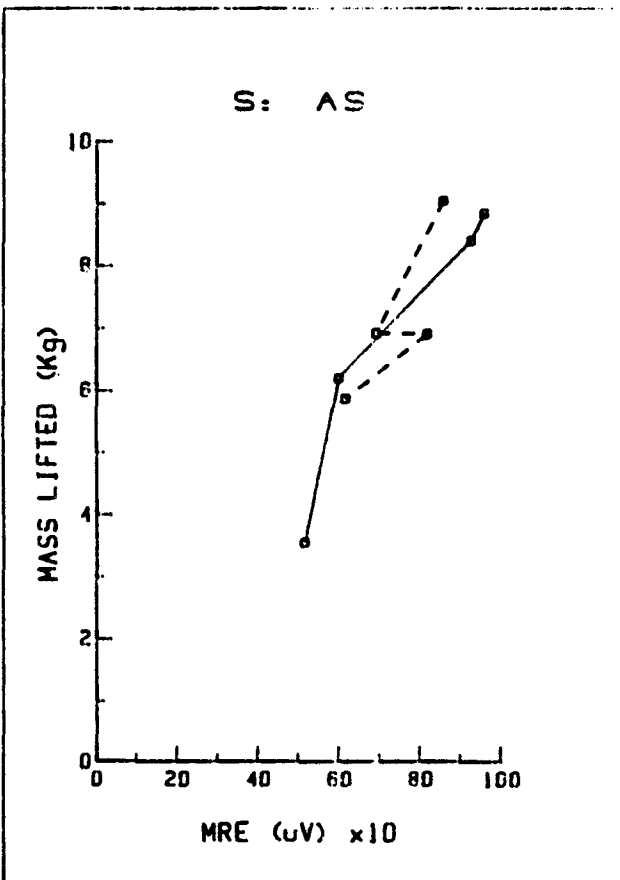


FRC + 2L





FRC + 2L



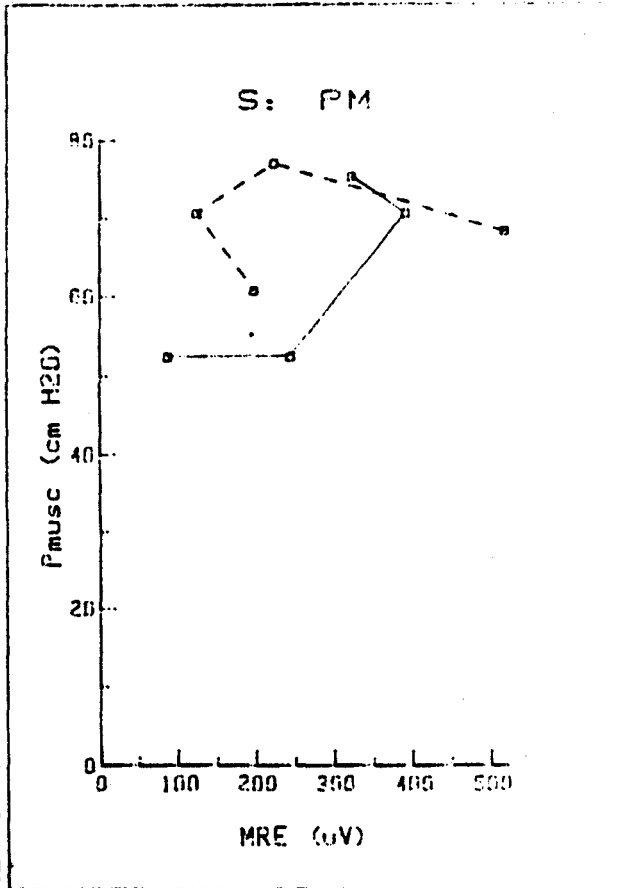
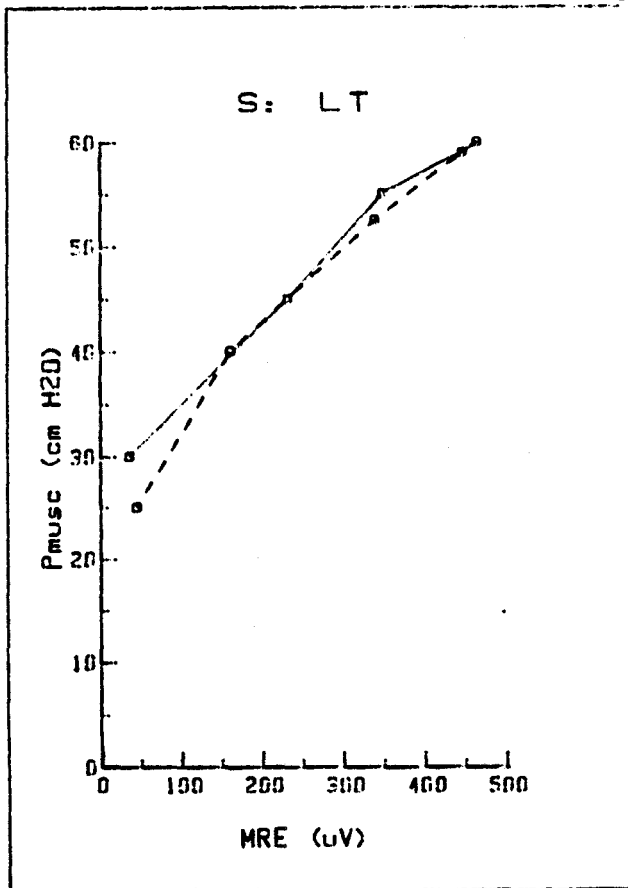
Head Lift Manoeuvre

SUBJECT	LUNG VOLUME	MEASUREMENT No. 1		MEASUREMENT No. 2	
		EMG uV	P <sub>musc</sub> cm H <sub>2</sub> O	EMG uV	P <sub>musc</sub> cm H <sub>2</sub> O
LT	FRC	462.220	60.000	462.220	60.000
		346.670	55.000	337.780	52.500
		231.110	45.000	160.000	40.000
		35.560	30.000	44.440	25.000
	FRC+2L	355.560	67.238	408.890	77.238
		213.330	57.238	142.220	57.238
		160.000	52.238	155.560	49.738
		26.670	42.238	35.560	42.238
PM	FRC	321.523	75.286	515.977	68.214
		389.504	70.481	222.156	76.947
		243.558	52.325	123.702	70.591
		87.195	52.257	197.385	60.743
	FRC+2L	120.000	75.159	260.000	80.159
		100.000	70.409	200.000	73.909
		70.000	62.034	90.000	67.959
		43.056	54.744	70.278	62.034

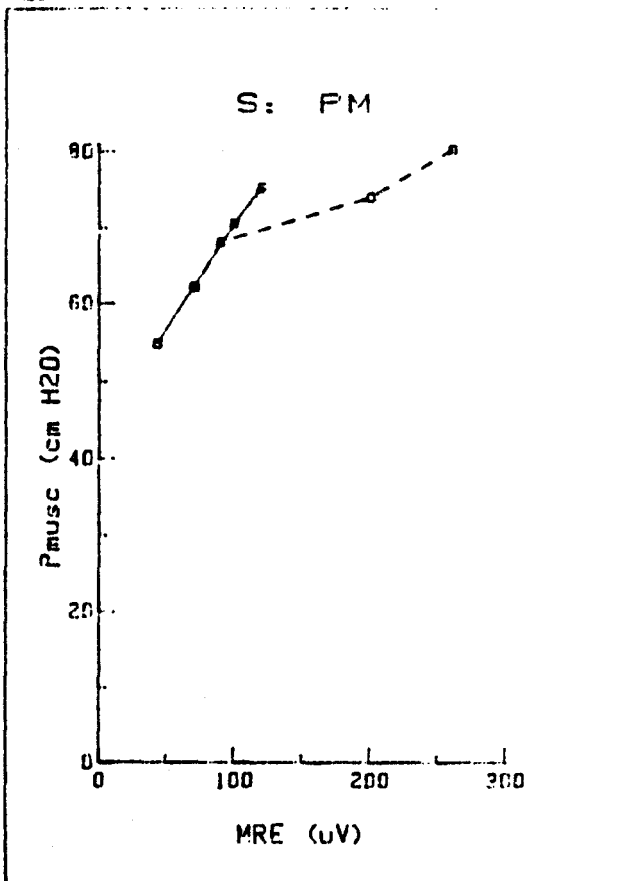
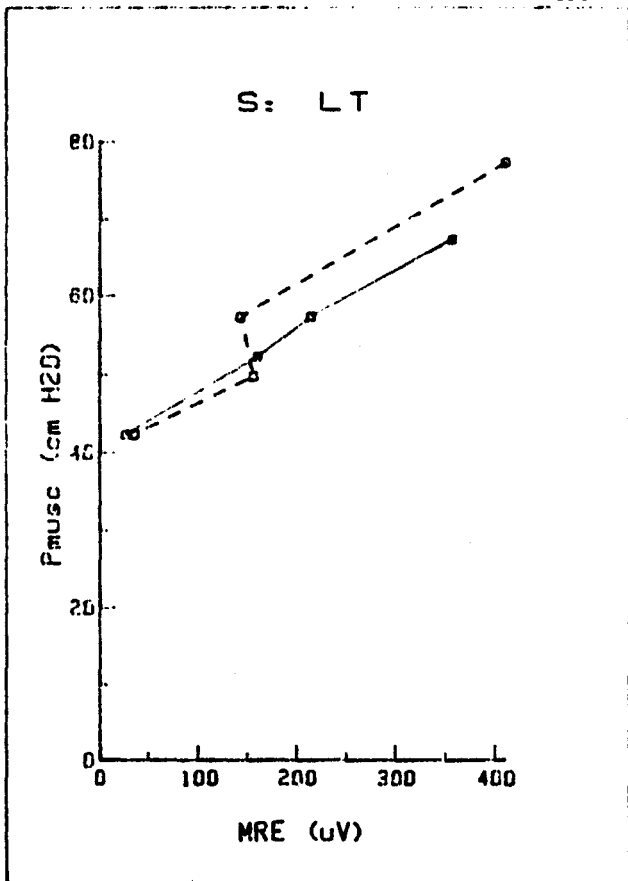
RM MANOEUVRE AT A HEAD HEIGHT OF 3cm ABOVE THE BED

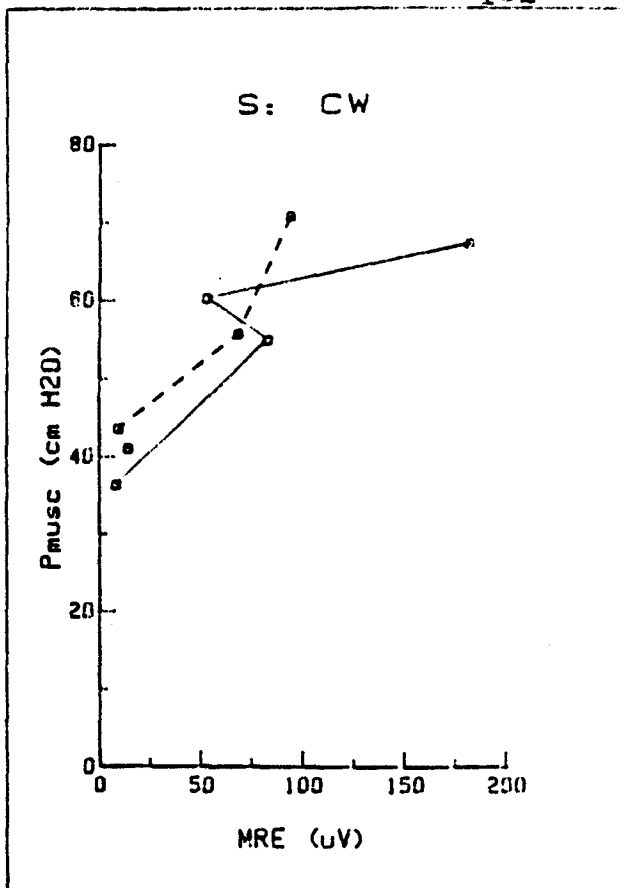
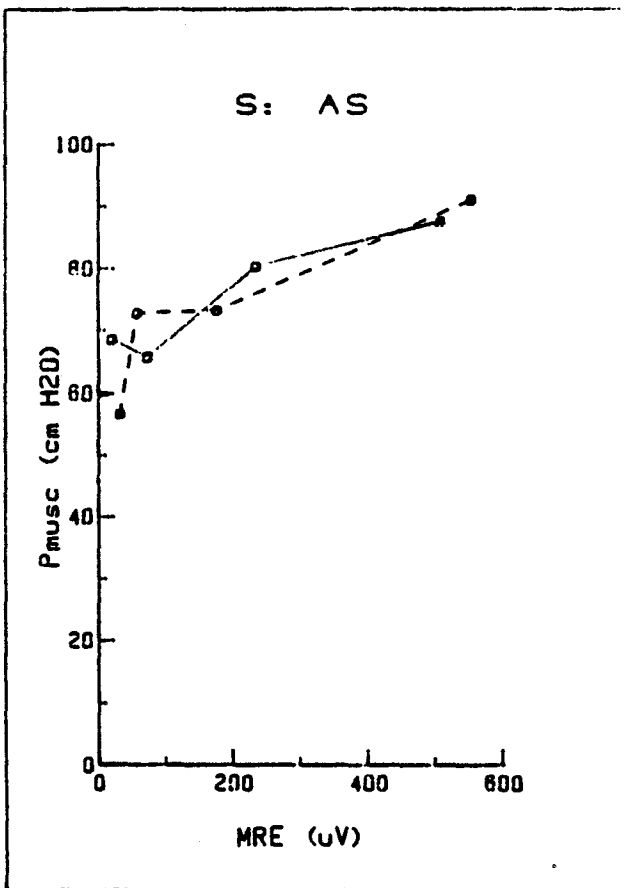
SUBJECT	LUNG VOLUME	MEASUREMENT No.1		MEASUREMENT No. 2	
		EMG uV	Pmusc cm H2O	EMG uV	Pmusc cm H2O
AS	FRC	659.882	89.786	524.118	82.714
		227.598	56.982	275.598	61.982
		227.598	56.982	148.402	60.518
		35.029	56.036	68.971	48.964
		6.343	45.518	17.657	41.982
	FRC+2L	505.373	87.441	550.627	90.977
		232.284	80.245	175.716	73.173
		72.558	65.673	57.842	72.745
		20.343	68.432	31.657	56.652
CW	FRC	161.040	64.821	226.760	66.509
		47.200	53.018	64.800	49.482
		24.063	40.518	11.493	36.982
	FRC+2L	181.778	67.209	93.782	70.745
		52.871	60.193	68.169	55.547
		82.770	54.782	9.230	43.588
		7.968	36.202	14.254	40.918

RM MANOEUVRE AT A HEAD HEIGHT OF 3cm ABOVE THE BED

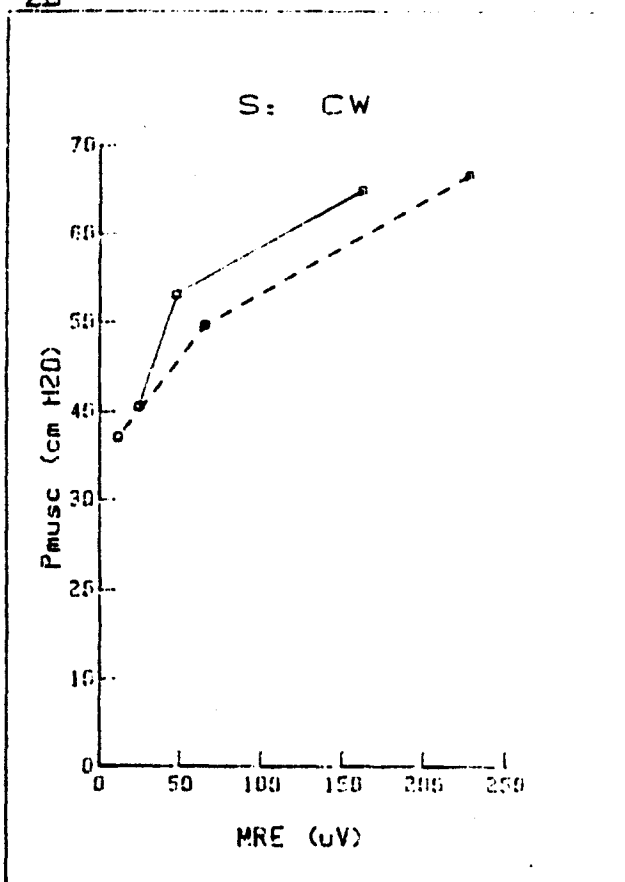
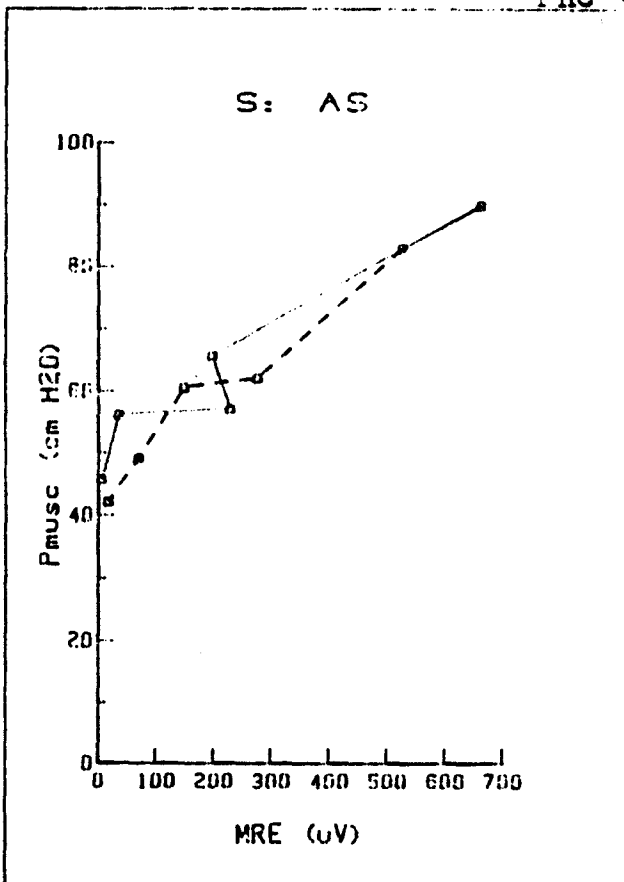


FRC + 2L





FRC + 2L



APPENDIX D



## APPENDIX D

### A MODEL OF THE NECK

Assume that the neck behaves like a hinge. The axis of rotation is located in the middle of the neck, as shown in Figure 1.

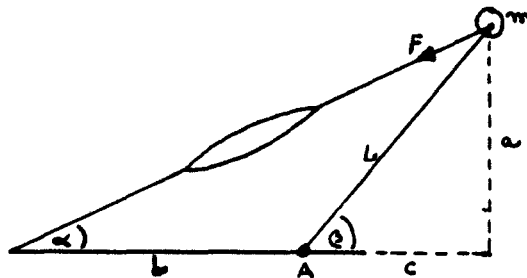


FIGURE 1

The mathematical analysis consists of finding the force  $F_1$  that is generated to support the weight  $mg$ . The method that is used here is the calculation of the total moment at the axis of rotation. From the geometry of the system, the force  $F$ , generated by the muscle, is found.

At equilibrium, the total moment around point A is:

$$F_1 \times L \sin \phi - (mg + F_2) \times L \cos \phi = 0 \quad D.1$$

where  $F_1 = F \cos \alpha$  and  $F_2 = F \sin \alpha$ .

By solving equation D.1, one gets an expression for the force  $F$  generated by the SCM muscle. This force is:

$$F = mg / \left( \frac{a}{c} \cos \alpha - \sin \alpha \right) \quad D.2$$

where  $mg$  is the total weight lifted during a specific manoeuvre.

The complexity of the neck system does not allow  $\alpha$  to be greater than 45 degrees, i.e.,  $0^\circ < \alpha < 45^\circ$ . This implies that  $\cos \alpha$  varies between 1 and 0.707, and  $\sin \alpha$ , between 0 and 0.707. These variations are small compared to the variation of the ratio  $a/c$ . As  $\alpha$  increases, the ratio  $a/c$  increases a lot because  $a$  increases and  $c$  decreases. Therefore, since  $mg$  is constant during a specific manoeuvre, the increase in head height gives rise to a decrease in the force  $F$  generated by the muscle to perform the same head lift. This decrease is inversely proportional to the ratio  $a/c$ .

The model applies also to RM manoeuvres. The weight  $mg$  has to be replaced by a system which has the same effect on the muscle. This system consists of representing the respiratory system by a piston in which a negative pressure exists. This pressure represents the inspiratory pressure performed during the manoeuvre.

**REFERENCES**

## REFERENCES

1. Agostoni, E. and P. Mogroni. Deformation of the chest wall during breathing efforts. *J. Appl. Physiol.* 21(6): 1827-1832, 1966.
2. Basmajian, J.V. *Muscle alive, their functions related by EMC.* The Williams & Wilkins company, 525p., 1974.
3. Bethea, R.M., B.S. Duran, and T.L. Boullion. *Statistical methods for engineers and scientists.* Dekker inc. 583p., 1975.
4. Bigland, E. and O.C. Lippold. Relation between force, velocity, and integrated electrical activity in human muscles. *J. Physiol.* 123: 214-224, 1954.
5. Bigland-Ritchie, B. EMC recordings and how they are affected by fatigue. *Am. Rev. Respir. Dis.*, 119: 95-97, 1979.
6. Campbell, E.J.M.. An electromyographic examination of the role of the intercostal muscles in breathing in man. *J. Physiol.* 129: 12-26, 1955a.
7. Campbell, E.J.M.. The role of the scalene and sternocleidomastoid muscles in breathing in normal subjects. An electromyographic study. *J. Anat.* 89: 378-386, 1955b.
8. Close, J.R., E.D. Nickle, and F.N. Todd. Motor-unit action-potential counts: their significance in isometric and isotonic contractions. *J. Bone & Joint Surg.* 42-A: 1207-1222, 1960.
9. Cnockaert, J.C., C. Lensel, and E. Pertuzon. Relative contribution of individual muscles to the isometric contraction of a muscular group. *J. Biomechanics* 8: 191-197, 1975.
10. Danon, J., et al. Relationship of inspiratory muscle electromyograms to pressure and lung volume during static inspiratory effort. *Physiologist* 14:128, 1971.
11. Danon, J., W.S. Druz, N.B. Goldberg, and J.T. Sharp. Function of the isolated paced diaphragm and the cervical accessory muscles in C1 quadriplegics. *Am. Rev. Respir. Dis.* 119: 909-919, 1979.
12. De Bruin, H.. Aspects of analysis and processing of electromyographic signals. Ph.D. Thesis Hamilton, Ont., Can.: McMaster University, 1976.
13. De Luca, C.J.. A model for a motor unit train recorded during constant force isometric contractions. *Biol.*

- Cybernetics 19: 159-167, 1975.
14. De Luca, C.J., and E.J. Vandyk. Derivation of some parameters of myoelectric signals recorded during sustained constant force isometric contractions. *Biophys J.* 15: 1167-1180, 1975.
  15. De Luca, C.J.. Physiology and mathematics of myoelectric signals. *IEEE Trans. on Biomed Eng BME-26(6)*: 313-325, 1979.
  16. Druz, W.S., et al. Approaches to assessing respiratory muscle function in respiratory disease. *Am. Rev. Respir. Dis.* 119(2): 145-149, 1979.
  17. Druz, W.S. and J.T. Sharp. Activity of respiratory muscles in upright and recumbent humans. *J. Appl. Physiol.: Respir. Environ. Exercise Physiol.* 51(6): 1552-1561, 1981.
  18. Figini, M. M. and B. Mambrico. Mathematical analysis of compound EMG signals. Abstract from the fourth congress of I.S.E.K., 1979.
  19. Green, J.R. and D. Margerison. Statistical treatment of experimental data., Elsevier, 382p., 1979.
  20. Hof, A.L. and J.W. Van Den Berg. Linearity between the weighted sum of the EMGs of the human Triceps surae and the total torque. *J. Biomechanics* 19: 529-539, 1977.
  21. Huggins, E.S., P.A. Parker, and R.N. Scott. EMG versus isometric force and muscle length. Abstract from the fourth congress of I.S.E.K., 1979.
  22. Knuttgen, H.C., J.F. Patton, and J.A. Vogel. An ergometer for concentric and eccentric muscular exercise. *J. Appl. Physiol.: Respirat, Environ. Exercise Physiol.* 53(3) " 784-788, 1982.
  23. Koepke, C.H., A.J. Murphy, E.M. Smith, and D.G. Dickinson. Sequence of action of the diaphragm and I.C. muscles during respiration. 1- Inspiration. *Arch. Phys. Med.* 39: 426-430, 1958.
  24. Komi, P.V. and J.H.T. Viitasalo. Signal characteristics of EMG at different levels of muscle tension. *Acta. Physiol. Scand.* 96: 267-276, 1976.
  25. Kurcda, E., V. Klissouras, and J.H. Milsum. Electrical and metabolism activities and fatigue in human isometric contraction. *J. Appl. Physiol.* 29(3): 358-367, 1970.
  26. Lynn, P.A., N.D. Bettles, A.D. Hughes, and S.W. Johnson. Influences of electrode geometry on bipolar recordings of the surface electrocyogram. *Med. & Biol. Eng. & Comput.* 16: 651-660, 1978.

27. Loring, H.S. and J.Mead. Action of the diaphragm on the rib cage inferred from a force-balance analysis. *J. Appl. Physiol.: Resp. Environ. Exercise Physiol.* 53(3): 756-760, 1982.
28. Manns, A. and M. Spreng. EMC amplitude and frequency at different muscular elongations under constant masticatory force or EMC activity. *Acta Physiol. Latino Am.* 27: 259-271, 1977.
29. Milner-Brown, H.S., R.B. Stein, and P. Yemm. The orderly recruitment of human motor units during voluntary isometric contractions. *J. Physiol.* 230: 359-370, 1973b.
30. Milner-Brown, H.S. and R.B. Stein. The relation between the surface electromyogram and muscular force. *J. Physiol.* 246: 549-569, 1975.
31. Missiuro, W., H. Kirschner, and S. Kozolowski. Electromyographic manifestation of fatigue during work of different intensity. *Acta Physiol. Polon.* 13: 11-23, 1962
32. Moore, A.D.. Synthesized EMC waves and their applications. *Amer. J. Phys. Med.* 46: 1302-1316, 1967.
33. Murphy, A.J. et al. Sequence of action of the diaphragm and I.C. muscles during respiration. 1- Inspiration. *Arch. Phys. Med.* 40: 337-342, 1958.
34. Mountcastle, V.B.. *Medical Physiology*, Mosby, vol.2, 1999p., 1980.
35. Netter, F.H. *Nervous System*, Ciba vol. 1, 168p., 1977.
36. Pansky, E. and E.L. House. *Review of Gross Anatomy*, Macmillan, 508p., 1975.
37. Pernkopf, E.. *Atlas of Topographical and Applied Human Anatomy*. vol. 1, 1963.
38. Ralston, H.J.. Uses and limitations of electromyography in the quantitative study of skeletal muscle function. *Am. J. Orthodontics*, 521-530, 1961.
39. Raper, A.J. et al. Scalene and Sternomastoid muscle function. *J. Appl. Physiol.* 21: 497-502, 1966.
40. Selkurt, E.E. *Physiology*, Little Brown Compagny, 879p., 1976.
41. Sharp, J.T. et al. Respiratory muscle function in patients with chronic obstructive pulmonary disease: Its relationship to disability and to respiratory therapy. *Am. Rev. Respir. Dis.* 110 (Supplement No.6. part 2): 154-167, 1974.

42. Stulen, F.B. and C.J. de Luca. The relation between the myoelectric signal and physiological properties of constant-force isometric contractions. *Encephal and Clin. Neurol.* 45: 681-698, 1978.
43. Tokizane, T. et al. Electromyographic studies on the human respiratory muscles. *Jap. J. Physiol.* 2: 232-247, 1952.
44. Warwick, R., L. Williams, and P. Longman. *Gray's Anatomy.*, 562p., 1973.
45. Woods, J.J. and B. Brigland-Richie. Integrated surface EMG vs force relationship and muscle fibre type composition and distribution. *Fed. Prcc.* 37: 786, 1978.
46. Zuniga, E.N. and D.C.Simons. Non-linear relationship between averaged electromyogram potential and muscle tension in normal subjects. *Arch. Phys. Med. and Rehab.*, 613-620, 1969.